REPORT NO.

CG-ONSCEN-01-89

(3)

DTIC FILE COPY

OMEGA SYSTEM PERFORMANCE ASSESSMENT

AD-A210 342

Peter B. Morris

THE ANALYTIC SCIENCES CORPORATION
55 Walkers Brook Drive
Reading, Massachusetts 01867

March 1989
Final Report

Prepared for:

U.S. DEPARTMENT OF TRANSPORTATION
UNITED STATES COAST GUARD
OMEGA Navigation System Center
Alexandria, Virginia 22310-3998

89

TECHNICAL REPORT DOCUMENTATION PAGE

1. REPORT NO.	2. GOVERNMENT ACCESSION NO.	3. RECIPIENT'S CATALOG NO.
CG-ONSCEN-01-89		

4. TITLE AND SUBTITLE	5. REPORT DATE
Omega System Performance Assessment	March 1989
	6. PERFORMING ORGANIZATION CODE

7. AUTHOR(S)	8. PERFORMING ORGANIZATION REPORT NO.
P.B. Morris	TR-5351-8-1

9. PERFORMING ORGANIZATION NAME AND ADDRESS	10. WORK UNIT NO. (TRAIS)
The Analytic Sciences Corporation 55 Walkers Brook Drive Reading, MA 01867	11. CONTRACT OR GRANT NO. DTCG23-86-C-20024 Task Order No. 88-0001

12. SPONSORING AGENCY NAME AND ADDRESS	13. TYPE OF REPORT AND PERIOD COVERED
U.S. Department of Transportation U.S. Coast Guard Omega Navigation System Center 7323 Telegraph Road Alexandria, VA 22310-3998	Final report June 1988 — March 1989
	14. SPONSORING AGENCY CODE

15. SUPPLEMENTARY NOTES

16 ABSTRACT

A measure of system performance, termed the system availability index, is introduced as: (1) an indicator of operational performance, (2) a probability of system access and utility to the system subscriber, and (3) a means of comparing system options. Theoretical development of the index is given in terms of a system availability model which is based on receiver/station reliability, signal coverage, and user geographic priorities. Sample calculations of the index are presented to illustrate comparison of system options, e.g., the effect of a station off-air. Techniques are presented to compute a station power level assignment and station off-air/maintenance schedule. Comparison of signals from the VLF communications stations and the Omega system in terms of signal coverage, receiver utilization, and government policy is also given.

17. KEY WORDS		18. DISTRIBUTION STATEMENT
OMEGA SYSTEM PERFORMANCE SYSTEM AVAILABILITY RELIABILITY OMEGA STATIONS	OMEGA RECEIVERS OMEGA SIGNAL COVERAGE VERY LOW FREQUENCY PROPAGATION PERFORMANCE INDEX OPTIMIZATION ALGORITHMS	Document is available to the U.S. Public through the National Technical Information Service, Springfield, Virginia, 22161

19. SECURITY CLASSIF. *(Of This Report)*	20. SECURITY CLASSIF. *(Of This Page)*	21. NO. OF PAGES	22. PRICE
UNCLASSIFIED	UNCLASSIFIED	140	

F910
6/21/88

NOTICE

This document is disseminated under the sponsorship of the Department of Transportation in the interest of information exchange. The United States Government assumes no liability for its contents or use thereof.

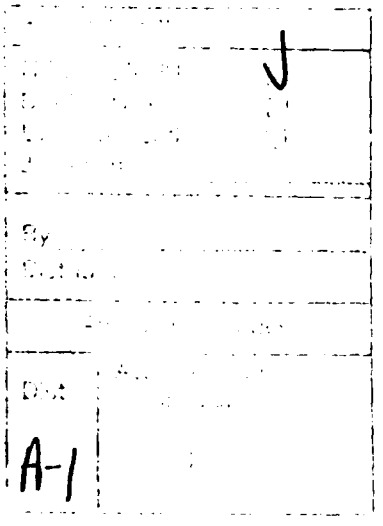

METRIC CONVERSION FACTORS

Approximate Conversions to Metric Measures

Symbol	When You Know	Multiply by	To Find	Symbol
	LENGTH			
in	inches	*2.5	centimeters	cm
ft	feet	30	centimeters	cm
yd	yards	0.9	meters	m
mi	miles	1.6	kilometers	km
	AREA			
in^2	square inches	6.5	square centimeters	cm^2
ft^2	square feet	0.09	square meters	m^2
yd^2	square yards	0.8	square meters	m^2
mi^2	square miles	2.6	square kilometers	km^2
	acres	0.4	hectares	ha
	MASS (weight)			
oz	ounces	28	grams	g
lb	pounds	0.45	kilograms	kg
	short tons (2000 lb)	0.9	tonnes	t
	VOLUME			
tsp	teaspoons	5	milliliters	ml
Tbsp	tablespoons	15	milliliters	ml
fl oz	fluid ounces	30	milliliters	ml
c	cups	0.24	liters	l
pt	pints	0.47	liters	l
qt	quarts	0.95	liters	l
gal	gallons	3.8	liters	l
ft^3	cubic feet	0.03	cubic meters	m^3
yd^3	cubic yards	0.76	cubic meters	m^3
	TEMPERATURE (exact)			
°F	Fahrenheit temperature	5/9 (after subtracting 32)	Celsius temperature	°C

*1 in = 2.54 (exactly). For other exact conversions and more detailed tables, see NBS Misc. Publ. 286, Units of Weights and Measures, Price $2.75, SD Catalog No. C13.10:286.

Approximate Conversions from Metric Measures

Symbol	When You Know	Multiply by	To Find	Symbol
	LENGTH			
mm	millimeters	0.04	inches	in
cm	centimeters	0.4	inches	in
m	meters	3.3	feet	ft
m	meters	1.1	yards	yd
km	kilometers	0.6	miles	mi
	AREA			
cm^2	square centimeters	0.16	square inches	in^2
m^2	square meters	1.2	square yards	yd^2
km^2	square kilometers	0.4	square miles	mi^2
ha	hectares (10,000 m^2)	2.5	acres	
	MASS (weight)			
g	grams	0.035	ounces	oz
kg	kilograms	2.2	pounds	lb
t	tonnes (1000 kg)	1.1	short tons	
	VOLUME			
ml	milliliters	0.03	fluid ounces	fl oz
l	liters	2.1	pints	pt
l	liters	1.06	quarts	qt
l	liters	0.26	gallons	gal
m^3	cubic meters	35	cubic feet	ft^3
m^3	cubic meters	1.3	cubic yards	yd^3
	TEMPERATURE (exact)			
°C	Celsius temperature	9/5 (then add 32)	Fahrenheit temperature	°F

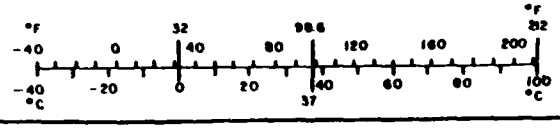

TABLE OF CONTENTS

TABLE OF CONTENTS (Continued)

LIST OF FIGURES

LIST OF TABLES

LIST OF TABLES (Continued)

1. EXECUTIVE SUMMARY

Fully operational since 1982, the Omega Navigation System is, by most definitions, a mature system. As the system matures, the U.S. Coast Guard must look to the future and project system resource availability and requirements over Omega's expected lifetime. In spite of the emergence of the NAVSTAR Global Positioning System, a highly accurate satellite-based navigation system which is scheduled for full operation by the early 1990's, Omega is expected to remain operational until at least the year 2000. Recent problems with Omega transmitting station antennas — in particular, the valley-span antenna at Omega station Hawaii (OMSTA Hawaii) — have brought these issues more sharply into focus, since decisions to make expensive repairs to station antennas clearly depend on the projected life of the system.

To provide supporting quantitative data which can facilitate decisions regarding future system options, the U.S. Coast Guard Omega Navigation System Center (ONSCEN) has sponsored a study to develop realistic models of system performance and methods for quantifying performance within the context of optional system structures or operational procedures. This report documents the important first step associated with the development of a quantitative methodology which is critical to assisting the decision process. Where possible throughout this report, system options regarding OMSTA Hawaii are emphasized.

The principal thrust of this report is the development of a measure of Omega system performance. Based on historical precedent and its probabilistic interpretation, the system availability index is selected to characterize expected system performance. System availability, as measured by this index, is defined as the probability that an Omega user, anywhere on the globe, will be able to receive and process three or more Omega signals for successful navigation or position-fixing. As a measure of performance, this index (which ranges from 0 to 1) addresses both receiver and transmitting station reliability. The complementary index, defined as the "system unavailability," is obtained by subtracting the system availability index from one. The station reliability (on-air probability) is translated into signal access probability via the signal coverage diagrams/database. By incorporating regional priorities for Omega usage and certain receiver characteristics, the system availability index can be tailored to an individual user or group of users. The system availability is defined at times given by the signal coverage database over time intervals which are constrained only by the validity of the station and/or receiver

reliability statistics. Besides its probabilistic definition from a user's viewpoint, the system availability index can serve as an overall measure of system performance which can be reported monthly or quarterly in support of system management/operations or as a reference by which the merit of system options may be compared. For system management/evaluation, an "inverse mode" of the system availability calculation may be used to determine those station reliability figures which yield a desired system availability index. Since current planning documents do not identify specific, external system availability requirements for Omega, a default minimum system availability figure of 0.95 is used here for numerical computations. Sample calculations of the system availability index indicate that for the hours/months/database tested, the index is reduced below 0.95 if the OMSTA Hawaii station signal is not available. From another viewpoint, these sample results mean that system unavailability increases by a factor of approximately 1.73 if no OMSTA Hawaii signal is transmitted. Other sample results show, for comparison, that a 10 dB increase in the power level at all stations, or, equivalently, a 10 dB increase in receiver sensitivity (in the presence of noise), increases system availability by 3-4%; in terms of system unavailability, this increase in station power/receiver sensitivity decreases unavailability by a factor of 4.63.

The numerical results and interpretations presented in this report serve primarily to illustrate application of the system availability model to system options of current interest. The numerical results appearing in the report are of two types: (1) sample calculations using the system availability algorithm and (2) approximate, "first-cut" calculations of system parameters (e.g., station power levels) for system alternatives/options (e.g., rescheduling off-air/maintenance periods). The type (1) numerical results are obtained with a fully developed algorithm but employ a previously-developed signal coverage database which is limited in dimensionality. The type (2) numerical results are based on first-cut approximations because the required databases are not yet fully developed and the proposed algorithms are not in an executable format. It is expected that more accurate, comprehensive results will be produced following the acceptance and implementation of this methodology.

The option of using the VLF communications stations as a substitute for one or more Omega stations is explored in terms of signal coverage, received signal utilization, and U.S. government policy. Comparison of the signal coverage which is limited by signal-to-noise ratio (SNR) is provided for OMSTA Hawaii and the Hawaii VLF communications station (NPM). In spite of the greater transmitted power, VLF station signals are likely to have spatially-extensive

regions of phase instability and thus exhibit equivalent, and possibly poorer, coverage than Omega. Comparison of the two systems in terms of received signal processing and government (Federal Aviation Administration and U.S. Navy) policy suggests that VLF communications signals, when used for navigation, should only serve in a support, or "backup," role to Omega signals.

Two other options addressed in this report include: (1) reduction of station power levels below the current value of 10kW (radiated) and (2) re-assignment of station off-air months for annual maintenance. Station power levels are sought which minimize the electric power generation costs to the system yet are high enough to achieve a minimally acceptable system availability figure. It is estimated that a 5 dB reduction in power at all stations increases system unavailability by a factor of 1.45 but is probably acceptable for a default minimum system availability figure of 0.95; a 10 dB reduction is expected to increase system unavailability by a factor of 1.75 and is probably unacceptable for a minimum acceptable system availability figure of 0.95. For comparison, if a *single* station (OMSTA Hawaii) suffers a power reduction of 5 dB, it is estimated that system unavailability will increase by a factor of 1.16 though system availability is likely to remain above 0.95; for a single station power level reduction of 10 dB, it is estimated that system unavailability will increase by a factor of 1.27 and system availability may range above and below 0.95 depending on the hour/month condition. An alternative off-air schedule is presented for annual maintenance at each station based on an approximate method which minimizes the coverage penalty for each station's off-air.

2. INTRODUCTION

2.1 BACKGROUND

The origins of Omega can be traced back to the 1940s during the period in which Loran was initially developed. The idea for the development of a VLF navigation system, which later evolved into the Omega System, was proposed in 1955 by J.A. Pierce in a letter to the Chief of Naval Research (Ref. 1). Omega developed slowly at first, with experimental stations established in Wales, Panama, San Diego, CA, Forestport, NY, and Trinidad. Of the current Omega transmitting station sites, Hawaii and Norway were the earliest, followed by North Dakota in 1971, Japan, Argentina, Liberia, and La Reunion in the mid-1970's, and Australia in 1982. While the transmitting stations were being constructed and brought on-air, Omega signal propagation was actively studied and multi-frequency propagation corrections were published in 1974 and 1980. A regional validation program was conducted from 1978-1988 to experimentally verify Omega signal coverage over the oceanic regions of the world.

Omega is now a mature system, co-existing with other navigation systems of various levels of spatial/temporal coverage and accuracy. Of the planned/existing global navigation systems, the most prominent alternative to Omega is the NAVSTAR Global Positioning System (GPS), an earth satellite-based system providing 100-meter, or better, accuracy in two or three dimensions. This system, which is primarily intended to serve U.S. Department of Defense navigation needs, is expected to be operational in the early 1990s. Based on these projections, the U.S. Department of Defense (currently, one of the Omega system's largest subscribers) plans to phase out airborne use of Omega by 1994 although use of Omega by the U.S. Navy may continue beyond that date (Ref. 2). Omega will likely continue operations well beyond this date, however, since civilian agencies such as the Federal Aviation Administration (FAA) recommend a 15 year phaseout period even after firm decisions are made to terminate the system. The International Omega Technical Commission (IOTC), composed of station host nation representatives with a charter to develop and coordinate Omega policy, considers that Omega operations should continue at least through the year 1998 (Ref. 3).

Apart from these external considerations, the Omega system faces internal issues of system longevity/resources. Recently, problems have been identified with the valley span antenna

at the Omega station in Kaneohe, Hawaii (OMSTA Hawaii). The estimated cost of repairs to this antenna is very high, precipitating a review of basic system operational parameters (e.g., number of stations and power levels) required for the next 10-20 years. In particular, since funds may or may not become available for these repairs, OMSTA Hawaii may be forced to operate in a low-power condition (one or more spans removed) or be permanently disestablished. Other station antennas may also require expensive repair/replacement during the projected lifetime of the system. These issues raise the following questions:

- Are all eight stations (in particular, OMSTA Hawaii) necessary for continued operation at an acceptable level of system performance for the projected life of the system?
- Could expensive antenna repair costs be partially offset by lower-power operation at one or more stations?
- Can operational doctrines (e.g., off-air schedules) be revised to improve system performance which may be degraded as a result of the actions above?
- Do current performance assessment estimates properly account for conventional Omega receiver system capabilities?
- Can the VLF communications station signals be used as a substitute for signals from one or more Omega stations?

These questions must be addressed in the context of the system-external issues mentioned above before proceeding with costly repairs or other actions. In order to address these questions, a quantitative measure of system performance must first be established.

2.2 OBJECTIVE

The principal goal of the work covered in this report is to develop a figure-of-merit, or index of performance for the Omega system which accounts for all (or, at least, most) of the attributes of the Omega system, including station performance, receiver performance, signal coverage characteristics, and the geographic patterns of users/user-requirements. The performance index must be quantitative so that numerical values of system performance may be compared for various system options. To provide a credible measure of system performance, calculation of the performance index must be based on a realistic model of system features and behavior. The index must synthesize the various system attributes into a single figure (or small set of figures) to simplify the evaluation process and facilitate decision-making on system

options. The index must also be sensitive to variations in important system features (e.g., station power levels) to distinguish clear-cut alternatives on system options.

An important objective of this report is to demonstrate how the system availability index and the model on which it is based can be used to quantify system options; the system options can then be logically and confidently compared by means of the system performance index. Algorithms are developed to compute the quantities/parameters associated with these system options and estimates are provided, where possible, using first-cut approximations. The following system options will be addressed:

- Use of the 23.4 kHz VLF communication station in Hawaii in place of OMSTA Hawaii
- Reduction of power levels at each Omega station below the current, nominal radiated power of 10 kW
- Alternative off-air schedules for annual maintenance at each station.

2.3 APPROACH

To achieve the goals/objectives listed above, an analytical approach is taken to insure objectivity and permit, at least in principle, optimization of system performance (e.g., maximizing a performance function or minimizing a cost function). System performance is defined in terms of system availability to any Omega user based on the expected reliability of the user's receiver and the stations' reliability which, from the user's perspective translates into an uncertainty in signal coverage. Because station reliability statistics are reasonably well-known and sufficient signal coverage information is available, a probabilistic model of system availability is adopted which can additionally embrace receiver reliability statistics (independent of station reliabilities) and Omega user geographic distributions through regional weighting applied to coverage maps. System options are first quantified in terms of the system parameters comprising the system availability model and then formulated as cost-penalty functions or performance functions subject to practical constraints on system parameters and options.

Algorithms are formulated to help resolve system options expressed in analytical form. The algorithms developed to compute alternative system parameters, e.g., power level assignment, are structured as an optimization, i.e., minimization of a cost function or maximization of a performance function. The algorithms indicate how a calculation is to proceed but do not include computer coding and numerical computation.

The numerical results appearing in this report are of two types: (1) sample calculations using the system availability algorithm and (2) approximate, "first-cut" calculations of parameters required for system alternatives/options. For the type (1) results, the two-hour/four-month 10.2 kHz coverage database is used with a fully developed system availability algorithm. The type (2) numerical results are based on first-cut approximations because the required databases are not yet fully developed and the proposed algorithms are not in an executable format. In some cases, the approximations/estimates are in the form of upper and lower bounds on the system parameters. Where possible, system options are focused on OMSTA Hawaii.

No specific requirement for a minimally acceptable Omega system availability figure has yet been articulated. The Federal Aviation Administration (FAA) and U.S. Coast Guard are jointly developing a Memorandum of Agreement which is expected to spell out requirements for Omega system availability (Ref. 36). For those cases in which a numerical value of a minimum threshold system availability figure is required (e.g., in sample calculations), a default value of 0.95 is used.

2.4 REPORT OVERVIEW

The system availability index and model is presented in Chapter 3. Historical precedent and motivation for the system availability index are given and the four elements comprising the model are described. The model structure is then developed and two modes of application for the index as an operational tool are discussed. Finally, sample calculations of the system availability index are presented.

VLF communication station signals as an alternative to Omega are discussed in Chapter 4. Signal-to-noise ratio (SNR) coverage figures for the current VLF station in Hawaii are presented and upper bound estimates of the coverage, including modal interference effects, are made. The second part of the chapter compares Omega/VLF receiver processing/utilization of the two types of signals and U.S. Government policies regarding use of the system.

Chapter 5 focuses on the problem of determining the minimum power level at each station such that a desired system availability is achieved. An algorithm is developed to minimize a cost function which includes the relative costs of producing power at each station. Numerical estimates are provided as upper and lower bounds on station power level with the assumption that all station power levels are equal.

The scheduling of station off-air periods for annual station maintenance is addressed in Chapter 6. An algorithm is developed to maximize a performance function subject to environmental/fiscal constraints on the allowable months at each station during which annual maintenance may be conducted. Based on signal coverage and a simplified algorithm, an estimated schedule is derived and compared to the current schedule.

Chapter 7 summarizes the work presented in the report and draws tentative conclusions from the numerical results based on first-cut estimates and approximations. Recommendations are outlined to develop databases and algorithms to permit precise calculation of system availability under contemplated system options.

The appendices include the mathematical details of the system availability model (Appendix A), a discussion of Omega receiver characteristics relevant to signal coverage (Appendix B), and a description of the signal coverage databases used in the report (Appendix C). The final two appendices describe the structure of the system power level assignment (Appendix D) and station off-air/maintenance scheduling algorithms (Appendix E).

3. A MODEL FOR CALCULATING THE OMEGA SYSTEM AVAILABILITY INDEX

This chapter introduces the system availability index as a measure of Omega system performance. The notion of system availability has historical precedent as noted in Section 3.1 of this chapter. By design, the index reflects a broad definition of system attributes, including Omega receivers, transmitting stations, signal coverage, and the geographical distribution of the system user population. Computation of this index requires a quantification of the system attributes/elements as described in Section 3.2. The basic assumptions required for this quantification, in addition to the connections between the system elements, collectively make up the system availability model whose structure is presented in Section 3.3. Finally, recommended modes of application for this model/index including sample numerical results are presented in Section 3.4.

3.1 BACKGROUND/OBJECTIVE

Prior to 1975, when Omega figured more prominently into the U.S. Navy's strategic planning, a Specific Operational Requirement (SOR 34-01) for the "Omega Long Range Navigation System" (Ref. 28, Section II) stated that:

> "...overall system availability shall be 95%. MTBF of the receiving system shall be at least 1000 hours. MTTR shall not exceed 30 minutes..."

In supporting documentation (Ref. 28, Section XIII), system availability was defined as the probability that at any point in time and at any point on the earth's surface, an Omega user's receiver would be properly functioning and three or more Omega signals could be effectively utilized* so that successful navigation/position-fixing could be performed.

As Omega moved under civil control, these operational requirements no longer directly applied, but the system management, formally organized through the International Omega Technical Commission (IOTC), sought to maintain the maximum level of system performance.

*This will be given more precise meaning in Section 3.2.3.

As representatives from nations hosting Omega transmitting stations, the IOTC naturally emphasized minimization of station off-airs (i.e., maximizing station reliability as a means of maximizing system performance).

The definition of P_{SA} given above, i.e., the probability that, at any geographic location/time, an Omega user's receiver functions properly with the reception of three or more effectively usable Omega signals, involves four general system features:

1. Omega receiver reliability
2. Omega station reliability
3. Omega signal coverage
4. Omega user regional priority.

These four elements, however, show that improving system availability involves more than just improving transmitting station reliability. Improved Omega receiver systems, demanded by the users and developed in consonance with advancing technology by the Omega receiver manufacturers, can also provide increased reliability. Improvements in signal coverage can be implemented through either: (1) increased station power output or station relocation by the system providers, or (2) increased receiver sensitivity or more sophisticated signal processing (such as use of long-path signals) by the Omega receiver manufacturers. Also, the availability of an accurate Omega system information/documentation base, providing information on which signals should be used in which areas and at what times, will permit users to realize the full performance potential of the system.

It is important that system availability be characterized by a single index which ties together the most crucial elements of overall system performance. In this way, the index can be used to assess the net effect (and sensitivity) of changes in the several components of system availability; e.g., an increase in overall station reliability coupled with a decrease in signal coverage (due, for example, to global propagation anomalies). From an operational viewpoint, a single index for system availability is easily monitored on a periodic (e.g., monthly) basis to detect short-term problems, such as an intense period of anomalous signal propagation, or long-term patterns which may indicate a problem with an equipment item which is common to all stations. By incorporating user regional priorities, the index can also furnish comparisons of the effect of system options (e.g., station power reductions) on various users. Thus, the index can provide critical support to both system operational and management functions.

The objective of this chapter is to present the Omega system availability index (herein referred to as P_{SA}) and the model upon which it is based. Sample results are also presented to illustrate the use of the index and some suggested applications.

3.2 ELEMENTS OF A PROBABILISTIC MODEL FOR COMPUTING SYSTEM AVAILABILITY

The system availability index for a global, multi-station network radiating signals (whose coverage pattern is highly time-dependent) to a multi-user environment with several levels of receiver sophistication and user classes has a rather intricate dependence on numerous, interdependent quantities. Without supporting tools and rationale for simplifying assumptions, the calculation of P_{SA} is a formidable task. Fortunately, a probabilistic model can be constructed which, with the aid of previously-developed coverage analysis tools, can be used to readily compute P_{SA}. The four elements of this model, introduced in Section 3.1, are described in this section and the model structure is explained in Section 3.3.

3.2.1 Receiver Reliability

The definition of P_{SA} includes two independent types of events: the proper functioning of an Omega receiver and the presence of three or more usable signals. Thus, by definition (at a particular location/time),

$$P_{SA} = P_R \, P_A$$

where P_R is the probability that the user's Omega receiver is both functioning normally and being operated correctly at the fixed point in time and space; P_A is the probability that three or more usable signals are accessible. P_R is considered to have a long-term time dependence as successive generations of receivers are expected to exhibit improved reliability. To illustrate the procedure, a uniform failure interval and repair time model is adopted which is characterized by two parameters: a mean time-between-failure (MTBF) and a mean time-to-repair (MTTR). In terms of these parameters, the receiver reliability is

$$P_R = 1 - \frac{MTTR}{MTBF}$$

In general, the MTBF and MTTR depend on the specific Omega receiver system (manufacturer/model) including the antenna installation, but for receivers within the same generic class (e.g.,

those on marine platforms or on meteorological balloons), these two parameters are approximately constant. Thus, more generally,

$$P_{R_i} = 1 - \frac{MTTR_i}{MTBF_i}$$

where *i* labels the receiver class.

3.2.2 Transmitting Station Reliability

Omega station reliability is clearly central to the calculation of system availability and has some important operational features which critically influence the development of the model as explained below. One of the most important features of station reliability is that all station off-air occurrences are classified as either

- unscheduled - random occurrence/duration
- scheduled - deterministic occurrence/duration.

Unscheduled off-airs occur as the result of unforeseen circumstances — usually equipment failure. Their individual occurrence may be considered random but occurrence statistics can be compiled which are characteristic of a particular Omega station. This characterization arises because of antenna type, environmental factors, and component replacement history. The off-air occurrence statistics are naturally derived from historical reliability figures for a particular Omega station. The statistics are best compiled on a month/year/station basis since

- the month (as a unit of time) is equal to or shorter than a climatically-important interval such as winter, summer, wet season, dry season, typhoon season, etc.
- the month is long compared to the time required to resolve a problem causing an emergency/unscheduled off-air condition.

Based on average off-air times for a given month/year (compiled from historical figures), it can be shown (Appendix A) that for simple, yet reasonably general off-air occurrence/duration probability functions, the probability that a particular station is in an unscheduled off-air condition at any given time during a specified month is approximately

$$\frac{T_{OA}}{T_{TOT}}$$

where T_{OA} is the average total off-air time (usually in minutes) for the specified month/station (based on earlier years for the same month/station) and T_{TOT} is the total time in the specified month (same units).

Scheduled off-airs are, as the name implies, planned conditions under which a station ceases operation. In this case "planned" refers to both the time at which the off-air begins and the off-air duration. The planning usually includes an advance notification to users of the scheduled off-air condition, although the amount of advance notice may vary considerably depending on the urgency of the work to be done during the off-air. Typical advance notice for scheduled off-airs (excluding annual maintenance, see below) is 1-2 weeks. From a user's viewpoint, these types of scheduled off-airs may be considered to have random occurrence times in terms of predictability on time scales longer than the advance off-air notice. Thus, at the beginning of a month,* a scheduled off-air probability is defined for the month for each station, similar to that for unscheduled off-airs, assuming that advance notification for one or more stations had not been received.

Annual maintenance periods are another type of scheduled off-air having two main features:

- The maintenance off-air period for maintenance and/or repair must occur in a specific, distinct month for each station. (see Fig. 6-1). Any antenna, electronics, or structural maintenance/repair which is not of an urgent nature *must* be scheduled during the station's annual maintenance period.
- The scheduled off-air period for annual station maintenance is planned well in advance and users are generally given notice 1-2 months in advance.

Because of the long lead time, these types of scheduled off-air events are deterministic for a monthly prediction interval. Deterministic events may be incorporated in a probabilistic model by assuming an "impulse-type" probability density function (see Appendix A). Thus, unscheduled off-airs and both types of scheduled off-airs, although following, in some cases, different probability distributions, nevertheless may be incorporated into a single probabilistic model of system availability.

Several important operational features concerning station off-airs are also included in the model. As interpreted by the model, these features may be grouped in two categories which identify exclusive events and independent events:

Exclusive Events:

- An unscheduled off-air event at a given station cannot be concurrent with a scheduled off-air event at the same station, i.e., an off-air must be either scheduled or unscheduled, not both.

*Unless otherwise specified, the month is the standard unit of time over which the probabilistic interpretation/prediction of system availability is applied.

- A scheduled off-air event at a given station cannot be concurrent with a *scheduled* off-air event at *any other station*. This operational doctrine is enforced by ONSCEN to avoid a substantial reduction in system coverage due to simultaneous station off-airs.

Independent Events:

- An unscheduled off-air event at a given station is independent of a concurrent unscheduled off-air event at any other station. This is due to the random nature of unscheduled off-airs.*
- An unscheduled off-air event at a given station is independent of a concurrent *scheduled* off-air at any other station. This is again due to the unpredictable nature of unscheduled off-air events.*

3.2.3 Omega Signal Coverage

In addition to the station and month dependence which characterize the station reliability model, the signal coverage model involves another time dimension (hour of the day) and two spatial dimensions (latitude and longitude on the earth's surface). Additional parameters, such as frequency (10.2 or 13.6 kHz) and signal access criteria (see below), also serve to define the signal coverage.

ONSCEN currently maintains two Omega signal coverage databases (Ref. 24): (1) the 2-hour/4-month/2-frequency database and (2) the 24-hour/4-month/2-frequency database. Both databases contain 10.2 and 13.6 kHz signal and noise parameters such as SNR, signal amplitude, and signal phase on radial paths extending from each station during the months of February, May, August, and November. Database (1) contains signal and noise data at 0600 and 1800 UT and, for 10.2 kHz, contains fractional coverage information for each combination of station signals. Database (2) contains signal and noise data at all 24 UT hours but the database structure is not currently in a format which permits coverage display and fractional coverage information on station signal combinations. Because of the current availability of the fractional coverage data on station signal combinations, the 2-hour/4-month/10.2 kHz database is referenced in most of the discussion and the sample results of this chapter. Future work, however, will permit calculations of P_{SA} at the geographic unit cell level using the 24-hour/4-month/2-frequency database. Signal access criteria, which describe the limits of signal usability (for a given

*The independence assumption for unscheduled off-airs is really an approximation but is expected to be valid for the distribution and duration of off-airs normally experienced by Omega stations.

scenario) are applied to the database to provide a display of Omega spatial coverage for each hour/month/frequency combination which is most meaningful to the user. In most applications, the following signal access criteria are invoked:

(1) SNR (100 Hz bandwidth (BW)) must be greater than -20 decibels (dB)

(2) Deviation of the total signal phase from the Mode-1 signal phase must be less than 0.2 cycle

(3) The geometric dilution of precision (GDOP) for the set of signals satisfying the first two criteria must be less than 1 km/centicycle of phase difference error.

Thus, for example, in the composite signal coverage diagram shown in Fig. 3.2-1, the region labeled "ACDH" in the upper left corner of the figure means that, at each point in the region, 10.2 kHz signals from Omega stations A, C, D, and H individually satisfy access criteria (1) and (2) and collectively satisfy access criterion (3) above. Appendix C describes the two databases and associated signal access criteria in greater detail.

It is important to note that the signal coverage component of the system availability model is deterministic, i.e., all coverage data are fixed and definite. Randomness is introduced into the system availability model through the uncertainty of operation expressed by receiver

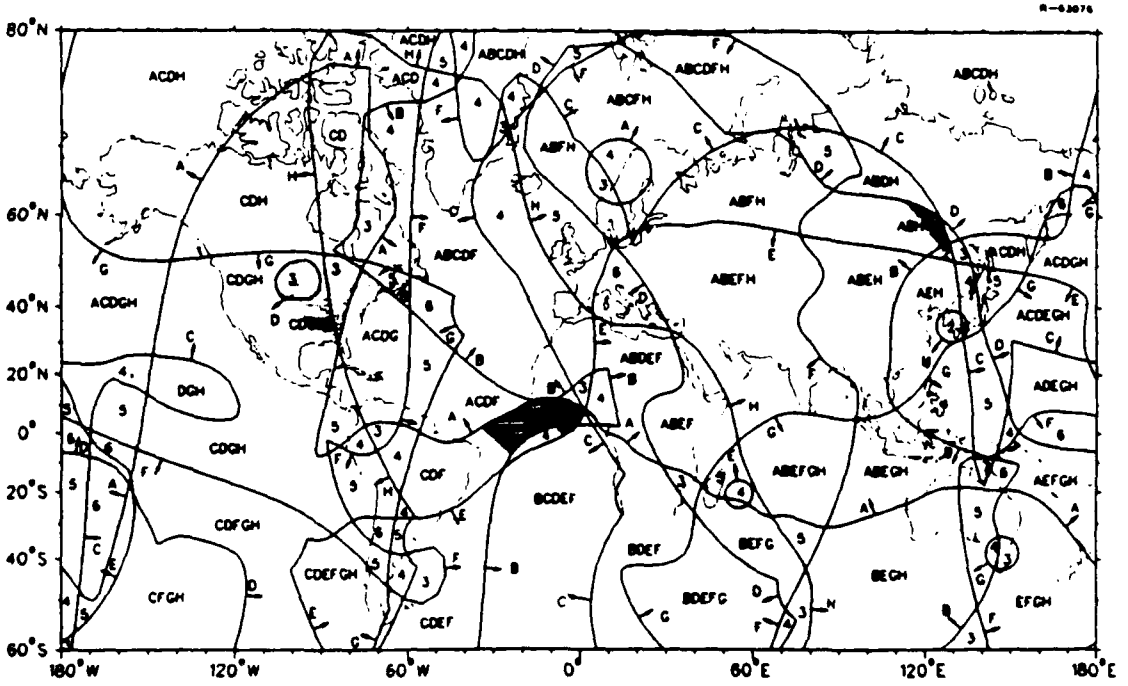

Figure 3.2-1 Composite Signal Coverage Prediction Diagram for 10.2 kHz at 0600 GMT in August

reliability and especially the transmitting station reliability. Extensive measurements of atmospheric noise (Ref. 20) have led to statistical definitions of random noise levels at Omega frequencies. Omega signal components also have a random variation although the distribution (e.g., amplitude) is much narrower than that for noise. These random variations may be combined to produce a probability distribution for signal-to-noise ratio. The model in its current form does not incorporate this random variation since the work described here focuses on the statistics of equipment reliability which can be controlled (to a degree) to improve system performance.

3.2.4 Omega User Regional Priority

The system availability index, P_{SA}, introduced in Section 3.1, is the probability that a user could, at a given time/time interval, operate his Omega receiver and process three or more usable station signals for successful navigation/positioning *at any geographic location on the earth*. This implies a uniform weighting in which a user has an equal need for Omega *anywhere* on the globe with no restrictions on topography/climate, and no consideration of historical actions or projected requirements. Most users do have geographical preferences, i.e., regions in which they are particularly concerned about the availability of usable Omega signals. To incorporate these needs, the model provides for the inclusion of a regional weighting map (Fig. 3.2-2 shows an example of such a map) which produces a P_{SA} that is sensitive to changes in coverage (e.g., hour-to-hour) in the user's region of interest.

The regional weighting is normalized so that the probabilistic interpretation is maintained. For example, assume that the surface of the earth is divided into cells, each with an area of approximately one square megameter, and the operating area (requiring use of Omega) for a particular user lies wholly within cell C. In this case, cell C would be weighted 1 and all other cells would be assigned weight 0. For this user, the definition of P_{SA} is modified to include only those geographic locations in cell C. If several cells encompass the operating area of interest, appropriate weights can be assigned to each of the cells to capture the typical or specific operational scenario of interest. Therefore, the weighting structure is general so as to accommodate a class of Omega users with a global/near-global operating area but with emphasis on specific or critical regions. Figure 3.2-2 illustrates a sample regional weighting for civil use of Omega emphasizing North Atlantic, North Pacific, and polar air routes and de-emphasizing regions of little Omega civil interest in the far southern oceanic regions.

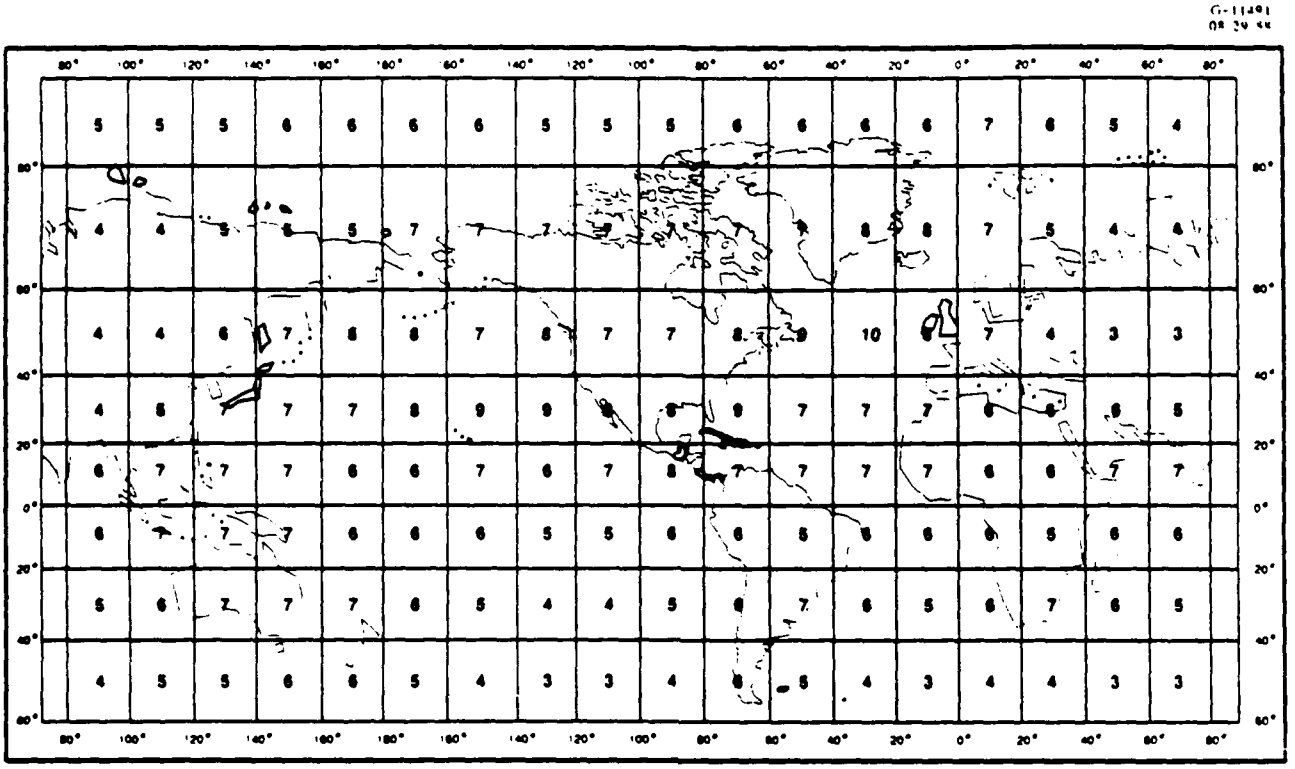

Figure 3.2-2 *Example of Regional Weighting: Omega Civil Use*

3.3 STRUCTURE OF THE PROBABILISTIC MODEL

3.3.1 Signal Access Probability

It is shown in Section 3.1 that P_{SA} can be decomposed into a product of the receiver reliability, P_R, and the probability of signal access, P_A, sufficient for conventional navigation/positioning. Define X_3 as the event that three or more usable signals are available at any point in space and time. This definition implicitly assumes the use of Omega-only navigation/positioning receivers. If signals/aids from other navigation systems are also available (as in, for example, a hybrid receiver), then perhaps as few as one or two Omega signals would be needed for successful navigation. The general approach described here can be used with an event defined for any minimum number of Omega signals, i.e., X_i ($i = 1,2,\ldots,8$), the event that i or more usable signals are available at any point in space and time. For the remainder of this report, however, only event X_3 will be used.

P_A has a global definition corresponding to the global definition of P_{SA} through the phrase "at any geographic location on the earth." Since X_3 is defined locally (i.e., a point

function of space and time), a weighted average of $P(X_3)$ over the earth's surface is taken to match the definition of P_A, i.e.,

$$P_A = < P(X_3(\theta, \phi, t)) >$$

where θ, ϕ are polar and azimuthal angles used in standard spherical coordinates and t is the time. For a spherical earth, P_A is given as

$$P_A = \frac{1}{N_w} \int_0^{2\pi} \int_0^{\pi} P(X_3(\theta, \phi, t)) w(\theta, \phi) R_E^2 \sin\theta \, d\theta \, d\phi \qquad (3.3\text{-}1)$$

where $w(\theta, \phi)$ is the regional weighting function, R_E is the earth's radius, and N_W is a normalizing factor given by

$$N_w = \int_0^{2\pi} \int_0^{\pi} w(\theta, \phi) R_E^2 \sin\theta \, d\theta \, d\phi$$

Notice that P_A is a function of the time, t, through $P(X_3(\theta, \phi, t))$. No time integration/averaging is carried out as done for space since, as is shown later in the development, time plays a special role in both the theory and application of the P_{SA} model.

Now, X_3 not only depends on space and time (as given by the Omega coverage database) but also on the particular Omega stations that are on-air/off-air. To explicitly include this dependence, the following complementary events are defined:

$T_i \equiv$ event that Omega station i is on-air (i = 1, 2, ..., 8)

$\overline{T}_i \equiv$ event that Omega station i is off-air (i = 1, 2, ..., 8)

It is important to note that the events making up the set $\{T_i\}$ (or $\{\overline{T}_i\}$) are not mutually exclusive. Thus it would not be desirable to express X_3 directly in terms of these sets of events. Mutually exclusive events are obtained by defining the following six sets of events*:

$B_0 \equiv$ event that no station is off-air

$\equiv T_1 T_2 T_3 T_4 T_5 T_6 T_7 T_8$

*In the set operations which follow, product indicates set intersection and addition indicates set union.

$$
\begin{aligned}
B_i &\equiv \text{event that only station i is off-air, } i = 1,2,...,8 \\
&\equiv T_1T_2...\overline{T}_i...T_8 \\
B_{ij} &\equiv \text{event that only stations } i \text{ and } j \text{ are concurrently off-air,} \\
&\quad i = 1,2,...,8;\ j = 1,2,...,8;\ i \neq j \\
&\equiv T_1T_2...\overline{T}_i...\overline{T}_j...T_8 \\
B_{ijk} &\equiv T_1...\overline{T}_i...\overline{T}_j...\overline{T}_k...T_8 \\
B_{ijkl} &\equiv T_1...\overline{T}_i...\overline{T}_j...\overline{T}_k...\overline{T}_l...T_8 \\
B_{ijklm} &\equiv T_1...\overline{T}_i...\overline{T}_j...\overline{T}_k...\overline{T}_l...\overline{T}_m...T_8
\end{aligned}
$$

where the B-events are symmetric under all possible permutations of indices, and no two indices are equal. Events with more than five stations off-air are not defined since, in that case, event X_3 could not occur under any circumstances. By expressing the set universe as the union of all possible (mutually exclusive) B-events, it is shown in Appendix A that

$$
\begin{aligned}
P(X_3(\theta,\phi,t)) &= P(X_3/B_o)P(B_o) + \sum_{i=1}^{8} P(X_3/B_i)P(B_i) + \ldots \\
&\quad + \sum_{i=1}^{8}\sum_{j=i+1}^{8}\sum_{k=j+1}^{8}\sum_{l=k+1}^{8}\sum_{m=l+1}^{8} P(X_3/B_{ijklm})P(B_{ijklm}) \qquad (3.3\text{-}2)
\end{aligned}
$$

Each term in the above expression is a product of two factors: the first factor deals mainly with signal coverage (given which stations are off-air) while the second factor deals strictly with station reliability. For a given spatial point (θ, ϕ), the first factor is called a local coverage element (LCE). When $P(X_3)$ is averaged over the earth's surface (see Eq. 3.3-1), the corresponding first factor in each term of the resulting expression is called a global coverage element (GCE). In either case, the second factor is called the network reliability factor (NRF).

3.3.2 Coverage Elements

The local coverage elements are best illustrated by the following examples. Suppose a point (θ, ϕ) on the surface of the earth at time t has effective access to signals from stations 2, 3, 6, and 8* only, when all 8 stations are on-air. Then, for example,

*Station numbers correspond to the usual station letter designations in alphabetic numerical sequence, e.g., A → 1, B → 2, ..., A → 8.

$$P(X_3(\theta,\phi,t)/B_{125}) = 1$$

since the only station off-air to affect coverage at (θ,ϕ,t) is station 2 which still leaves stations 3, 6, 8 to provide 3-station coverage. As another example, consider that

$$P(X_3(\theta,\phi,t)/B_{38}) = 0$$

since, with stations 3 and 8 off-air, fewer than 3 stations are accessible at (θ,ϕ,t).

To provide further understanding of global coverage elements, make the simple (but totally unrealistic) assumption that stations 1, 2, 3, 4 cover exactly half the earth's surface and stations 5, 6, 7, 8 cover the other half (note that the coverage area does not have to be contiguous, i.e., the 1234 station coverage may occur in patches which, when summed, gives an area equal to half the earth's surface area). In this case,

$$< P(X_3/B_o) > = 1$$

since the globe is everywhere covered by 3 or more stations. On the other hand,

$$< P(X_3/B_{345}) > = 0.5$$

since only the second half of the world is covered by 3 or more stations. In the same way,

$$< P(X_3/B_{1278}) > = 0$$

In actual practice, the local coverage elements are computed for a "cell", typically of size 10° (latitude) x 10° (longitude). Global coverage elements then may be computed by summing over local coverage elements and normalizing. Alternatively, P_A may be computed at the local level and averaged over the globe, as expressed in Eq. (3.3-1).

3.3.3 Network Reliability Factors

Section 3.2 described unscheduled and scheduled off-air events including the operational discipline which excludes concurrent scheduled off-air events and the uncontrollable factors which make unscheduled off-airs independent of all other events. Here, that discussion is quantified by first decomposing the off-air event for the i^{th} station as

$$\bar{T}_i \equiv \bar{T}_i^u + \bar{T}_i^s \quad i = 1,2,...,8$$

$\bar{T}_i^u \equiv$ unscheduled off-air event for the i^{th} station

$\bar{T}_i^s \equiv$ scheduled off-air event for the i^{th} station
$i = 1,2,...,8$

By definition, these events are mutually exclusive, i.e.,

$$\bar{T}_i^u \, \bar{T}_i^s = 0 \quad i = 1,2,...,8 \ .$$

Also, the exclusion of two concurrent scheduled off-airs, as noted above, is expressed as

$$\bar{T}_i^s \, \bar{T}_j^s = 0 \quad i,j = 1,2,...,8 \ ; \ i \neq j \ .$$

Finally, the approximate independence of an unscheduled off-air event at a given station from unscheduled/scheduled off-air events at other stations may be written

$$\left.\begin{aligned} P(\bar{T}_i^u \, \bar{T}_j^u) &= P(\bar{T}_i^u)P(\bar{T}_j^u) \\ P(\bar{T}_i^u \, \bar{T}_j^s) &= P(\bar{T}_i^u)P(\bar{T}_j^s) \end{aligned}\right\} \begin{array}{c} i,j = 1,2,...,8 \\ i \neq j \end{array}$$

Based on these assumptions, the NRFs which occur as the second factor in each term in Eq. 3.3-2 may be computed. For example,

$$\begin{aligned} P(B_1) &= P(\bar{T}_1 T_2 T_3 ... T_8) \\ &= P[(\bar{T}_1^u + \bar{T}_1^s) \, T_2 T_3 ... T_8] \end{aligned}$$

This expression can be reduced (see Appendix A) to one involving only single-station reliability figures, e.g., $P(\bar{T}_j^s)$, $P(T_j)$, $P(\bar{T}_k^u)$. Numerical values for these quantities are readily available from historical station reliability data (usually specified by month/year) as discussed in Section 3.2.2. The specific definitions of the events B_i, B_{ij}, etc., given above mean that station reliability data cannot be directly substituted for the corresponding NRF. For example, as shown above,

$$P(B_1) \neq P(\bar{T}_1)$$

This can be understood by noting that event B_1 specifies that stations 2-8 are on-air whereas event $\bar{T}_1$ carries no such requirement. Even if the interdependence is neglected, the historical

reliability database is insufficient to specify/estimate multi-station off-air probabilities, e.g., $P(B_{12})$ or $P(B_{2578})$. The effect of the interdependence may be seen from the relationship (derived in Appendix A).

$$P(T_1T_2) = P(T_1)P(T_2) - P(\overline{T}_1^s)P(\overline{T}_2^s)$$

If the scheduled off-air probabilities are small, then the second term may be ignored and the station on-air events are essentially independent. However, scheduled off-air probabilities for stations during their annual maintenance months may be 0.5 or higher, thus making station on-air events highly dependent.

3.3.4 Final Expression for P_{SA}

To develop the expression for P_A, the averaging/integration indicated in Eq. 3.3-1 is carried out, using Eq. 3.3-2. The result is

$$P_A(t) = Q_oR_o + \sum_{i=1}^{8} Q_iR_i + \ldots + \sum_{i=1}^{8}\sum_{j=i+1}^{8}\sum_{k=j+1}^{8}\sum_{l=k+1}^{8}\sum_{m=j+1}^{8} Q_{ijklm}\, R_{ijklm} \tag{3.3-3}$$

where the GCEs are defined by*

$$Q_{ijk\ldots} = \frac{1}{N_w}\int_0^{2\pi}\int_0^{\pi} P(X_3(\theta,\phi,t)/B_{ijk\ldots})w(\theta,\phi)R_E^2 \sin\theta \, d\theta d\phi$$

and the NRFs are defined by

$$R_{ijk\ldots} = P(B_{ijk\ldots})$$

Note that the time dependence of P_A enters explicitly through the $Q_{ijk\ldots}$ via the signal coverage database which depends on hour/month and implicitly through the $R_{ijk\ldots}$ via the station on-air probabilities which depend on month/year. Time integration/averaging (hour and month) could be performed and for some applications that may be useful. However, for most applications, the time-dependent form given by Eq. 3.3-3 is the most appropriate.

Combining the results obtained above with those of Section 3.2.1 gives, as the final expression for P_{SA},

*N_w, $w(\theta,\phi)$, and R_E are defined in connection with Eq. 3.3-1.

$$P_{SA} = P_{R_i} P_A(t)$$

where *i* labels the receiver class. Note that P_A has a dependence on *i* through the GCEs since the signal coverage depends on the signal access criteria, one of which is SNR. Generally, it is expected that different classes of Omega receivers will have different minimum SNR thresholds, thus changing the signal coverage (through the GCEs) and, hence, P_A. Also, it should be recognized that P_{R_i} is probably a long-term (1-2 year) function of time (receiver reliability may improve with succeeding generations of receiver), if long-term time averaging (greater than one year) of P_{SA} is required.

Another implicit parameter on which P_{SA} depends (through the GCEs) is frequency (10.2 or 13.6 kHz). P_{SA} is not averaged over this parameter because of the several different types of multi-frequency signal phase processing used in conventional Omega receivers: serial, parallel, combining with 11-1/3 kHz phase, etc. Thus, for the applications envisioned, it remains as an implicit parameter.

3.4 APPLICATIONS OF THE PROBABILISTIC MODEL

This section focuses on: (1) operational use of the system availability index, P_{SA}, and (2) use of the index to compare system options. The operational use of P_{SA} is presented in terms of a direct mode, which is a direct calculation of P_{SA}, given known station reliability figures, and an inverse mode which computes the station reliability figures, given a fixed, required P_{SA}. The comparison of system options employs sample calculations of P_{SA} using the 24-hour/4-month/10.2 kHz database and historical reliability figures.

3.4.1 Direct Mode: Evaluate P_{SA} for Assumed Station Reliability

Figure 3.4-1 shows the computational flow for the calculation of P_{SA} given the required inputs (direct mode). The operational use of this mode is best described by considering the inputs and outputs to the computational functional blocks shown in the figure.

Time is the most important input parameter since it enters at all stages of the calculation. For example, both the GCE and the NRF require month as an input. One difficulty is that the signal coverage database provides data only for the months of February, May, August, and

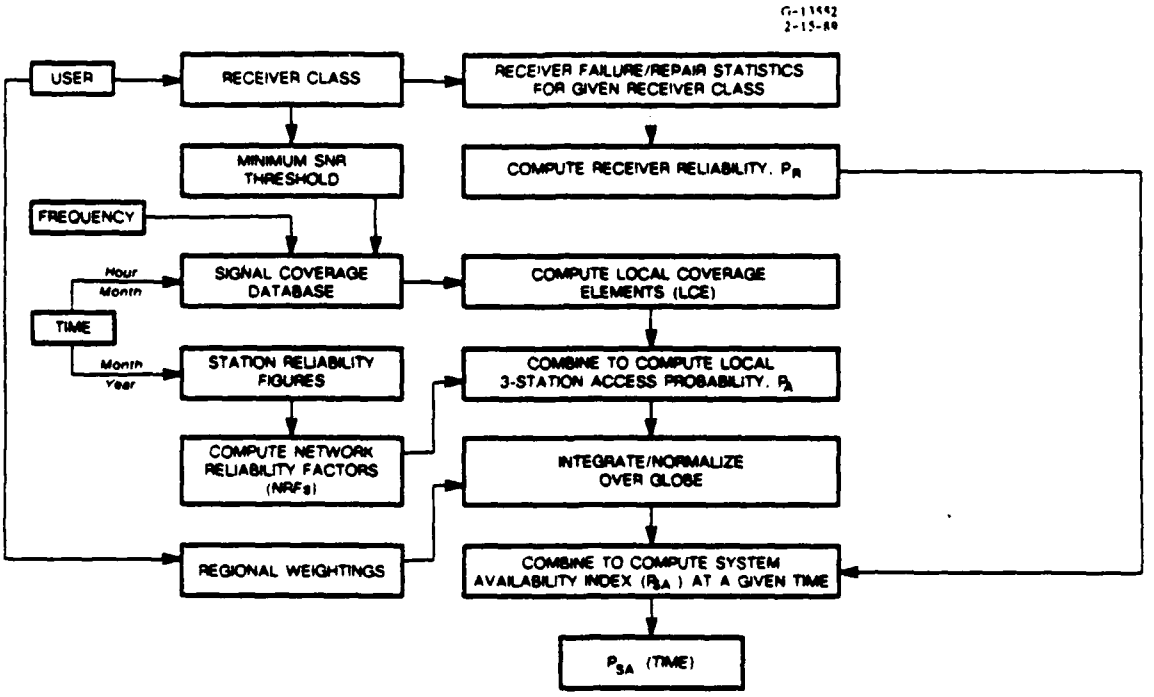

Figure 3.4-1 Computational Flow for Direct Mode of System Availability Calculation

November while the station reliabilities are specified for all 12 months. Since coverage generally does not change dramatically with month-of-the-year, a linear interpolation of P_{SA} between coverage-specified months is justified. This issue is discussed further in Chapter 6. System availability figures could be included with station reliability figures, which are compiled and reported monthly, thus providing a month-to-month comparison of the system-wide index. Since coverage does not depend on the particular year, comparison of P_{SA} could be made between the current month and the same month one year earlier to see the combined effect of differing station reliabilities (over a period of a year or more, receiver reliabilities should be checked for possible upgrade).

The hour(s) must be specified for the signal coverage database: 2 hours (0600 and 1800 UT) are provided by the 2-hour/4-month database and all 24 hours (*on* the UT hour) for the 24-hour/4-month database. An evaluator of the system could, for example, compute the average P_{SA} over the hours given in the database and/or compute the maximum/minimum P_{SA} over the set of hours. A given value of P_{SA} (e.g., 0.95) could serve as a minimum (to be exceeded at all hours) or as a target average.

P_{SA} could be evaluated/reported for both frequencies (10.2 and 13.6 kHz) and/or as the average P_{SA} over the two frequencies. Alternatively, it is possible to redefine coverage for two types of receiver mechanization:

AND: Local coverage is assumed if three or more station signals are accessible at *both* frequencies

OR: Local coverage is assumed if three or more station signals are accessible at *either* frequency.

It is clear that the AND condition is generally more difficult to achieve than the OR condition. It is also inclusive in the sense that if a target value of P_{SA} is satisfied for the AND condition, it is certainly satisfied for the OR condition. Appendix B addresses Omega receiver mechanization issues.

The type of user is also important to the calculation and use of system availability since the user type is tied to one or more receiver classes each of which may have a characteristic minimum SNR threshold. The minimum SNR threshold directly affects the GCEs/LCEs and thus P_{SA}. The user also has characteristic geographical patterns of use which can be specified in terms of regional weightings. These regional weightings directly affect P_{SA} as shown in Figs. 3.2-2 and 3.4-1. For example, Omega system management could specify a target P_{SA} to be satisfied by those users operating the least sensitive types of Omega receivers (highest minimum-SNR thresholds). This would ensure that users of more advanced equipment would experience a P_{SA} greater than the target value. Alternatively, the target P_{SA} could be computed for a uniform distribution (equal weights for all cells) or for a specific regional weighting describing the needs of a large, important user, e.g., the U.S. Navy or U.S. air carriers.

3.4.2 Inverse Mode: Evaluate Station Reliabilities for Assumed Target Value of P_{SA}

The above discussion of P_{SA} target values implies that actions could be taken by the system manager to increase or decrease system availability. The "simplest" way (for the system operator) to increase P_{SA} is by increasing/improving station reliability. Thus, for some applications it is important to know the station reliability figures which are required to achieve a required/desired P_{SA}. This is the objective of the inverse mode of the system availability calculation although, in a general sense, calculation of any quantity (or quantities) which normally serves as input (given that all other input/output quantities are fixed/known) is defined as an inverse mode calculation.

The major difficulty associated with the inverse mode calculation is that, in general, the station reliabilities represent eight distinct quantities which therefore cannot be uniquely determined from a single expression for P_{SA}. Eight relations, obtained from any eight sets of month/hour/frequency combination, are needed to solve for the eight station reliabilities. Even with eight relationships, the strong non-linearity of the resulting equations makes the calculation exceedingly complex.

A far simpler, although less realistic, procedure is to assume the station reliabilities are all equal so that only one quantity is to be determined. Even in this case a closed form analytic solution is not feasible so that an interactive scheme is used. This procedure can be made somewhat more realistic by using average ratios of unscheduled to scheduled off-air durations over a given year. Thus, although the total on-air probabilities (and thus off-air probabilities) for the eight stations are assumed to be the same, the partitioning of the off-air probabilities between unscheduled and scheduled conditions can be tied to station-specific historical data. This procedure is employed in the sample calculations presented in Section 3.4.3.

Figure 3.4-2 shows the computational flow for the inverse mode which is similar to that for the direct mode except for the iteration over station reliabilities and the P_{SA} input. The principal use of the inverse mode outputs by a system evaluator is likely to be the comparison of the computed minimum station reliability figures (unequal or equal) with those actually measured over a given period. If the computed figures are less than the measured figures, the system availability is above the minimum acceptable value and no action needs to be taken. If (some or all of) the measured reliabilities are less than the computed minimum values, corrective action is indicated to upgrade the reliability of those stations with below-threshold on-air probabilities so that the system can achieve the target P_{SA}. The time, frequency, and user/receiver-class input can be used in the same fashion as described in Section 3.4.1.

3.4.3 Sample Results

In this section, sample calculations are shown for system availability in both the direct and inverse modes to illustrate the effects of various system options. The results are based on the 2-hour/4-month/10.2 kHz signal coverage database mentioned earlier. The station reliability figures are based on monthly reliability statistics for 1985, 1986, and 1987 compiled by

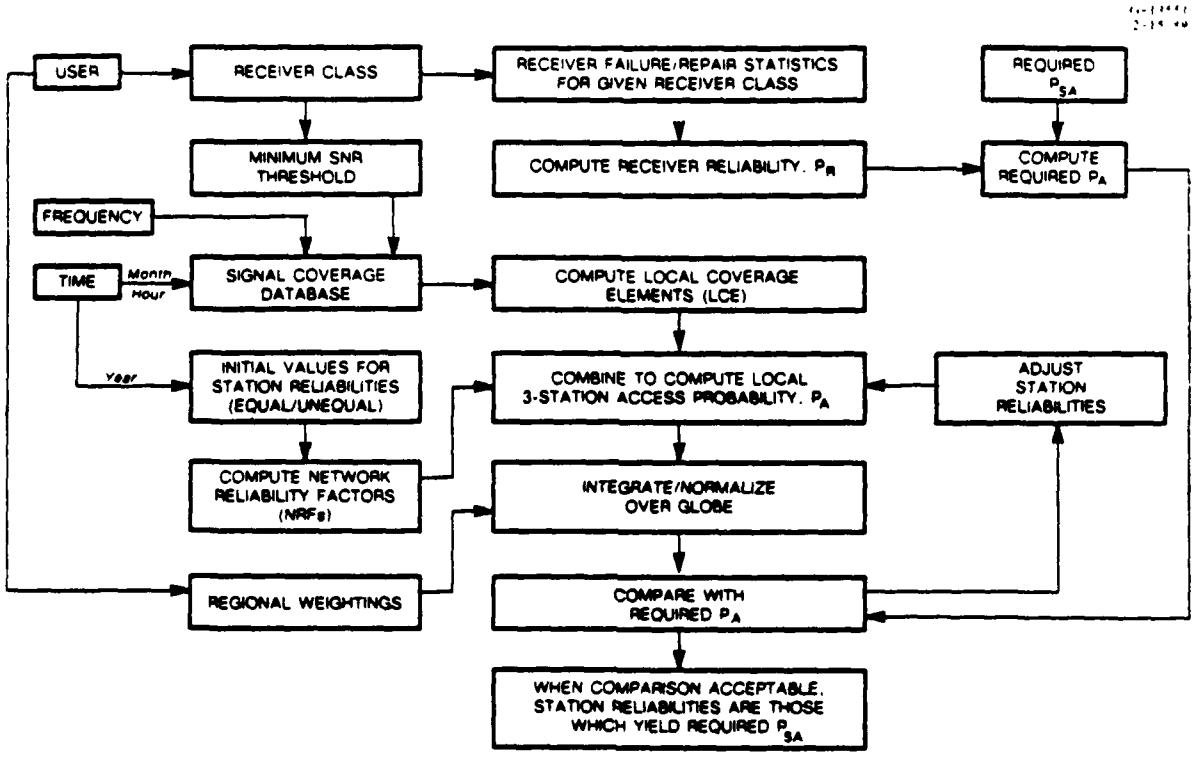

Figure 3.4-2 Computational Flow for Inverse Mode of System Availability Calculation

ONSCEN (Ref. 25). A uniform regional weighting is assumed and, unless otherwise specified, the following signal access criteria serve to define coverage:

- SNR $\geq$ -20 dB (100 Hz BW)
- Phase deviation $\leq$ 20 centicycles
- GDOP $\leq$ 1 km/centicycle*.

Table 3.4-1 lists the scheduled and unscheduled station off-air probabilities ($x10^4$) for the months in the signal coverage database (February, May, August, and November) and for years 1985-87. Inspection of the table shows that, in many cases, no unscheduled and/or scheduled off-air was reported for a particular month/year/station. According to the general rule developed in Appendix A for approximating the probability that a station is off-air at a given time during the month, the off-air probability should be zero for these cases. However, when the

*Here "centicyle" refers to 0.01 cycle of phase-difference (LOP) error, assumed the same on all paths. This hyperbolic-mode GDOP is checked only for those regions with less than 5-station coverage (in regions having $\geq$ 5-station coverage, the GDOP is assumed to be less than the threshold for at least one three or four station combination).

Table 3.4-1 Station off-air Probabilities (Unscheduled and Scheduled) $\times 10^4$ for the Months of February, May, August, and November during the Years 1985, 1986, and 1987

STATION	UNSCHED(U) OR SCHED(S)	1985				1986				1987			
		FEB	MAY	AUG	NOV	FEB	MAY	AUG	NOV	FEB	MAY	AUG	NOV
A	U	1.2	1.9*	1.6	1.9*	1.9*	1.9*	0.7	2.1	1.2	9.0	1.9*	1.9*
	S	26.9†	26.9†	697.6	26.9†	26.9†	26.9†	564.3	26.9†	26.9†	26.9†	2055.1	26.9†
B	U	29.5	16.4	6.7	13.0	250.2	8.1	49.7	8.1	23.4*	33.6	0.4	6.9
	S	2981.1	3.7†	3.7†	3.7†	4205.1	3.7†	47.7	3.7†	3184.5	3.7†	3.7†	3.7†
C	U	1.0	2.8*	0.7	1.9	2.8*	2.8*	4.7	11.3	2.8*	2.8*	11.9	1.9
	S	207.3	360.4†	360.4†	360.4†	360.4†	360.4†	360.4†	360.4†	360.4†	9999.9‡	17.2	360.4†
D	U	3.7*	3.7*	6.7	3.0	0.5	1.6	3.7*	5.1	1.5	3.7*	6.3	3.7*
	S	2.4†	2.4†	2.4†	2.4†	2.4†	2.4†	2.4†	2.4†	2.4†	2.4†	2.4†	2.4†
E	U	3.7	2.5	0.9	1.2	1.2	1.8	258.8	0.7	9.2	2.2	7.2	21.8
	S	16.3†	16.3†	282.3	16.3†	16.3†	16.3†	16.3†	16.3†	16.3†	16.3†	16.3†	16.3†
F	U	6.8*	6.3	6.9	4.6	1.5	0.9	4.7	0.5	43.2	6.8*	20.6	4.6
	S	3.0†	3.0†	3.0†	3.0†	3.0†	3.0†	3.0†	3.0†	3.0†	3.0†	3.0†	3.0†
G	U	3.5	1.2*	17.0	1.2*	1.5	1.2*	1.2*	3.0	1.2*	1.2*	1.2*	1.6
	S	6.1†	6.1†	6.1†	294.7	6.1†	6.1†	6.1†	207.9	6.1†	6.1†	6.1†	15.3
H	U	1.5	0.9	0.2	1.4	0.5	2.5	2.2*	0.5	2.2*	4.5	9.0	2.2*
	S	0.7	0.9	0.9	0.5	1.0	0.9	0.9	0.9	1.0	0.5†	0.5†	0.5†

*No unscheduled off-air for the indicated month; value shown is default based on station's average unscheduled off-air for years 1985-1988.

†No scheduled off-air for the indicated month; value shown is default based on station's average scheduled off-air (excluding annual maintenance month) for years 1985-1988.

‡No scheduled on-air for the indicated month; value shown is default adjustment.

average off-air probability is exactly zero, the probabilistic arguments developed in Appendix A become invalid as does the probabilistic interpretation of P_{SA}. In order to retain both P_{SA}'s probabilistic interpretation and its use as a system availability index, a set of *default* scheduled and unscheduled off-air probabilities is introduced. For unscheduled off-airs, default probabilities for a given station are obtained by averaging all monthly unscheduled off-air probabilities for that station over the years 1985-1988 (Ref. 25).

Default scheduled off-air probabilities are obtained in a similar way except that the averaging for each station is carried out over scheduled off-air probabilities for each month *excluding the annual maintenance month* for that station. This is done to preserve the probabilistic interpretation of P_{SA}. Whereas the annual maintenance schedule for a given month may be known 1-2 months in advance, other types of scheduled off-air may be known only 1-2 weeks in advance. Thus at the beginning of a month, it is unlikely that any scheduled off-air to be taken by a station (excluding annual maintenance) will be known so that a statistical expectation, which must be largely dependent on historical data, can be represented by the default scheduled

off-air probabilities. In one case shown in Table 3.4-1, Station C was off-air for an entire month (May, 1987). Based on arguments similar to those just given on *off-air* defaults, an on-air default adjustment of 10^{-5} is used to indicate a finite on-air probability (assuming that an entire month's off-air was not a certainty at the beginning of the month).

As explained in Section 3.4.2, the inverse mode calculations performed for these sample results assume that the station reliability figures are all equal and thus the total off-air probabilities for each station are also the same throughout the network. However the partitioning of each station's total off-air probability between scheduled and unscheduled conditions is different for each station and is obtained from historical data (years 1985-1987). Table 3.4-2 shows the ratio of unscheduled to scheduled station off-air probabilities used in the inverse mode calculations. The partitioning is given by

$$O_i^s = \frac{1 - P_T}{1 + R_i} = \text{Scheduled off-air probability for station } i = 1, 2, ..., 8$$

$$O_i^u = R_i O_i^s = \text{Unscheduled off-air probability for station } i = 1, 2, ..., 8$$

Table 3.4-2 Ratios of Unscheduled/Scheduled Station Off-Air Probabilities for Years 1985–1987

STATION	1985	1986	1987
A	0.50	2.09	1.16
B	8.24	14.06	6.95
C	0.42	14.42	0.38
D	3.42	15.89	7.12
E	0.59	3.22	0.64
F	5.53	1.42	8.23
G	12.29	4.34	0.93
H	0.37	11.89	1.53

where:

P_T = station on-air probability (same for all stations)

R_i = ratio of unscheduled/scheduled off-air probabilities for station $i = 1, 2, ..., 8$

The ratios, R_i, are given in Table 3.4-2.

For the sample results given below, the system "unavailability" ($1-P_{SA}$) is also discussed to provide another perspective in evaluating the effect of system options. Because no hard requirements exist for a minimally acceptable P_{SA} for Omega, a default value of 0.95 is used in the numerical calculations. It is important to remember that this number could be, for example, 0.98 or 0.90 depending on future requirements.

In the tables which follow, P_{SA} is carried out to five decimal places because, for a month, the last decimal place indicates, approximately, half-minutes (in time units) which is just below the threshold reporting level (1 minute) for off-airs. For the inverse mode station reliability figures, four decimal places are used because of the less accurate, iterative procedure required for their calculation.

3.4.3.1 Effect of High-GDOP Exclusions on P_{SA} — Table 3.4-3 shows the effects on system availability due to the exclusion from coverage of those regions (with < 5-station coverage) having station combinations with GDOP > 1 km/cec. The results are shown for November, 1800 UT and for three years (1985, 1986, 1987) to illustrate the consistency of the results. P_{SA} increases only 1-2% by lifting the GDOP restriction but the common station reliability figure, P_T, (inverse mode) decreases by 3-4%. P_T decreases when no GDOP criterion is invoked because signal coverage increases and thus the station reliability needed to achieve $P_{SA} = 0.95$ diminishes. In more dramatic terms, the system *unavailability* decreases by a factor of 1.48 (from about 0.040 to 0.027) as a result of lifting GDOP restrictions.

3.4.3.2 Effect of OMSTA Hawaii Off-air on P_{SA} — Table 3.4-4 shows the effects on system availability due to Omega station Hawaii* being off-air. In this case, no default adjustments for Station C reliabilities are used - the station is completely off-air during the time conditions assumed. Results are shown for 1985 during all four coverage months at 0600 UT

*Referred to as OMSTA Hawaii, Station C, or simply "C"

Table 3.4-3 Effect of High-GDOP Exclusions

INPUT SIGNAL COVERAGE DATA: 10.2 kHz/ALL STATIONS 10 kW
NOVEMBER (NOV) 1800 UT
MIN SNR THRESHOLD = -20 dB

MODE	P_{SA} CRITERION	STATION RELIABILITY FIGURES	GDOP ≤ 1 km/cec FOR 3- AND 4-STATION COMBINATIONS	NO GDOP RESTRICTIONS
DIRECT	N.A.*	NOV 1985	P_{SA} = 0.96036	P_{SA} = 0.97303
DIRECT	N.A.	NOV 1986	P_{SA} = 0.96043	P_{SA} = 0.97316
DIRECT	N.A.	NOV 1987	P_{SA} = 0.96032	P_{SA} = 0.97318
INVERSE	0.95	All Station Reliabilities Equal†	P_T = 0.9589	P_T = 0.9220
INVERSE	0.95	All Station Reliabilities Equal‡	P_T = 0.9593	P_T = 0.9231
INVERSE	0.95	All Station Reliabilities Equal§	P_T = 0.9587	P_T = 0.9215

*N.A. denotes Not Applicable
†Ratios of Unscheduled/scheduled off-air durations based on average 1985 figures
‡Ratios of Unscheduled/scheduled off-air durations based on average 1986 figures
§Ratios of Unscheduled/scheduled off-air durations based on average 1987 figures

and two UT times (0600/1800) in November. P_{SA} decreases 2-4% as a result of Station C's off-air with the maximum change (of nearly 4%) in August at 0600 UT. From a complementary viewpoint, exclusion of Station C signals increases system unavailability by a factor of 1.73 (from about 0.037 to 0.064). Interestingly, P_{SA} decreases from above 0.95 to below 0.95. Thus, for this sample case, a minimum required P_{SA} of 0.95 means that Station C cannot be permanently off-air. The same result is reflected in the P_T values which shows that even with all stations at 100% reliability, a P_{SA} of 0.95 cannot be achieved with Station C off-air. Table 3.4-4 shows that P_T must increase about 6% (0.93881 to 1) for February 0600 UT in order to maintain the same P_{SA} with station C off-air. For August 0600 UT, this required P_T increase escalates to nearly 14%. If the results for 0600 UT/1985 are representative of all UT hours and years, the results suggest that August is the least desirable month for Station C to be off-air.

3.4.3.3 Effect of Concurrent Scheduled Off-air Exclusion on P_{SA} — Table 3.4-5 shows the effect on system availability of the concurrent scheduled off-air exclusion. As for the

Table 3.4-4 Effect of OMSTA Hawaii Off-air

INPUT SIGNAL COVERAGE DATA: 10.2 kHz
MIN SNR THRESHOLD = -20 dB
GDOP ≤ km/cec FOR 3-AND 4- STATION COMBINATIONS

MODE	P_{SA} CRITERION	STATION RELIABILITY FIGURES	SIGNAL COVERAGE CONDITION	OMSTA HAWAII 10 kW	OMSTA HAWAII OFF-AIR
DIRECT	N.A*.	FEB 1985	FEB 0600UT	P_{SA} = 0.95552	P_{SA} = 0.93415
DIRECT	N.A.	MAY 1985	MAY 0600UT	P_{SA} = 0.96879	P_{SA} = 0.94121
DIRECT	N.A.	AUG 1985	AUG 0600UT	P_{SA} = 0.96801	P_{SA} = 0.92952
DIRECT	N.A.	NOV 1985	NOV 0600UT	P_{SA} = 0.96093	P_{SA} = 0.93303
DIRECT	N.A.	NOV 1985	NOV 1800UT	P_{SA} = 0.96036	P_{SA} = 0.94105
INVERSE	0.93877	All Station Reliabilities Equal†	FEB 0600UT	P_T = 0.9388	P_T = 1.0
INVERSE	0.94179	All Station Reliabilities Equal†	MAY 0600UT	P_T = 0.8920	P_T = 1.0
INVERSE	0.93681	All Station Reliabilities Equal†	AUG 0600UT	P_T = 0.8625	P_T = 1.0
INVERSE	0.93789	All Station Reliabilities Equal†	NOV 0600UT	P_T = 0.9119	P_T = 1.0
INVERSE	0.94251	All Station Reliabilities Equal†	NOV 1800UT	P_T = 0.9326	P_T = 1.0

*N.A. denotes Not Applicable
†Ratios of Unscheduled/scheduled off-air durations based on average 1985 figures

previous example, the results are given for all signal coverage months in 1985 at 0600 UT and additional November results for 1800 UT. It is expected that this exclusion will improve system availability since the probability of concurrent station off-airs is reduced. The calculations in the table show a small increase (<1%) in P_{SA} and a similarly small decrease in the unavailability because the scheduled off-airs used for the calculations are comparatively short. If several stations had relatively lengthy scheduled off-airs during a month, the improvement in P_{SA} due to the exclusion rule would be much more dramatic. The inverse mode calculations show a larger effect with decreases in P_T of almost 3% (August 0600 UT) as a result of the concurrent scheduled off-air exclusion.

3.4.3.4 Effect of 12-hour Change on P_{SA} — Table 3.4-6 shows the effect on system availability as the result of a 12-hour change (0600 UT to 1800 UT) in November. Results for

Table 3.4-5 Effect of Concurrent Scheduled Off-air Exclusion

INPUT SIGNAL COVERAGE DATA: 10.2 kHz/ALL STATIONS 10 kW
MIN SNR THRESHOLD = -20 dB
GDOP ≤ 1 km/cec FOR 3-AND 4- STATION COMBINATIONS

MODE	P_{SA} CRITERION	STATION RELIABILITY FIGURES	SIGNAL COVERAGE CONDITION	INDEPENDENT SCHEDULED OFF-AIRS	DEPENDENT SCHEDULED OFF-AIRS
DIRECT	N.A.*	FEB 1985	FEB 0600UT	P_{SA} = 0.95545	P_{SA} = 0.95552
DIRECT	N.A.	MAY 1985	MAY 0600UT	P_{SA} = 0.96878	P_{SA} = 0.96879
DIRECT	N.A.	AUG 1985	AUG 0600UT	P_{SA} = 0.96773	P_{SA} = 0.96801
DIRECT	N.A.	NOV 1985	NOV 0600UT	P_{SA} = 0.96082	P_{SA} = 0.96093
DIRECT	N.A.	NOV 1985	NOV 1800UT	P_{SA} = 0.96031	P_{SA} = 0.96036
INVERSE	0.95	All Station Reliabilities Equal	FEB 0600UT	P_T = 0.9738	P_T = 0.9714†
INVERSE	0.95	All Station Reliabilities Equal	MAY 0600UT	P_T = 0.9451	P_T = 0.9219†
INVERSE	0.95	All Station Reliabilities Equal	AUG 0600UT	P_T = 0.9406	P_T = 0.9119†
INVERSE	0.95	All Station Reliabilities Equal	NOV 0600UT	P_T = 0.9607	P_T = 0.9524†
INVERSE	0.95	All Station Reliabilities Equal	NOV 1800UT	P_T = 0.9642	P_T = 0.9589†

*N.A. denotes Not Applicable
†Ratios of Unscheduled/scheduled off-air durations based on average 1985 figures

years 1985, 1986, and 1987 are shown for comparison. P_{SA} changes over 12 hours can only be due to signal coverage and the results show the changes in P_{SA} to be small (<1%). P_{SA} values for 0600 UT are slightly higher than those for 1800 UT but the differences are too small to make any conclusive statement. System unavailability increases slightly, from 0.03843 to 0.03963 during this 12-hour period. The inverse mode calculations also show insignificant changes, with P_T changing by less than 1%. More complete information on P_{SA} changes over 12 hours can be obtained from similar calculations for February, May, and August and other 12-hour intervals (e.g., 1100 to 2300 UT which would require data from the 24-hour/4-month database).

3.4.3.5 Effect of 10 dB System Power Level Increase — In Section 3.4.3.2, P_{SA} is evaluated for a single station (Station C) off-air (power reduced to zero). In contrast, this example considers a scenario in which all stations' power is *increased* by 10 dB. The results are given in

Table 3.4-6 Effect of 12-Hour Change

INPUT SIGNAL COVERAGE DATA: 10.2 kHz/ALL STATIONS 10 kW/NOVEMBER (NOV)
MIN SNR THRESHOLD = -20 dB
GDOP ≤ 1 km/cec FOR 3-AND 4- STATION COMBINATIONS

MODE	P_{SA} CRITERION	STATION RELIABILITY FIGURES	SIGNAL COVERAGE CONDITION: 0600UT	SIGNAL COVERAGE CONDITION: 1800UT
DIRECT	N.A.*	NOV 1985	P_{SA} = 0.96093	P_{SA} = 0.96036
DIRECT	N.A.	NOV 1986	P_{SA} = 0.96140	P_{SA} = 0.96043
DIRECT	N.A.	NOV 1987	P_{SA} = 0.96238	P_{SA} = 0.96032
INVERSE	0.95	All Station Reliabilities Equal†	P_T = 0.9524	P_T = 0.9589
INVERSE	0.95	All Station Reliabilities Equal‡	P_T = 0.9533	P_T = 0.9593
INVERSE	0.95	All Station Reliabilities Equal§	P_T = 0.9522	P_T = 0.9587

*N.A. denotes Not Applicable
†Ratios of Unscheduled/scheduled off-air durations based on average 1985 figures
‡Ratios of Unscheduled/scheduled off-air durations based on average 1986 figures
§Ratios of Unscheduled/scheduled off-air durations based on average 1987 figures

Table 3.4-7 for February 0600 UT during 1985, 1986, and 1987. P_{SA} increases by 3-4% in changing from a 10 kW/station system to a 100 kW/station system. The corresponding system unavailability decreases by a factor of 4.63 (from 0.0454 to 0.0098). For the inverse mode, P_T shows substantial decreases of 23-25% with the maximum change occurring in 1987. The year-to-year changes in P_{SA} and P_T differ only because of the year-to-year differences in off-air probabilities. This scenario is completely equivalent (in terms of system availability) to one in which all stations are at a 10 kW power level but the minimum SNR threshold is -30 dB (100 Hz BW) instead of -20 dB (100 Hz BW).

3.4.3.6 Dependence of P_{SA} on the Common Station Reliability Figure — In the examples presented here, the common station reliability figure nearly always changes substantially more than does P_{SA} for the particular scenario/condition addressed. The reason for this difference in sensitivity is that P_{SA} is a relatively "flat" function of P_T for the range of parameters

Table 3.4-7 Effect of 10 dB Power Level Increase at all Stations

INPUT SIGNAL COVERAGE DATA: FEB 0600 UT/10.2 kHz
MIN SNR THRESHOLD = -20 dB
GDOP ≤ 1 km/cec FOR 3-AND 4- STATION COMBINATIONS

MODE	P_{SA} CRITERION	STATION RELIABILITY FIGURES	ALL STATION POWER LEVELS = 10 kW	ALL STATION POWER LEVELS = 100 kW
DIRECT	N.A.*	FEB 1985	P_{SA} = 0.95552	P_{SA} = 0.99034
DIRECT	N.A.	FEB 1986	P_{SA} = 0.95366	P_{SA} = 0.98997
DIRECT	N.A.	FEB 1987	P_{SA} = 0.95475	P_{SA} = 0.99018
INVERSE	0.95	All Station Reliabilities Equal†	P_T = 0.9714	P_T = 0.7165
INVERSE	0.95	All Station Reliabilities Equal‡	P_T = 0.9717	P_T = 0.7478
INVERSE	0.95	All Station Reliabilities Equal§	P_T = 0.9714	P_T = 0.7127

*N.A. denotes Not Applicable
†Ratios of Unscheduled/scheduled off-air durations based on average 1985 figures
‡Ratios of Unscheduled/scheduled off-air durations based on average 1986 figures
§Ratios of Unscheduled/scheduled off-air durations based on average 1987 figures

normally considered. Figure 3.4-1 shows a plot of P_{SA} as a function of P_T for February 0600 UT for 1985 (inverse mode). Two curves are shown: the upper one for all stations at 100 kW power level and minimum SNR of -20 dB (or, equivalently, a power level of 10 kW and a minimum SNR of -30 dB) and the lower one for all stations at 10 kW and a minimum SNR of -20 dB. From the intersections of these curves with the P_{SA} = 0.95 line, the large shift in P_T is immediately seen. In general this means that any changes in the required P_{SA} will result in large changes in the required minimum station reliabilities (P_T).

3.4.3.7 Summary of Sample Results — It should again be emphasized that P_{SA}=0.95 is used in these examples as a reference, or default, system availability requirement. The changes in system availability/unavailability under the system options considered are independent of a minimum P_{SA} threshold, but the inverse mode reliability figures and the acceptability of P_{SA} computed for a particular option are dependent on such a threshold. In summary, the sample results presented in this section indicate that:

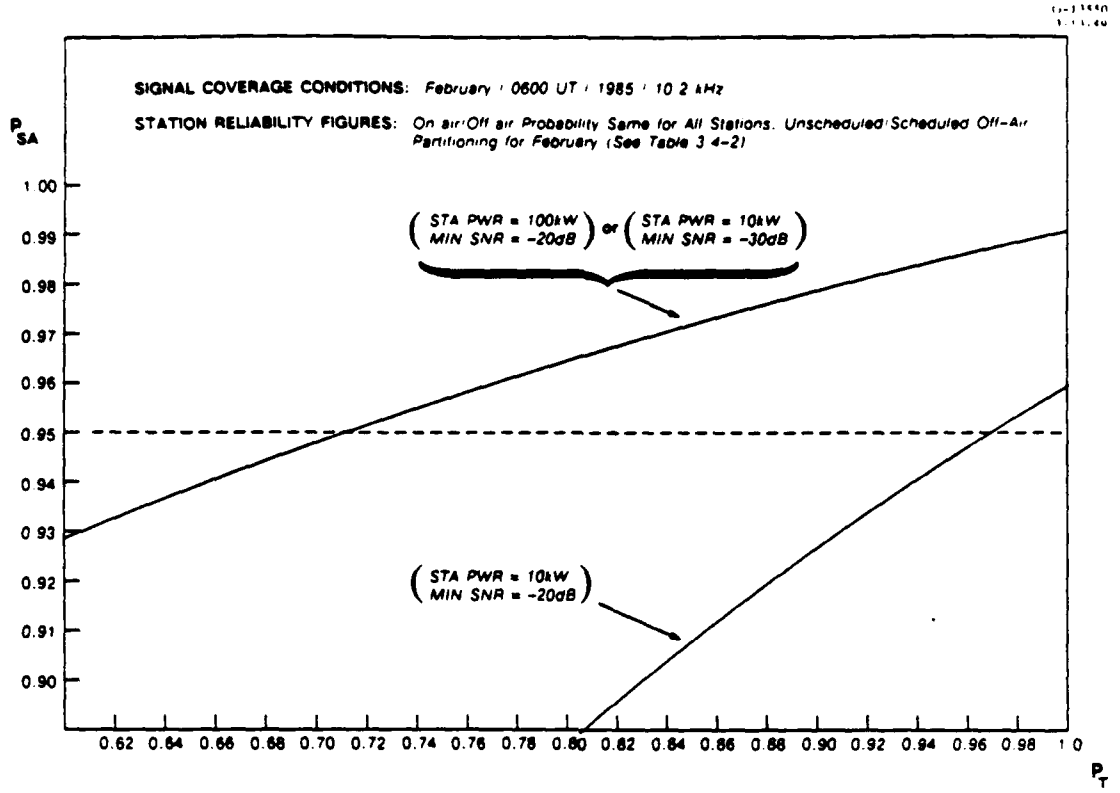

Figure 3.4-3 Illustration of Inverse Mode Calculation (P_{SA}= 0.95) showing Large Decrease in P_T when Station Power Levels are Increased by 10 dB (or, equivalently, when minimum SNR is decreased by 10 dB)

- Coverage exclusion due to geometry reduces P_{SA} by about 1% and thus is not a major consideration
- Absence of a single station from the system (due to off-air or disestablishment) has a substantial effect on system availability/unavailability; in the case of OMSTA Hawaii off-air, P_{SA} is reduced below 95% for all time conditions considered and system unavailability is increased by a factor of 1.73
- The operational practice of excluding concurrent scheduled off-airs has a small (< 1%) effect on system availability/unavailability when scheduled off-airs are few and short in duration but is expected to show a dramatic improvement in P_{SA} when lengthy scheduled off-airs at several stations occur during a month; even a relatively small number/duration of scheduled off-airs such as those occurring in 1985 have a noticeable effect (1-3%) on the minimum common station reliability, P_T
- Changes in coverage over a 12-hour period have little effect on system availability/unavailability and P_T for the month and specific 12-hour period considered; other months/periods may show larger effects
- Increasing all station power levels by 10 dB (or decreasing minimum detectable SNR by 10 dB) increases P_{SA} from about 0.95 to 0.99 and thus decreases unavailability by a factor of 4.63; the required P_T is correspondingly decreased by about 15%.

4. VLF AND OMEGA SYSTEM UTILIZATION TRADEOFFS

In this chapter, comparisons are made between the Omega Navigation System and the VLF Communications Station Network in terms of signal coverage, signal utilization by navigation receivers, and government policy issues. These comparisons are drawn to help resolve the question of whether the VLF communications stations could effectively act as an alternative to the Omega Navigation System. In this chapter, attention is focused on station NPM in Lualualei, Hawaii since it is proximate to Omega Station Hawaii, a station whose future is uncertain due to projected costly antenna repairs. In broad terms, however, many of the comparisons made for NPM can be applied to other VLF stations. Omega and VLF signal coverage are compared in Section 4.1 while Section 4.2 provides a comparison of the two systems in the areas of received signal utilization and government policy.

4.1 NAVIGATION SIGNAL COVERAGE AND THE VLF COMMUNICATIONS STATIONS

Signals from the network of VLF communications stations (Table 4.1-1) are primarily intended (by the system providers) for communications and thus "coverage" has a different meaning than for signals used purely for navigation. Information for navigation is obtained by comparing parameters of the signal waveform itself (e.g., the zero-crossing) with an external standard (or independent signal), whereas communications signal processing usually detects characteristic changes in the signal waveform itself. Thus, in VLF navigation, processes which affect the phase stability over time scales of minutes and longer are of concern; for communications, processes which influence the cycle-to-cycle coherence of the signal are given the most attention. As a result, a larger variety of physical mechanisms affect the navigational capability of signals than the communications capability. Thus, more parameters are needed to define navigational signal coverage (i.e., Omega) than communications signal coverage. The signal coverage parameters for the Omega 2-hour/4-month 10.2 kHz database, described in Chapter 3, are phase deviation (due to the presence of higher-order modes), signal-to-noise ratio (SNR), and

Table 4.1-1 The VLF Communications Station Network

STATION ID	LOCATION	LATITUDE	LONGITUDE	FREQUENCY (kHz)	POWER (kW)
GBR*	Rugby, U.K.	52° 22'N	1° 11'W	16.0	65
JXZ*	Noviken, Norway	66° 58'N	13° 53'E	16.4	−200
NDT†	Yosami, Japan	34° 58'N	137° 01'E	17.4	38
GBZ*	Anthorne, U.K.	54° 55'N	3° 16'W	19.0	80
NSS†	Annapolis, MD, U.S.	38° 59'N	76° 27'W	21.4	390
NWC†	Exmouth, Australia	21° 49'S	114° 10'E	22.3	1800
NPM†	Lualualei, HI, U.S.	21° 26'N	158° 09'W	23.4	530
NAA†	Cutler, Me, U.S.	44° 39'N	67° 17'W	24.0	1740
NLK†	Jim Creek, Washington, U.S.	48° 12'N	121° 55'W	24.8	192

*Operated by the North Atlantic Treaty Organization (NATO).

†Operated by the U.S. Navy (USN).

signal arrival geometry*. The sample results presented in Chapter 3 suggest that geometrical effects have a rather small impact on overall system availability so they are ignored in the applications described in this chapter. This leaves phase deviation and SNR as the important parameters for Omega signal coverage. Since, from the discussion above, VLF communications are affected primarily by short-time-scale (10-100 ms) phenomena (e.g., atmospheric noise), SNR and signal amplitude are the only parameters needed to determine VLF communications station signal coverage. As a result, many of the models used for VLF signal evaluation compute only SNR and signal amplitude.

The VLF communications network transmits carrier signals modulated for communication using a minimum shift keying (MSK) format. For more than 10 years, navigational receivers have been built to demodulate the MSK signal and extract the navigational information from the carrier waveform (Refs. 4,5). However, since the signals are intended for communication,

*The 24-hour/4-month/2-frequency database includes other coverage parameters such as long-path/short-path ratio and path/terminator crossing angle.

accompanying signal propagation information, such as propagation correction (PPCs) and signal deselection algorithms (Ref. 6), are not available. Because the objective here is to compare Omega and VLF *navigation* and since only SNR information is readily available as a (navigation) coverage parameter for VLF signals above 14 kHz, quantitative comparison of coverage for OMSTA Hawaii and NPM is made on the basis of SNR only. Though important for navigation, adequate information on VLF modal interference (above 14 kHz) is not readily available as discussed below. Aside from the lack of VLF modal information, the comparison between NPM and OMSTA Hawaii is greatly facilitated by the close proximity between the transmitting stations (approximately 40 km). Thus, the spatial electromagnetic characteristics (e.g., the distribution of ground conductivity levels) are the same and only the signal frequency, noise, and radiated power level differences remain.

4.1.1 Comparisons of SNR Coverage for NPM and OMSTA Hawaii

Calculations of SNR at VLF (above 14 kHz) are readily made using the computer program VLFACM developed by the Naval Research Laboratory (Ref. 7). This program computes signal amplitude based on a semi-empirical model of VLF wave propagation and calculations of VLF noise are based on the WGL-NRL noise model (Ref. 9).

For the Omega signal coverage database used in this study, calculations of SNR at Omega frequencies are obtained using full-wave models (Ref. 8) of signal amplitude and phase. The noise model is the same as that used in the VLFACM program. The calculations were performed at two frequencies (10.2 and 13.6 kHz), on selected radials from all eight Omega stations, at 96 times (24 hours x 4 months), and the results stored in a database (Ref. 10).

The comparison of SNR coverage for NPM and OMSTA Hawaii is based on the signal coverage conditions and access criteria shown in Table 4.1-2. Calculations along radial paths from each station are made at bearings spaced by 10° (beginning at geographic north). Twelve additional radial paths are used to probe special geophysical regions (e.g., Greenland) whose angular extent is less than 10° measured from the stations. Range is computed by finding the point (data was given at points spaced at about 500 km along the path) with the lowest SNR greater than the minimum SNR threshold. If the SNR is greater than the minimum SNR threshold at 19 Mm (1 Mm from the antipode) along the path, the range is set to 19 Mm to avoid antipodal and long-path effects.

Table 4.1-2 Signal Coverage Conditions and Access Criteria for SNR Coverage Comparison of NPM and OMSTA Hawaii

MONTH	HOUR (UT)	MINIMUM SNR (dB/100 Hz BW)	VLF FREQUENCY (kHz)	OMEGA FREQUENCIES (kHz)
February	0600	-20	23.4	10.2, 13.6
February	1000	-20	23.4	10.2, 13.6
February	1800	-20	23.4	10.2, 13.6
February	2200	-20	23.4	10.2, 13.6

Table 4.1-3 presents a sample range comparison between the NPM (23.4 kHz, 530 kW) signal and the OMSTA Hawaii (10.2 and 13.6 kHz, 10 kW) signal during a representative day in February at 2200 UT. The minimum SNR threshold is assumed to be -20 dB (100 Hz BW). From Table 4.1-3, it can be seen that in most cases NPM range exceeds that of OMSTA Hawaii 13.6 kHz which, in turn, is nearly always greater than that for 10.2 kHz. The greater range is partly due to propagation characteristics since the signal attenuation rates at 10.2 and 23.4 kHz are roughly the same but those at 13.6 kHz are smaller (depending on path bearing and the average path conductivity; see Ref. 11). Atmospheric noise is probably a contributing factor since the median noise at 23.4 kHz is about 5 dB lower (for the same bandwidth) than that at 13.6 kHz which is, in turn, about 5 dB lower than that for 10.2 kHz. The largest effect is certainly due to the radiated power which is 17.2 dB higher at NPM than OMSTA Hawaii.

The fractional coverage given in Table 4.1-4 is based on the maximum range at each bearing, at each of the four universal times indicated in Table 4.1-2. The UT-hours portray "day" (2200 UT which is noon at the station)* and "night" (1000 UT which is midnight at the station) coverage conditions as well as 0600 and 1800 UT which are the signal coverage times for the 2-hour/4-month database. Coverage at OMSTA Hawaii is shown at both 10.2 and 13.6 kHz to permit coverage comparison between the two Omega frequencies as well as with NPM. Table 4.1-4 compares the fractional coverage (relative to the earth's surface area) of the three signals. The first feature worth noting is that NPM covers most of the earth (94-97%) and

*Because of the long range of VLF signals, many of the signals propagate well beyond the hemisphere of illumination containing the station. However, the universal times for noon and midnight at the station(s) can still serve as a reference for coverage comparisons.

Table 4.1-3 Comparison of Range for the 23.4 kHz NPM Signal Transmitted at 530 kW and the 10.2 and 13.6 kHz OMSTA Hawaii Signal Transmitted at 10 kW Based on a Minimum SNR of -20 dB (100 Hz BW) for February 2200 UT

BEARING (DEGREES)	RANGE, NPM (MM)	RANGE, OMSTA HAWAII (MM)	
		10.2 kHz	13.6 kHz
0	17.1	17.0	19.0
5	17.4	16.0	17.0
10	15.5	12.7	17.2
20	15.0	9.5	10.3
25	14.8	9.8	10.5
27	15.0	10.6	13.4
30	16.8	13.0	17.2
40	19.0	10.5	14.5
50	19.0	15.0	19.0
60	19.0	10.4	14.3
70	19.0	13.0	18.8
80	19.0	19.0	19.0
90	19.0	19.0	19.0
100	19.0	19.0	19.0
110	19.0	19.0	19.0
120	19.0	11.0	19.0
130	19.0	11.4	19.0
140	19.0	13.0	19.0
150	19.0	14.3	19.0
152	19.0	13.5	18.5
160	19.0	13.8	18.0
163	19.0	13.2	14.5
167	18.0	12.4	12.6
170	14.2	12.2	12.4
180	14.6	13.0	13.2
185	14.9	13.1	13.2
190	14.0	12.4	12.7
200	15.0	11.6	12.1
205	19.0	12.9	16.0
207	19.0	12.9	19.0
210	19.0	11.5	17.1
220	19.0	9.0	19.0
230	19.0	7.8	19.0
240	19.0	7.2	10.0
250	19.0	6.9	9.0
260	19.0	7.0	14.5
270	19.0	7.4	9.5
280	19.0	7.7	10.8
290	19.0	12.7	19.0
300	17.2	15.2	15.2
310	16.1	10.0	14.0
320	14.4	9.8	15.5
330	15.9	11.8	14.0
332	16.0	11.8	14.0
340	13.1	11.3	13.0
343	14.4	12.5	14.5
347	16.9	19.0	19.0
350	17.1	19.0	19.0

Table 4.1-4 Comparison of SNR Coverage (Expressed as a Fraction of the Earth's Surface Area) For NPM (23.4 kHz) and OMSTA Hawaii (10.2 and 13.6 kHz) Based on a Minimum SNR Threshold of -20 dB (100 Hz BW)

MONTH/HOUR (UT)	FRACTIONAL COVERAGE		
	NPM (530 kW)	OMSTA HAWAII (10 kW)	
	23.4 kHz	10.2 kHz	13.6 kHz
FEB/0600	0.969	0.761	0.779
FEB/1000	0.968	0.849	0.901
FEB/1800	0.938	0.777	0.878
FEB/2200	0.951	0.608	0.840

changes little with hour (maximum of 3%). This is partly due to a "saturation" effect in which increasing power level adds marginally less coverage due to the large number of radials for which the signal range extends to the antipodal regional (19 Mm). Increasing the power level will not increase coverage along such "full" radials which account for 54% of the total radials shown in Table 4.1-3. Another distinguishing feature of the comparison in Table 4.1-4 is that NPM coverage is always greater than OMSTA Hawaii 13.6 Khz coverage which, in turn is always greater than OMSTA Hawaii 10.2 kHz coverage. The comparison between coverage at the Omega frequencies is consistent with the observation that 13.6 kHz signal attenuation and noise are less than those for 10.2 kHz (Ref. 11) (station power level is assumed the same at the two frequencies). The widest disparity between 10.2 and 13.6 kHz, which occurs at 2200 UT, the "daytime" case, is supported by the fact that the daytime difference in the two frequencies' attenuation rates is substantially larger than the nighttime difference (Ref. 11). Coverage at 10.2 kHz varies widely (more than 25%) across the computation hours whereas 13.6 kHz coverage varies by less then half the 10.2 kHz variation. At 0600 UT, 10.2 and 13.6 kHz coverage are nearly the same (and 20% less than NPM coverage) but at other hours the differences are much greater. The maximum Omega coverage occurs at 1000 UT ("nighttime" case) when 13.6 kHz coverage attains 90% but still nearly 7% less than the NPM coverage.

4.1.2 Modal Limitations to Coverage

In the coverage comparison of NPM and OMSTA Hawaii in Section 4.1.1, modal effects are ignored because of insufficient modal information at 23.4 kHz. However, if VLF signals are to be used for navigation in *the same way as Omega signals* (excluding network synchronization), coverage exclusions due to modal interference could offset the SNR coverage advantage of the NPM signals indicated in Table 4.1-4. Thus, before comparing VLF *navigation signal* coverage with Omega signal coverage, the extent of modal interference at VLF must be determined. A very brief survey of the available observational data and theoretical results for NPM is presented in the following two subsections.

4.1.2.1 Observations of the NPM Signal — Much of the recorded data on the NPM signal includes only a few distinct paths and thus does not provide the spatial diversity required for prediction or comparison with theory. Fixed-site observations do not lend themselves well to extracting modal information since time-dependent modal effects are often indistinguishable from those of atmospheric noise. Signals recorded on airborne platforms traversing a radial path from a station may exhibit the long-period spatial oscillations characteristic of modal interference. However, airborne signal recordings, *by necessity, mix* the space-and time-dependence of the signals. Thus, though an aircraft can fly along an entire radial path (either away from or toward the station) of reasonable length while that path is in darkness, the actual ionosphere changes with time at night. This means that recordings taken while flying outbound along a radial path at night may not be well-correlated with those taken along the inbound path on the same or following night. In spite of this space/time mixing, aircraft recordings are frequently the only way to unambiguously identify modal interference.

Table 4.1-5 lists some of the known radial path airborne observations of the NPM signal (Refs. 22, 23) and Fig. 4.1-1 shows sample signal traces from two of the recordings. These data suggest the presence of modal interference (both night and day) but insufficient information exists to interpolate/extrapolate the *spatial extent* or *degree* of the modal interference.

4.1.2.2 Theoretical Calculation of NPM Signal Parameters — Most of the published calculations of the 23.4 kHz NPM signal parameters are obtained from a version of the Segmented Waveguide (SW) program developed by Naval Ocean Systems Center (NOSC) (Ref. 12). This computer-intensive program includes routines for path segmentation, eigenvalue search/calculation, and a synthesis of the path-segment calculations using a mode conversion procedure (Ref. 13). The program is usually executed with a horizontally homogeneous

Table 4.1-5 Airborne Observations of the 23.4 kHz NPM Signal on Nighttime Radial Paths (Refs. 22 and 23)

DATE	RADIAL PATH FLIGHT	DISTANCE (Mm) ALONG PATH OVER WHICH RECORDINGS WERE MADE
2 Feb 1969	NPM to Wake Island	3.5
3 Feb 1969	Wake Island to NPM	3.5
7 Feb 1969	NPM to Ontario, CA	4.0
27 Jan 1969	NLK to NPM	4.3
29 Jan 1969	NPM to Samoa	4.1
31 Jan 1969	Samoa to NPM	4.1
11 Jan 1977	Fairbanks, AK to NPM	4.7
06 Dec 1976	NPM to NLK	4.3

ionosphere (although the ionosphere conductivity profile can be varied along the path) during the day and night portions of the path. The ground conductivity and geomagnetic field models are similar to those used in the propagation correction (PPC) model (Ref. 14).

Figure 4.1-2(a) and (b) show the frequency dependence of VLF signals along day and night radial paths. Examination of the information in the figures reveals

- Daytime signals became increasingly modal as the signal frequency increases; at the Omega frequencies the daytime signals, outside the station near-field, are usually non-modal but this is not the case projected for the NPM signals
- Nighttime signals become increasingly modal with increasing signal frequency
- There is a significant change in modal structure sensitivity to frequency between 17.124 and 21.794 kHz.

These results confirm the view that Omega modal-effects information/experience cannot be extended to the high VLF frequencies (e.g., to 23.4 kHz, radiated by the NPM station).

Extensions of these results to a wide variety of radial paths from NPM are precluded for the same reason found in connection with the observational results: lack of sufficient spatial

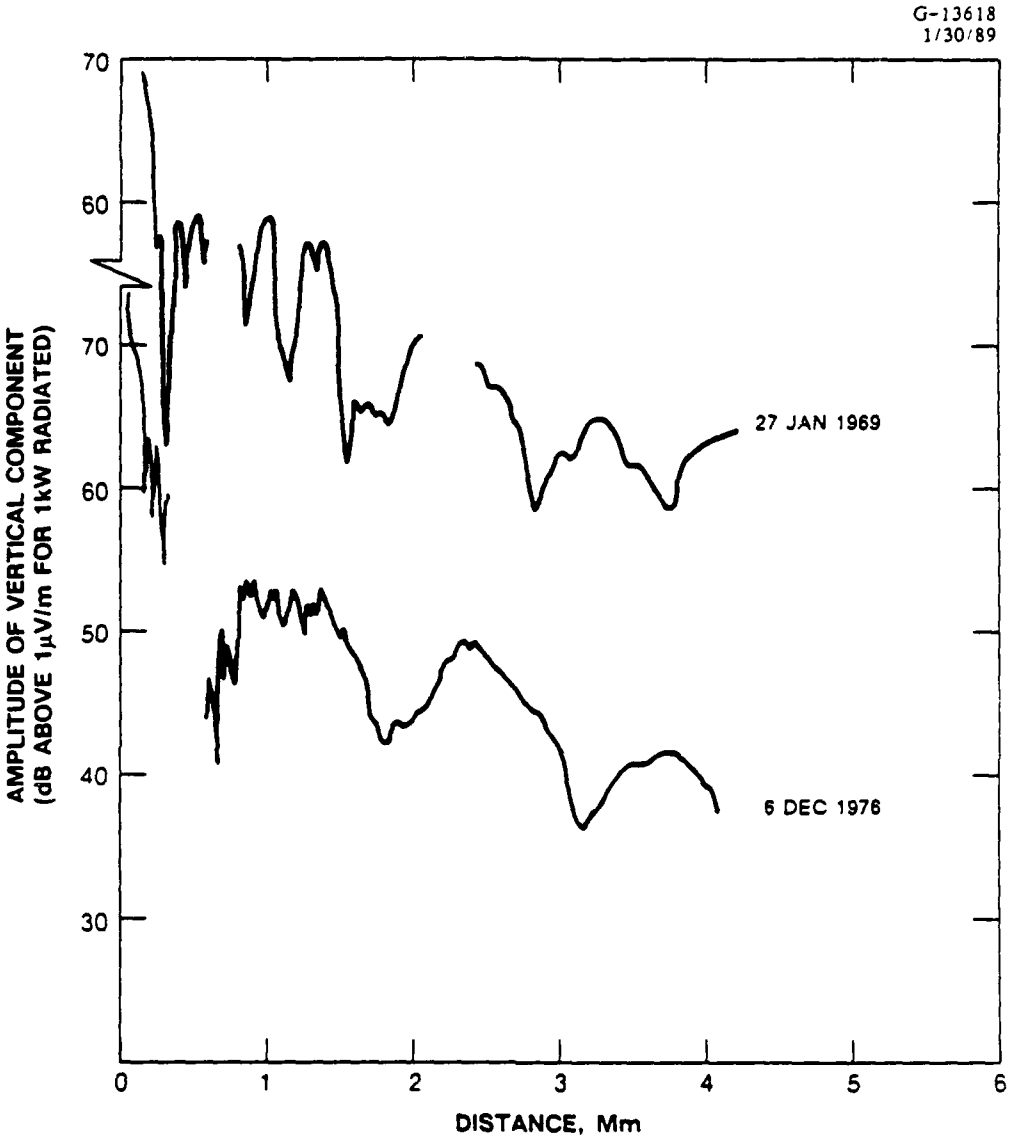

Figure 4.1-1 NPM (23.4 kHz) Signal Amplitude Measured on Flight Between NLK and NPM in 1969 and 1976 (Ref. 23)

diversity in the available path calculations. Another difficulty in specifying/identifying modal interference conditions at VLF is the reference signal. For Omega, the reference is Mode-1 phase since the PPCs used for Omega navigation are based on Mode-1 phase models. Since VLF navigation receivers do not universally employ PPC's, it is not clear what the reference signal should be or if one is needed. One possibility is to simply specify the spatial variation (from the mean) of the mode-sum signal phase over a radial/angular interval of 1-2 Mm. In any case,

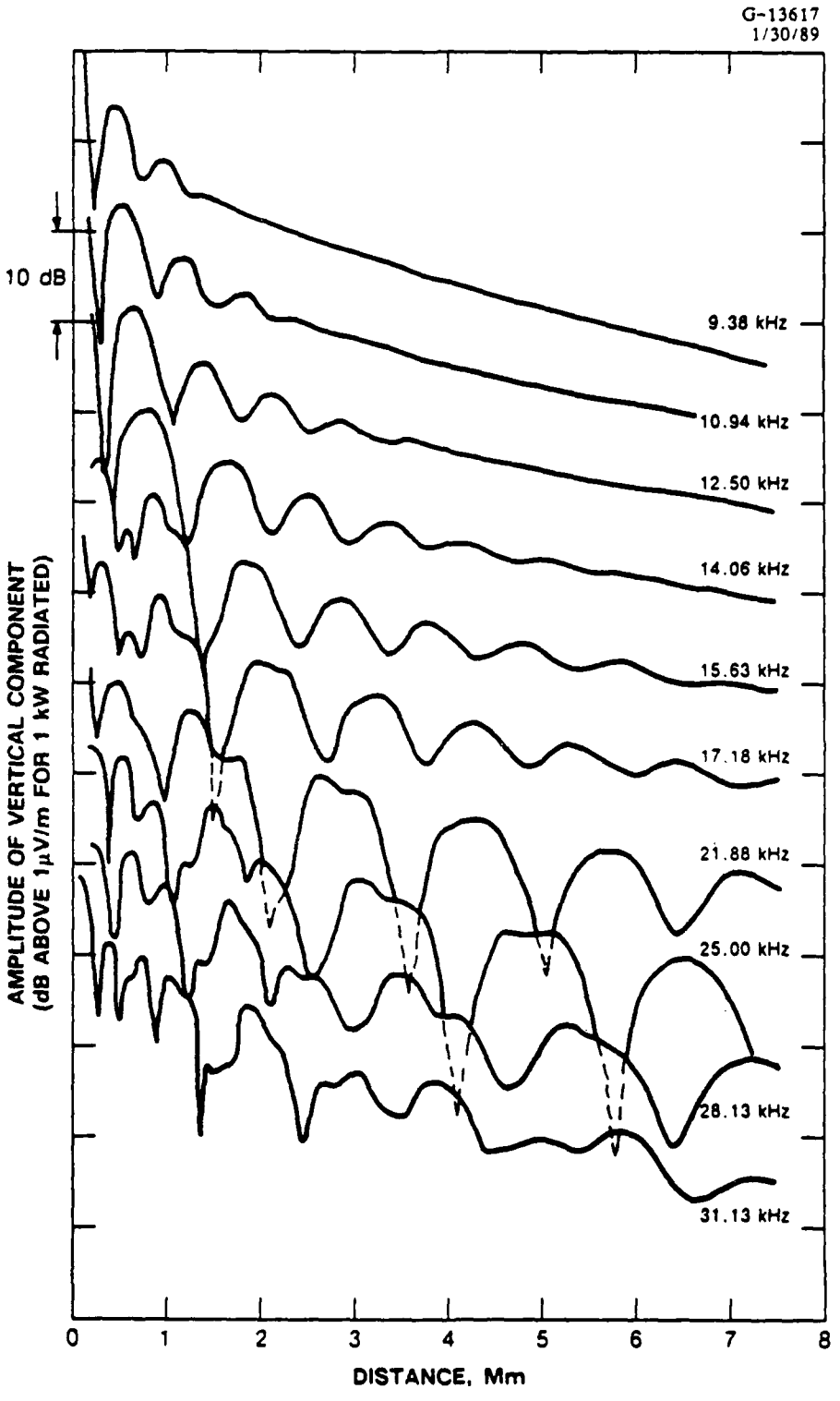

Figure 4.1-2(a) Theoretical Daytime Amplitude for Propagation from Hawaii through Southern California (Ref. 22)

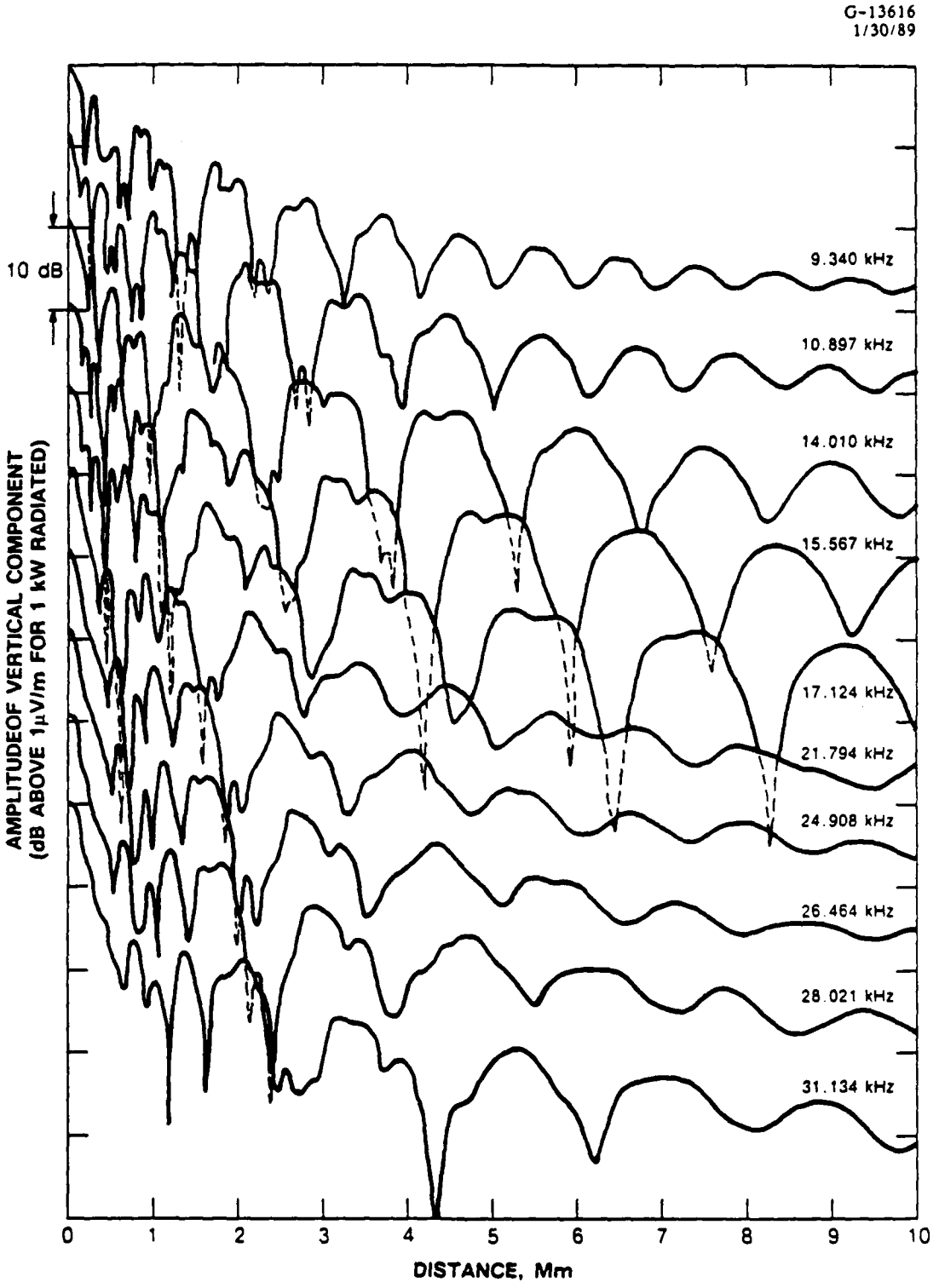

Figure 4.1-2(b) Theoretical Nighttime Amplitude for Propagation from Hawaii through Southern California (Ref. 22)

the phase deviation threshold of 20 centicycles is not likely to change much since deviations of 1/4 cycle (from an assumed phase "reference") can be shown to result in false phase changes of one or more cycles. (Ref. 24).

4.1.3 Estimates of NPM SNR/Modal Interference Coverage

Results of Section 4.1.2 suggest that VLF modal interference at frequencies above 14 kHz is pervasive but the available information is insufficient to specify the spatial extent of modal interference, both night and day. If it is *assumed* that the extent/degree of modal interference for NPM (23.4 kHz) is at least as great as that for OMSTA Hawaii (13.6 kHz), then an upper bound can be determined on NPM coverage limited by SNR and modal interference.

Although OMSTA Hawaii nominally radiates 10 kW signals, the equivalent coverage for a 530 kW station (17.2 dB above 10 kW) can be easily obtained by reducing the minimum receiver SNR threshold from -20 dB to -37.2 dB (100 Hz BW) for a 10 kW station. From this SNR coverage data (with OMSTA Hawaii at an equivalent 530 kW), the reduction in fractional coverage (ΔC) may be computed by subtracting OMSTA Hawaii (at an equivalent 530 kW) 13.6 kHz SNR coverage under the same conditions but *including* modal interference. This coverage reduction, ΔC, is then applied to the NPM SNR coverage given in Table 4.1-4 to obtain an upper-bound estimate of the NPM coverage limited by SNR and modal interference at the sample times. Table 4.1-6 shows the result of these calculations. One interesting feature of the data in the table is that with an equal station power level, 13.6 kHz SNR coverage exceeds that for 23.4 kHz (both signals radiated from stations in Hawaii) at all UT-hours except 0600 UT. This result implies that the lower 13.6 kHz signal attenuation rate dominates the 5 dB noise advantage at 23.4 kHz. The table shows the lowest estimate of coverage (0.442) to occur at 1800 UT

Table 4.1-6 Estimated Upper Bound for the Fractional Coverage Limited by SNR and Modal Interference of NPM at Four UT-Hours in February Assuming that Modal Interference at 23.4 kHz is at Least as Extensive as for 13.6 kHz

MONTH/HOUR (UT)	OMSTA HAWAII			NPM	
	COMPUTED SNR COVERAGE (530 kW:13.6 kHz)	COMPUTED SNR PLUS MODAL COVERAGE (530 kW:13.6 kHz)	ΔC	SNR COVERAGE (530 kW:23.4 kHz)	ESTIMATED UPPER BOUND ON SNR PLUS MODAL COVERAGE (530kW:23.4 kHz)
FEB/0600	0.941	0.581	0.360	0.969	0.609
FEB/1000	0.973	0.536	0.437	0.968	0.531
FEB/1800	0.973	0.496	0.477	0.938	0.461
FEB/2200	0.973	0.590	0.383	0.951	0.568

which is consistent with the fact that the sunrise terminator is just west of the station so that the nighttime westerly modal regions are excluded from coverage as well as many of the distant daytime regions to the east (due to the high daytime signal attenuation). For the opposite reason (daytime and nighttime regions reversed), the highest estimated coverage occurs 12 hours later, at 0600 UT.

4.2 COMPARISON OF OMEGA AND VLF SIGNAL UTILIZATION

Comparison of Omega station and VLF station signal coverage is hindered by a lack of signal coverage information at frequencies above 14 kHz - specifically, the spatial extent of modal interference. The missing information is that which is needed to support a *navigation* signal whereas the system provider (U.S. Navy/NATO) intends only that the VLF transmissions be used as a *communication* signal for which adequate information exists. This use of a navigational signal for communication has consequences beyond those of signal coverage discussed in Section 4.1; the implications for system subscribers and government policy are presented in this section.

4.2.1 User-Operation Issues

Omega/VLF receiver characteristics pertinent to signal coverage are presented in Appendix B. These characteristics include features of the signal processing software (e.g., station selection algorithms) in addition to hardware attributes (e.g., receiver sensitivity). One important feature of Omega/VLF receivers is the difference in the algorithms which guide the processing of Omega and VLF signals. Some of these distinctions arise from inherent differences in the two transmitting systems. For example, the stations in the VLF network are not synchronized (although the carrier signals are synthesized from precise standards) and thus no receiver acquisition of a time-frequency pattern is required as for Omega signals. This also means that signal phase from different stations cannot be compared to determine position as for other radionavigation systems such as Omega and Loran-C. Because the radiated signal field is quite stable over a period of several hours (in the absence of propagation anomalies), VLF navigation depends on an initial calibration (where known coordinates are fed to the receiver) and a "cycle count" (toward or away from the station) for each VLF station. Following initial calibration, accurate navigation requires an onboard precise frequency standard or additional VLF signal measurements to estimate the frequency/time offset of the receiver's internal clock. Another

important difference in processing signals from the two systems is that all known Omega/VLF receivers use PPCs to correct the measured Omega phase prior to use in the navigational filter whereas only one known manufacturer's receiver corrects VLF signal measurements using a simple algorithm for PPCs (Ref. 15). This means that, for most receivers, the received VLF signal phase is not accurately related to distance over the ground, a problem which is not necessarily ameliorated by redundant measurements. A related processing difference found in most receivers is the external deselection of modal signals* for Omega (based on U.S. Coast Guard-supplied modal maps) but not for VLF (due to lack of sufficient information). Failure to deselect modal signals is potentially a more serious problem for navigation than the lack of VLF PPCs since modal phase excursions can be large and sudden, often resulting in cycle slips/advances.

As a result of these system/system-support differences, receiver processing algorithms usually treat signals from the two systems differently. Once acquired (synchronized to the Omega format) and initialized, Omega-only signal processing is robust and will fail only under unusual circumstances (e.g., cycle shifts or fewer than three signals above the minimum SNR). VLF signal processing schemes generally rely on the presence of Omega signals and other aids in the receiver's navigation filter. In most receivers, VLF signals are closely monitored with frequent cross-consistency checks which, if not successful, result in signal deselection. Normally, a receiver will initialize with Omega/VLF or Omega alone, but at least two manufacturers' receivers permit initialization using VLF signals alone, although this represents a "forced mode" for one of the receiver types. While enroute, most receivers can operate, at least temporarily, in a VLF-only mode, although the receiver recognizes this to be a degraded state, similar to a "DR mode."

In summary, Omega and VLF signals are not interchangeable in terms of receiver signal processing. Because of the lack of system synchronization and signal propagation information, VLF signals are generally treated as backup support to Omega signals in the navigation filter. Although most receivers can operate temporarily in a VLF-only mode, the operation is degraded and would be unsatisfactory on a permanent basis to nearly all Omega subscribers.

*A modal signal is defined as a signal whose phase is perturbed by more than 20 centicycles from the signals Mode-1 phase due to the presence of strong higher-order modes in the signal.

4.2.2 Transportation Policy Issues

As noted in Section 4.1, one of the major problems in using the VLF station signals for navigation is that the system providers (U.S. Navy/NATO) intend only that the system be used for special naval communications. The implications of this policy for the transportation industry as well as government regulatory agencies responsible for developing civil policy are briefly explored here. NATO policy on this issue has not been studied and thus is not addressed further.

4.2.2.1 U.S. Navy Policy on the Use of VLF Station Signals for Navigation — Since 1972, the U.S. Department of Transportation has negotiated with the U.S. Department of Defense (DoD) on the use of VLF signals transmitted by the U.S. Naval Communication Stations (NAVCOMMSTAs) for navigation. The negotiations intensified as airborne use of Omega rapidly developed in the early 1970s and manufacturers became aware of the supplementary value of the VLF NAVCOMMSTA signals. At that time Omega was financed by the U.S. Navy (USN) although the system was intended for navigational use by both the civil and military sectors. The mission of the VLF NAVCOMMSTAs, however, remained focused on providing high-priority communications to submerged vessels. Thus, for reasons of national security, USN reserved the right to turn stations on and off, change frequencies and modulation rates, and schedule maintenance periods without advance public notice. These issues apparently did not overly concern military users since, presumably, many had access to advance notification messages. Civil users, of course, did not have such advance notice and although VLF signals were generally used for backup, concern was expressed for the uncertain availability of VLF signals. The concern was generally limited to the airborne navigation sector since marine navigation was dominated by TRANSIT satellite use as a result of general dissatisfaction with first-generation Omega receivers. Consequently the Federal Aviation Administration (FAA) became involved with the issue through the need to certify Omega/VLF receivers for civil air use. This set the stage for a formal request in 1975 (Ref. 16) by the FAA Administrator that the USN adopt a navigation mission for the VLF stations, specifically requesting

> "...scheduled outages, output variations, and signal format changes be kept to a minimum."

and

> "...all outage information be made available to the international NOTAM system in a timely manner."

A few months later, DoD declined the FAA request (Ref. 17) citing

> "...fundamental inconsistencies between a communication system intended for contingency communication purposes and a communication system intended for navigation purposes."

In subsequent correspondence, DoD clarified its position, acknowledging the navigational use of VLF signals but urging that VLF users be cautioned about unannounced changes in signal format, modulation, and frequency. In the late 1970's the U.S. Naval Observatory (USNO) was given the responsibility of providing information for a joint Omega/VLF Notice to Airmen (NOTAM) which included scheduled maintenance periods, planned changes in transmission frequency(ies) and emission levels, scheduled repair periods, and "after-the-fact" outages of more than 10 minutes. This information is supplied in addition to the routinely reported phase/time data on the VLF and Omega signals recorded at USNO. The advance information now carried in the Omega/VLF NOTAMs probably covers the great majority of the actual anomalous VLF station events which occur but the USN still reserves (and occasionally exercises) the right to make unannounced changes in the VLF transmitted signals.

4.2.2.2 FAA Policy on the Use of VLF Station Signals for Navigation — The USN policy on the use of VLF station signals outlined above limits the policy options of the FAA regarding the use of these signals. Use of multiple, independent navigation aids is a fundamental precept of prudent navigation. Thus, the addition of VLF signals to those of Omega* is considered advantageous to the user. The FAA, however, cannot certify for commercial use a receiver which critically depends on signals from a system which apparently does not meet some or all of the requirements for a navigation aid. The approach that the FAA has adopted is to accept Omega/VLF receivers for certification but insure that the receiver systems satisfy certification requirements using *Omega signals alone*. A recent FAA Advisory Circular (Ref. 18) states that

> "The Omega/VLF navigation system, while it may use VLF communications stations to supplement and enhance the Omega system (increase areas of coverage, improve performance, etc.), should be capable of accurate navigation using Omega signals alone."

This statement succinctly summarizes FAA policy on the use of VLF station signals for navigation and the policy is not likely to change in the immediate future.

---

*The two systems' signals are not independent since they are both affected by certain types of ionospheric phenomena, e.g., sudden ionospheric disturbances (SIDs)

5. STATION POWER LEVEL ASSIGNMENT

Chapter 3 describes the system availability model which is used to compute the system availability index (P_{SA}) and related quantities in this report. For the system options considered in this chapter, P_{SA} is used as a measure of system performance. The structure of a station power level assignment algorithm is developed below in terms of a cost function and an appropriate constraint. Estimates are also given for an upper bound on station power level reductions consistent with a minimum required P_{SA}.

5.1 OBJECTIVE

Based on early measurements of VLF transmissions and a general knowledge of signal attenuation rates, the architects of the eight-station Omega Navigation System (Ref. 19) recommended an effective radiated power of 10 kW on all frequencies from each station. The recommendation was implemented and, in retrospect was well-chosen since, in spite of occasional complaints of coverage "holes" (which may result from modal effects, independent of station power), Omega coverage is considered excellent.

Now that Omega is a mature, fully operational system with increasingly available signal coverage information and supporting data, the determination of the appropriate station power levels should be revisited. This determination is given special impetus since there is some evidence to suggest that station power levels can be reduced while maintaining an acceptable P_{SA}. Reduced station power levels mean lower electric power costs and greater component reliability, e.g., power-amplifier tube life.

The appropriate station power levels are determined as a trade-off between a desire to maximize the system performance, as measured by P_{SA}, and the need to minimize power consumption at each station. The objective here is to quantify this trade-off and describe an algorithm to compute the resulting station power levels. Since the algorithm has not been translated into computer code and the supporting databases have not been fully developed, numerical estimates are perforce based on rather extensive approximations and assumptions.

5.2 SYSTEM AVAILABILITY CONSTRAINT AND POWER LEVEL COST FUNCTION

As noted above, one part of the trade-off is to maximize system performance. This can be done by adjusting system parameters to maximize P_{SA}. For this investigation, the system parameters that can be freely varied are station power level and reliability. There is some evidence that station reliability varies with the station power level being maintained, but this correlation is ignored here and the station reliabilities are assumed to be fixed. Thus, increased P_{SA} requires increased station power levels (through increased signal coverage), a requirement which directly conflicts with the second part of the trade-off, the reduction of power consumption. In this case, it would be necessary to specify the relative importance of improving system performance and reducing power level costs through a series of weights. This difficulty can be avoided by redefining the problem to one of finding the minimum station power levels required to achieve a level of performance above some minimum acceptable threshold. This reduces the problem to defining a minimum acceptable threshold.

In Chapter 3, it is noted (as background information) that a system availability figure of 0.95 was specified for the Omega System in one of the original Navy requirements documents. Investigation into more recent Omega system availability requirements indicate that no hard requirement for Omega service has yet been enuniciated (Ref. 21). The most recent (U.S.) Federal Radionavigation Plan (FRP) (Ref. 20) mentions three measures of Omega system reliability/availability. These measures have associated numerical values which are stated as system *characteristics* (based on historical experience) and not requirements. The three system measures/characteristics cited in the FRP are:

1) Omega availability (exclusive of scheduled off-air/maintenance periods) is greater than 99% per year for each station
2) Omega availability (exclusive of scheduled off-air/maintenance periods) is greater than 95% per year for three stations,
3) Annual system availability has been greater than 97% with scheduled off-air time included.

The first item above applies only to signal transmission reliability and does not address *system* availability which embodies signal coverage, receiver reliability, etc. The second item may be interpreted (if "three stations" means "any three stations") as a statement that any combination of three station signals must be available (irrespective of the availability of the other five station signals) at least 95% of the time (exclusive of scheduled off-air/maintenance periods). Because

of the exclusion of scheduled off-air/maintenance periods, this definition is not quite equivalent to that for P_{SA} given in Chapter 3. The third item includes scheduled off-air periods but does not define system availability. Thus, no firm requirement for Omega system availability can be inferred from the FRP. As a result, an arbitrary minimum system availability threshold, P_{SAT}, will be used in discussing the power level assignment algorithm. Thus, $P_{SA} \geq P_{SAT}$ is the requirement imposed on P_{SA}. Where numerical results are needed, a default of P_{SAT}=0.95 will be used.

The above condition on P_{SA} may be interpreted as a constraint on the amount by which the power levels may be reduced at each station. Hence, the implicit assumption is made that, for the current 10 kW station power levels, P_{SA} is greater than P_{SAT}. Since the free system parameters in this problem are limited to the station power levels, P_{SA} may be written as a function of the eight station power levels. Thus the condition above may be written in vector form as

$$P_{SA}(\vec{P}) \geq P_{SAT} \; ; \; \vec{P} = (P_1, P_2, \ldots P_8) \qquad (5.2\text{-}1)$$

where P_i $(i = 1, 2, \ldots, 8)$ is the power level for station i.

To quantify the other aspect of the tradeoff, the minimization of station power level cost, the relative reductions in power among the stations need to be considered. For example, in a two-station system with power levels (P_1, P_2), a method is needed to decide which of the allocations (3 kW, 5 kW) or (4 kW, 4 kW), is "better" given that they both satisfy $P_{SA} \geq P_{SAT}$. To do this, a cost function is specified which controls the relative amounts by which the power levels are reduced at each station. The cost function is then minimized subject to the constraint given by Eq. 5.2-1.

A linear cost function may be written as

$$CF = \beta \sum_{i=1}^{8} a_i P_i \qquad (5.2\text{-}2)$$

where: $\beta = 1 / \sum_{i=1}^{8} a_i$

P_i = power level for station i

CF = System Power Level Cost Function

In this expression, β is a normalizing factor and the a_i are coefficients which determine the relative reduction of station power levels. Setting a_i=1 for all i=1,2,...8, means that the marginal

impact of reducing power at each station would be the same. However, in terms of a cost impact on the *system*, the coefficient a_i should represent the cost of providing electric power at station *i*. Moreover, these costs should be referenced to a standard cost basis (e.g., U.S. dollars).

Table 5.2-1 lists the coefficients a_i for each station. The coefficients are given in units of U.S. dollars/kW-hour and the cost function is thus referenced to a unit hour. Since the power levels P_i, $i = 1,2,...8$ are given in kilowatts, P_i would nominally vary from 0 to 10 although, in principle, it could be larger. Thus, the cost function, CF is also a number between 0 and 10.

5.3 STATION POWER LEVEL ASSIGNMENT ALGORITHM

The problem of determining "optimal" station power levels has been quantified by use of Eqs. 5.2-1,2 and can be stated as follows:

> Find the set of power levels $\{P_i\}$ i=1,2,...8, i.e., the vector $\vec{P}$, such that the cost function, CF (Eq. 5.2-2), is minimum subject to the constraint specified by Eq. 5.2-1.

As stated, the problem is equivalent to a mathematical minimization problem in eight dimensions (each dimension corresponding to a station's power level) subject to a constraint. Since

Table 5.2-1 Values of the Coefficients in the System Power Level

COEFFICIENT	STATION	VALUE (U.S. Dollars/kW-hour*)
a_1	NORWAY	0.0475
a_2	LIBERIA	0.1650
a_3	HAWAII	0.0830
a_4	NORTH DAKOTA	0.0479
a_5	LA REUNION	T.B.D.
a_6	ARGENTINA	0.0130
a_7	AUSTRALIA	0.0450
a_8	JAPAN	0.1443

*The figures include a combination of energy and demand costs transformed to a kW-hour basis. Other costs (e.g., fuel charge) computed on a kW-hour basis are also included. Miscellaneous charges, e.g., subscription or transformer fees are excluded since they are small compared to the kW-hour costs.

the cost function, CF, is linear in $\vec{P}$, it is represented by a seven-dimensional hyperplane embedded in the eight-dimensional space. The region of primary interest in this space is an eight-dimensional hypercube with each edge having values between 0 and 10 kW. Since P_{SA} is a highly non-linear function of $\vec{P}$, a given value of P_{SA} is represented by a complicated seven-dimensional hypersurface in the space. The constraint (Eq. 5.2-1) represents the eight-dimensional space between the $P_{SA} = P_{SAT}$ hypersurface and the $P_i = 10$ kW hyperplanes. However, since both CF and P_{SA} increase (decrease) with increasing (decreasing) $\vec{P}$, only the intersection of the CF hyperplane with $P_{SA} = P_{SAT}$ hypersurface needs to be considered. The problem then reduces to the following:

> Find the minimum value of CF which intersects the $P_{SA} = P_{SAT}$ hypersurface at a point $\vec{P}$ inside the hypercube.

In designing an algorithm to solve this problem, the general shape of the $P_{SA} = P_{SAT}$ hypersurface is important. Two classes of surfaces are distinguished in this type of minimization problem:

1) The $P_{SA} = P_{SAT}$ hypersurface is *convex** with respect to the origin
2) The $P_{SA} = P_{SAT}$ hypersurface is *concave*† with respect to the origin.

Figure 5.3-1 illustrates these ideas by showing a two-dimensional cut through this space. Figure 5.3-1(a) illustrates the minimization process for a convex form of the $P_{SA} = P_{SAT}$ hypersurface. Several contours are shown for $P_{SA} = \gamma$ where γ is a parameter decreasing from the upper right to the lower left. The contour corresponding to $\gamma = P_{SAT}$ represents the constraint. Overlayed on these contours are the lines representing the cost function, parameterized by CF = η where η also decreases from upper right to lower left. The lines CF = η intersect the $P_{SA} = P_{SAT}$ contour in several places but the line CF = η' corresponds to the minimum value of η for an intersection (at P_1', P_2') inside the 10 kW × 10 kW square (interestingly, there may exist values of $P_1 > 10$ kW for which CF is smaller). Note that for a slightly different (though still convex) contour or for a CF line with greater (negative) slope, it is possible to have a minimum cost function defined at two widely separated points on the boundary. It is characteristic of a

---

*Any two points inside a *convex* surface are connected by a straight line which does not cut the surface.

†Some pairs of points inside a *concave* surface are connected by straight lines which do cut the surface.

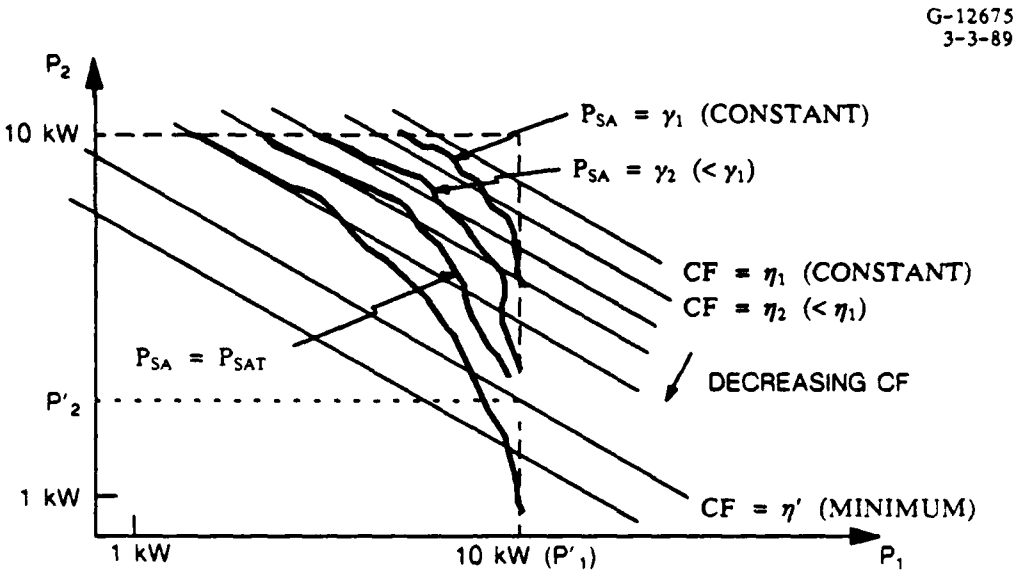

a) Convex Form of P_{SA} Contour

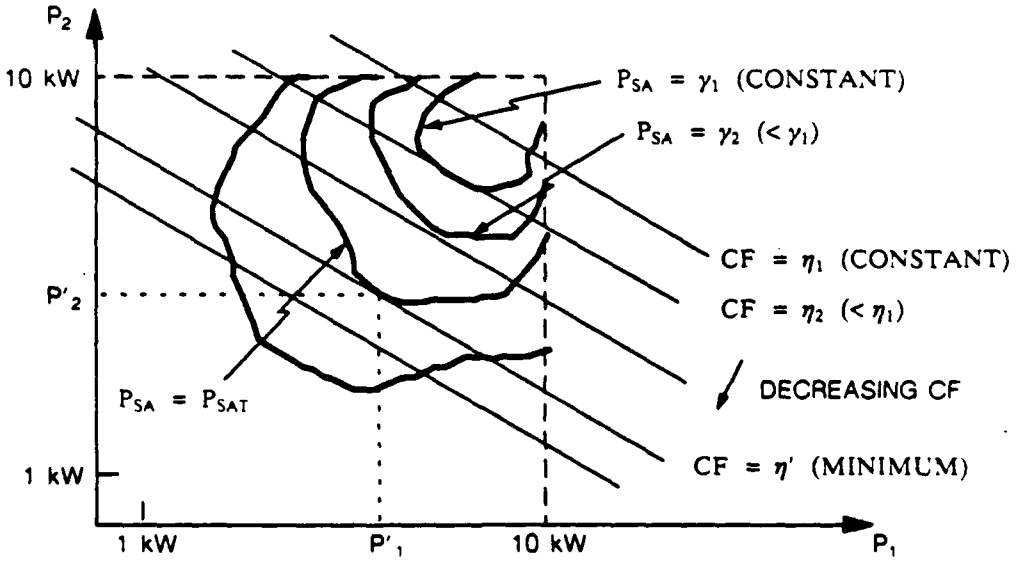

b) Concave Form of P_{SA} Contour

Figure 5.3-1 Illustration of Station Power Level Assignment Algorithm in Two Dimensions for Two Types of P_{SA} Contours Defined by $P_{SA} = P_{SAT}$

convex surface, defined within a space, to have a minimum cost function (of the kind considered here) on the boundary of the space.

Figure 5.3-1(b) illustrates the minimization process for a concave form of the $P_{SA}=P_{SAT}$ hypersurface. This figure is similar to that described above, except that the minimum occurs at a unique point (P_1', P_2' in the figure) inside the space, thus simplifying the search algorithm.

The actual dependence of P_{SA} on the power levels is very complex and the characteristics of $P_{SA} = P_{SAT}$ hypersurface are not computed in detail. Since coverage never decreases with increasing power level, the eight components of the gradient of P_{SA} are all non-negative. This *suggests* a convex surface but it is quite possible the surface could be locally concave.

As discussed above, a concave form of the $P_{SA} = P_{SAT}$ surface is likely to yield a minimum cost function at a well-defined point (power level assignment) in the "central sector" of the eight-dimensional power level space. From a system management viewpoint, this is probably a satisfying result since station power levels would be within a few kilowatts of each other and little additional action (e.g., engineering modifications) would need to be taken.

In contrast, the convex form of the $P_{SA} = P_{SAT}$ hypersurface minimizes the cost function at the boundary of the allowed space (hypercube) with possible degeneracy (multiple minima at widely separated points). This has two important implications from a system management viewpoint:

1) Power level assignments in which one or more stations have "boundary" power levels (0 or 10 kW) are likely to be "polarized", i.e., some stations at very high power and others at very low power. This may require a redesign of the station transmitter and/or other subsystems which were originally designed for efficient operation at a radiated power of 10 kW.

2) Power level assignments under conditions of degeneracy or near-degeneracy may fluctuate wildly since slight changes in station reliabilities (e.g., month-to-month) change the $P_{SA} = P_{SAT}$ hypersurface slightly which can cause the minimum point to shift from one boundary to another. Extension of the upper boundary to greater than 10 kW might mitigate the degeneracy/fluctuation problem but would require re-design of the transmitter for higher power.

Algorithms for both concave and convex forms of the $P_{SA} = P_{SAT}$ hypersurface are given in Appendix D. Once the characteristic shape of the $P_{SA} = P_{SAT}$ hypersurface is determined for the desired month/hour/frequency, the appropriate algorithm may be used to determine the

system power level assignment which minimizes the cost function but maintains P_{SA} at a fixed value given by P_{SAT}.

5.4 STATION POWER LEVEL ASSIGNMENT ESTIMATES

As described in Section 5.3, the problem of determining the "optimal" station power level assignment is quite involved, complicated by the high-dimensionality (8) of the space and the detailed dependence of P_{SA} on $\vec{P}$. Even if the $P_{SA} = P_{SAT}$ hypersurface were computed to sufficient resolution, rigorous calculations of station power level assignments are not possible until the algorithms are converted to code and the supporting databases are fully developed. Thus, any attempt to estimate the station power level assignment must invoke extreme simplifications. For the estimates considered in this section, a default value of 0.95 will be assumed for P_{SAT}.

Rather than estimate a $\vec{P}$ which minimizes CF subject to $P_{SA} = 0.95$, estimates are given for the upper and lower bounds on the power level assignments assuming equal station power levels (corresponding to a diagonal of the hypercube) and similar coverage statistics among the stations. As noted in Chapter 4, a change in station power level does not affect the occurrence of modal interference (change in power is proportionally divided into all the modes). Station power level changes also do not affect long-path interference (power level change divides proportionally into the short- and long-path), path/terminator crossing angle, or station signal arrival geometry. Thus, SNR is the only signal access parameter affected by station power level.

Taking the receiver reliability, P_R, to be 1, the system availability model described in Chapter 3 gives

$$P_{SA} = P_A$$

and, approximating P_A by the first term in Eq. 3.3-3* yields (time dependence is suppressed in the expressions which follow)

$$P_A = Q_o R_o \qquad (5.2\text{-}3)$$

where: $Q_o = < P(X_3(\theta, \phi)/B_o) >$ (weighted average over the globe)

$R_o = P(B_o)$

*Sample calculations show that the error in this approximation is normally about 7%. The error could be much larger for a lengthy station annual maintenance off-air.

Attention is focused on Q_o which is the only quantity depending on the power levels $\vec{P}$.

Assume that all stations are initially at 10 kW and that the power levels are gradually decreased equally at each station. Consider a global grid structure with nearly equal-area cells having a nominal 10° (latitude) × 10° (longitude) size. As the station power levels are equally reduced, some signals will dip below the SNR threshold and coverage at a given cell will change from, for example, five to four. These changes will affect the general expression for P_{SA} but not the approximation above, $P_{SA} = Q_o R_o$, which is affected only by those cells which are reduced from three-station coverage to two-station coverage as a result of the decrease in station power levels. Thus, for a given reduction in power levels ΔP, SNR levels in three-station coverage cells must be examined to see if any will drop below threshold as a result of the reduction ΔP. It is possible that four-station coverage cells would drop below the three-station limit if two or more signals are reduced below the SNR threshold as a result of the reduction ΔP. It can be shown that this possibility is much less probable (by a factor of about 20) than the three-station —> two-station case and can be ignored for purposes of this estimate. Higher-order changes, e.g., five-station —> two-station, are similarly ignored.

From the 24-hour/4-month 10.2 and 13.6 kHz OMSTA Hawaii database (the description of this database is given in Appendix C), the relative fraction of spatial cells with SNRs in the range (all quantities in dB)

$$-20 < \text{SNR} \leq -20 + \Delta P$$

can be calculated. Table 5.4-1 shows the results of this calculation for ΔP=5 dB and 10 dB. The relative fractions are computed for the month of February, at 2200 UT (noon at OMSTA Hawaii) and 1000 UT (midnight) for both 10.2 and 13.6 kHz. If the cells are chosen at random, the

Table 5.4-1 Fractional Coverage of Non-modal* OMSTA Hawaii Signals which Lie within Specified SNR Intervals

MONTH/HOUR/FREQUENCY	-15 dB<SNR≤-20 dB	-10 dB<SNR≤-20 dB
FEB/2200 UT/10.2 kHz	0.0586	0.1104
FEB/2200 UT/13.6 kHz	0.0500	0.1059
FEB/1000 UT/10.2 kHz	0.0541	0.0811
FEB/1000 UT/13.6 kHz	0.0293	0.0653

*Signals having phase deviations within 20 cec of Mode 1 phase and with Mode 1 dominant.

relative fractions shown in the table may be interpreted as the probability that the SNRs are within the indicated intervals. As noted in the table caption, these relative fractions include only *non-modal* signals, i.e., only those which are affected by power level changes.

Since data on SNR distributions are available only for OMSTA Hawaii, it must be assumed that *all* Omega stations have the same relative fractions/probabilities of SNRs within the indicated intervals shown in Table 5.4-1. The veracity of this assumption is not known but it is known that, in terms of overall pattern, OMSTA Hawaii coverage does not represent an "extreme," as does, for example, OMSTA Norway (minimum modal region; major blockage by Greenland) or OMSTA Liberia (maximum modal regions).

Based on these results, the quantity ΔQ_o (see Eq. 5.2-3) due to a change ΔP in *all* station power levels may now be computed as

$$\Delta Q_o = P(3)\ P(A_1 + A_2 + A_3)$$

where: $P(3) \equiv$ probability that a given cell will have exactly three-station coverage
$A_i \equiv$ event that the station i SNR will lie in the range $-20<SNR\leq -20+\Delta P$
i does not label a particular station but only one of the three-station signals accessible to the cell.

P(3) may be estimated by assuming an average station coverage fraction of 0.6* and assuming no strong correlation in coverage among any set of stations. Thus, with p=0.6,

$$P(3) = \binom{8}{3} p^3(1-p)^5 = 0.1239$$

which is in approximate agreement with results obtained from the 2-hour/4-month database (see Table C.1-1). Since the events A_i are independent but *not* mutually exclusive and $P(A_i)=P(A)$ as assumed above (all stations have the same relative SNR distribution),

$$P(A_1 + A_2 + A_3) = 3P(A) - 3(P(A))^2 + (P(A))^3$$

In general, P(A) depends not only on ΔP but also on the average SNR value over the interval.

With these results, estimates can be made of ΔQ_o from which ΔP_{SA} may be computed as

$$\Delta P_{SA} = R_o \Delta Q_o$$

*This represents a rough average over the stations and times given by the 2-hour/4-month 10.2 kHz database; compare also with the data given in Table 4.1-7 (13.6 kHz coverage).

Table 5.4-2 illustrates the results for power reductions of 5 dB and 10 dB (from 10 kW) at all stations under the same signal coverage conditions used in Table 5.4-1. The table indicates that power reductions of 5 dB (i.e., from 10 kW to 3.16 kW) at all stations reduces P_{SA} by about 1-2%. The sample results presented in Chapter 3 (for 10.2 kHz) give P_{SA} values ranging from 0.955 to 0.969 (depending on year/month/hour) under normal conditions. Combining the sample results with the (10.2 kHz) estimates given in Table 5.4-2 suggests that, with *all* stations at approximately 3 kW, P_{SA} would range above and below 0.95 (default value of P_{SAT}) depending mostly on the month and hour. Table 5.4-2 also indicates that for a 10 dB reduction in all station power levels (from 10 kW to 1 kW), P_{SA} would be reduced by about 2-3%. This estimate, together with the sample results (at 10.2 kHz) suggests that a reduction of all station power levels to 1 kW would reduce P_{SA} to the default threshold or lower under all month/hour conditions tested. It is interesting to note that Table 3.4-7 suggests that a 10 dB *increase* in all station power levels produced a 3-4% increase in P_{SA}, somewhat larger than the estimated P_{SA} change for a 10 dB power reduction.

The approximate methods developed in this section can also be used to estimate the decreases in P_{SA} due to reductions in OMSTA Hawaii power levels of 5 dB and 10 dB. The change in the GCE Q_o due to a reduction in power at a single station is

$$\Delta Q_o = P(3)\ P(A)$$

For a 5 dB Station C power reduction, the 10.2 kHz data in Table 5.4-1 (middle column) is averaged over 1000 and 2200 UT (February) to yield P(A) = 0.0564. Thus, using P(3) = 0.1239, it follows that ΔQ_o = 0.0070 and, with a typical value of 0.8524 for R_o,

$$\Delta P_{SA} = 0.0060 \quad \text{(5 dB power reduction at Station C)}$$

Table 5.4-2 Reductions in P_{SA} as a Result of Power Level Decreases (ΔP) from the Nominal 10 kW Values at all Stations

MONTH/HOUR/FREQUENCY	ΔP=5 dB	ΔP=10 dB
FEB/2200 UT/10.2 kHz	0.0175	0.0313
FEB/2200 UT/13.6 kHz	0.0151	0.0301
FEB/1000 UT/10.2 kHz	0.0162	0.0237
FEB/1000 UT/13.6 kHz	0.0090	0.0193

Similar calculations for a 10 dB Station C power reduction show that $\Delta Q_0 = 0.0119$ and

$$\Delta P_{SA} = 0.0101 \quad \text{(10 dB power reduction at Station C)}$$

When combined with the sample results (10.2 kHz) from Section 3.4, the above calculations indicate that a reduction of OMSTA Hawaii power level by 5 dB probably does not reduce P_{SA} below the default threshold of 0.95, but a reduction of 10 dB might reduce P_{SA} below the default threshold for some hour/month conditions.

Based on these estimates and the sample results from Chapter 3, the tentative conclusion is drawn that, if the goal is to maintain $P_{SA} = 0.95$ as an *average* system availability index over time (hour/month), then a power level of 3 kW at each station is perhaps acceptable. For a power level of 1 kW for all stations, however, P_{SA} is apparently less than 0.95 for most of the time and thus serves as a lower bound on the "optimal" station power level (assuming all station power levels are the same). In terms of system unavailability, a 5 dB power level decrease at all stations implies an increase in unavailability by a factor of 1.45; a 10 dB power level reduction at all stations increases unavailability by a factor of 1.75. Another tentative conclusions is that if the power level of a single station (OMSTA Hawaii) is reduced from 10 kW to 3 kW, the decrease in P_{SA} (−0.6%) is probably not enough to reduce P_{SA} below the default P_{SA} threshold of 0.95, but a power reduction to 1 kW leading to a P_{SA} decrease of about 1% is likely to reduce P_{SA} below the default threshold for some hour/month/frequency conditions. From the viewpoint of system unavailability, a 5 dB power level reduction at OMSTA Hawaii yields a factor of 1.16 increase in unavailability; a 10 dB power level reduction at OMSTA Hawaii increases unavailability by a factor of 1.27. More definitive results on the station power level assignment must await the complete development of the algorithm (including coding/testing) described in Section 5.3.

6. STATION OFF-AIR/MAINTENANCE SCHEDULING

The system availability index is again used in this chapter as a reference for comparing system options. Instead of optional station power level assignments, the focus here is on station off-air/maintenance scheduling options. Scheduled and unscheduled station off-air models are described in some detail in Chapter 3. The concern in this chapter is directed at a particular type of scheduled off-air, the annual maintenance period.

ONSCEN management policy dictates that each Omega station should perform those maintenance functions which require off-air, in addition to those repairs which can be safely postponed until the maintenance period, during a pre-scheduled time interval unique to each station. To simplify the scheduling arrangements, a month has been established for each station to schedule its necessary maintenance and/or repairs. Typically, stations are off-air for a few days (occasionally going on-air at night) during the maintenance month and rarely more than 1-2 weeks.

Figure 6-1 illustrates the current (1989) monthly schedule for each station's annual maintenance period. The origins of this schedule are somewhat obscure and individual stations have occasionally switched maintenance months since the system became operational.*

6.1 OBJECTIVE

The objective in this chapter is to develop an algorithm which can be used to determine the month/station annual maintenance schedule which maximizes system performance, as measured by the system availability index P_{SA}. Instead of minimizing a cost function, as for station power level assignment, a "performance" function is maximized. Using the notation introduced in previous chapters, the performance function may be written as

$$PF = \sum_{i=1}^{8} w_i \, \bar{P}_{SA} \, (\vec{P}_i, m_i) \qquad (6.1\text{-}1)$$

*For example, in 1985, OMSTAs Hawaii and La Reunion switched maintenance months following approval by the IOTC.

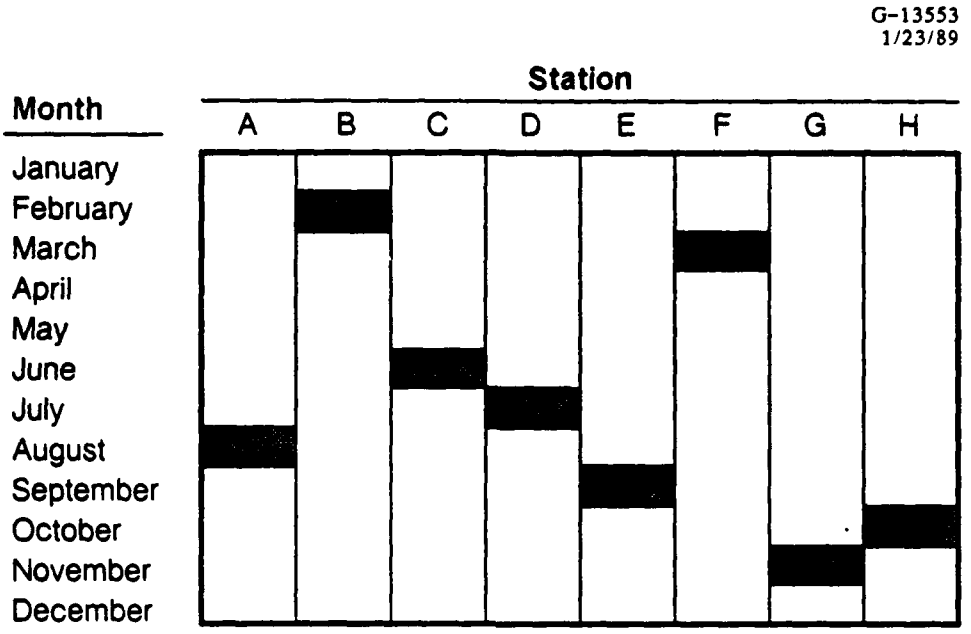

Figure 6-1 Omega Station Annual Maintenance Months

where: $\overline{P}_{SA}(\vec{P}_i, m_i)$ = P_{SA} averaged over 24 hours (or hours found in the database) for month m_i and station power level vector $\vec{P}_i$

$\vec{P}_i$ = station power level vector in which all stations are at 10 kW except station *i* which is off-air (0 kW) for annual maintenance, e.g., $\vec{P}_3$ = (10,10,0,10,10,10,10,10)

w_i = weighting function for station *i*

m_i = annual maintenance month for station *i*

With this formulation, the objective of the problem is to find the values of $m_1, m_2, ...m_8$ which maximize the performance function, PF. This problem could, in principle, be solved as currently presented; however, real, practical constraints exist on the allowable values for m_i. These constraints are not of the type introduced in Chapter 5 to help formulate the power level assignment problem. These constraints are external to the performance function defined above and are described in Section 6.2.

6.2 CONSTRAINTS ON OFF-AIR/MAINTENANCE SCHEDULING

Omega station maintenance often involves the antenna which, for 10-14 kHz signals, is a very large structure and takes one of three forms: grounded tower, insulated tower, and valley span. Maintenance on these structures requires the coordination of men and machinery under the best possible weather conditions in order that it be performed correctly and in minimum time. Thus, local weather/climatological considerations are critical in selecting a station's annual maintenance month. Additional considerations arise in some countries from long-term arrangements with maintenance contractors, budgetary timing, and cost ceilings.

The above considerations place limits on the allowable months for each station's annual maintenance. Figure 6.2-1 shows the allowable monthly intervals for annual maintenance at each station based on the above considerations. The intervals are 4-5 contiguous monthly periods. The current annual maintenance month is shown as a shaded portion of the interval.

6.3 MONTHLY INTERPOLATION OF SYSTEM AVAILABILITY/COVERAGE

One issue that must be addressed before proceeding to a monthly scheduling algorithm is that Omega signal coverage databases (both 2-hour and 24-hour) are limited to four

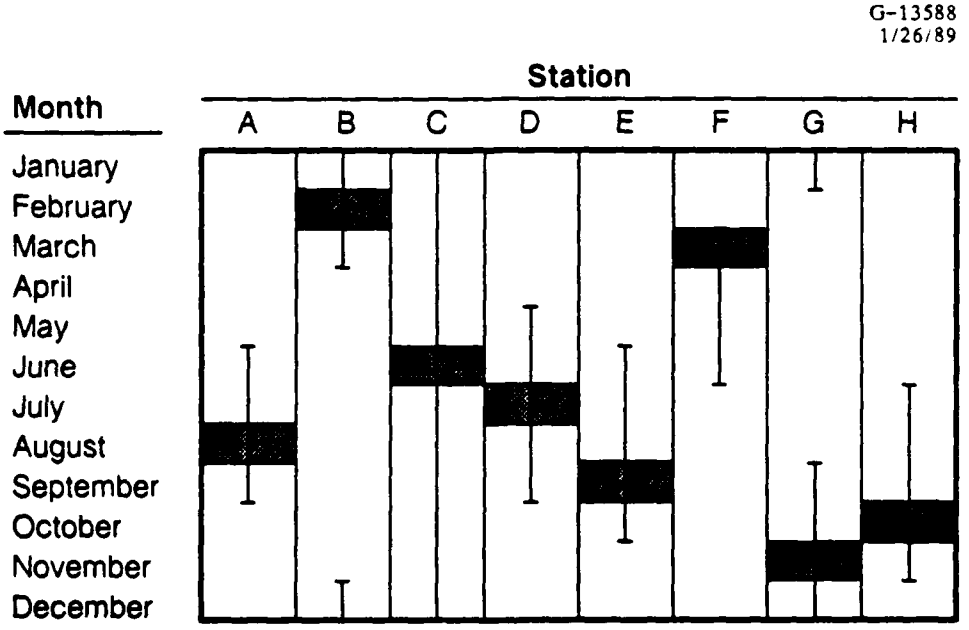

Figure 6.2-1 Allowable Monthly Intervals for Each Station's Annual Maintenance Month (Current Maintenance Month is Shaded)

months — February, May, August, and November — whereas monthly scheduling requires relative coverage/availability at each month. This problem is briefly addressed in Section 3.4 where it is mentioned that monthly changes in P_{SA} are expected to be small enough to warrant linear interpolation. The sample results seem to confirm this assumption with changes of approximately 1% between coverage months (3 months apart). It is expected that local signal quantities, such as signal amplitude and phase have a month-to-month variation depending largely on solar zenith angle. The fact that solar zenith angle has a regular periodic variation over a year suggests that local signal quantities would best be interpolated using a low-order sinusoidal function. However, global quantities like signal coverage and system availability mix solar zenith angle dependence from both northern and southern hemispheres leaving only differences due to north-south asymmetries in station distributions and geophysical properties. This suggests that, by default, linear interpolation is acceptable for globally-defined signal quantities. Thus, for example, P_{SA} for the month of March would be given in terms of P_{SA} computed from the months in the database as

$$P_{SA}\ (MAR) = (2P_{SA}\ (FEB) + P_{SA}\ (MAY))/3$$

6.4 STATION OFF-AIR/MAINTENANCE SCHEDULING ALGORITHM

The performance function, PF (Eq. 6.1-1), is a weighted sum over hour-averaged P_{SA} for eight separate months. For each month m_i, the corresponding station i is assumed to be off-air. Except for annual maintenance figures, the station reliability statistics, based on historical data (see Chapter 3), are assumed to be incorporated in the calculation of P_{SA}. For the i^{th} term in the sum, station i is assumed off-air in the calculation of P_{SA} (*no default invoked*) so the historical reliability figures for any scheduled/unscheduled off-air condition including annual maintenance for station i are not used. For other stations included in the P_{SA} calculation for the i^{th} term, only annual maintenance scheduled off-air probabilities are deleted. This is done to allow testing of m_i for months other than the current/historical maintenance month associated with station i. For this reason the weight w_i is inserted to give historical perspective to a particular station's likely off-air duration for annual maintenance. Thus, for example, if a particular station i historically has longer-than-average off-air durations for annual maintenance, w_i would be larger than for other stations because P_{SA}'s importance should be magnified for this term. This follows since the station is likely to be off-air longer than average and, hence, the corresponding P_{SA} will

be in effect for a longer time period. Signal coverage data are only used to average P_{SA} over the available hours and for monthly (m_i) interpolated coverage data excluding corresponding station *i*.

For unconstrained m_i, the number of possible station/month assignments is about 2×10^7. By constraining the m_i to intervals of 4-5 months, however, the number of possibilities is reduced to a few thousand. Appendix E describes this algorithm in further detail.

6.5 ESTIMATED OFF-AIR/MAINTENANCE SCHEDULE

Since P_{SA} calculations are not available to the extent required by the above algorithm (hour-averaged P_{SA} with single station off-airs for all station/month combinations), a much simpler approach is used for the estimate. For purposes of estimation, the individual stations are assumed to be 100% reliable so that only coverage data is used.

The basic approach is to determine the month for which a particular station's coverage is minimum. This month will be that initially proposed for annual maintenance since the penalty for its absence from coverage is minimal. Due to the environmental/monetary constraints resulting in the allowable monthly intervals for station annual maintenance shown in Fig. 6.2-1, however, the initially recommended annual maintenance month may not be allowed. Because of this strong possibility, each station's coverage is ranked from highest (1) to lowest (12) over the months and the highest-ranking month falling within the allowable monthly interval is selected. Conflicts are then resolved by comparing relative ranking among the stations, i.e., lower rankings will displace higher rankings since the penalty is greater for lowering an existing low ranking.

The 2-hour/4-month database provides individual station coverage at 10.2 kHz for 0600 UT and 1800 UT during the months of February, May, August and November. Averaging the coverage fraction for 0600 and 1800 UT for each month yields the data displayed in Table 6.5-1. The table shows that a given station's coverage varies over the four months from about 3% (of the earth's surface) for the equatorial stations to 8% for the high-latitude stations. The station-to-station coverage variation for a given month averages about 11%. OMSTA Japan shows the highest average coverage, followed by La Reunion and Australia.

A linear interpolation of the Table 6.5-1 fractional coverage data over months results in a full 12-month fractional coverage/station matrix shown in Table 6.5-2. Since it is derived

Table 6.5-1 Fractional Coverage at 10.2 kHz Averaged Over 0600 and 1800 UT for the Four Signal Coverage Months; Data Taken from the 2-hour/4/month Database

STATION	FEBRUARY	MAY	AUGUST	NOVEMBER
A	0.5635	0.4862	0.5567	0.5688
B	0.5500	0.5544	0.5238	0.5577
C	0.5511	0.5060	0.4916	0.5333
D	0.5788	0.5011	0.5137	0.5685
E	0.6017	0.6290	0.5890	0.6160
F	0.5818	0.5947	0.5928	0.5780
G	0.6367	0.5765	0.5714	0.6065
H	0.6368	0.5971	0.6052	0.6406

Table 6.5-2 Interpolated Fractional Coverage at 10.2 kHz Averaged Over 0600 and 1800 UT for all Station/Month Combinations; Data from Linear Interpolation of Four-month Coverage Values in Table 6.5-1

MONTH	STATION							
	A	B	C	D	E	F	G	H
JAN	0.5653	0.5526	0.5452	0.5754	0.6065	0.5805	0.6266	0.6381
FEB	0.5635	0.5500	0.5511	0.5788	0.6017	0.5818	0.6367	0.6368
MAR	0.5377	0.5515	0.5361	0.5529	0.6108	0.5861	0.6166	0.6236
APR	0.5120	0.5529	0.5210	0.5270	0.6199	0.5904	0.5966	0.6103
MAY	0.4862	0.5544	0.5060	0.5011	0.6290	0.5947	0.5765	0.5971
JUN	0.5097	0.5442	0.5012	0.5053	0.6157	0.5941	0.5748	0.5998
JUL	0.5332	0.5340	0.4964	0.5095	0.6023	0.5934	0.5731	0.6025
AUG	0.5567	0.5238	0.4916	0.5137	0.5890	0.5928	0.5714	0.6052
SEP	0.5607	0.5351	0.5055	0.5320	0.5980	0.5879	0.5831	0.6170
OCT	0.5648	0.5464	0.5194	0.5502	0.6070	0.5829	0.5948	0.6288
NOV	0.5688	0.5577	0.5333	0.5685	0.6160	0.5780	0.6065	0.6406
DEC	0.5670	0.5551	0.5392	0.5719	0.6112	0.5793	0.6166	0.6393

from linear interpolation, the coverage range over months (for a fixed station) and over stations (for a fixed month) are the same as for Table 6.5-1. Note also that December and January values were interpolated between November and February signal coverage data.

The entries in Fig. 6.5-1 are ranked in inverse order of fractional coverage over the 12 months for each station. For example, in the case of station A (Norway), May is ranked 1 (lowest coverage), June is ranked 2, etc. These rankings are overlayed on the allowed monthly interval chart for annual station maintenance (Fig. 6-1) to determine the best choice of annual maintenance month for each station. The rankings shown in Fig. 6.5-1 are only those necessary to cover the allowable months for each station.

For each station, the highest ranking month (lowest number) in the allowable interval is selected as the candidate maintenance month. This is done for each station in sequence, excluding Hawaii which effectively has no constraints on the allowable maintenance month. When month selection for all seven stations is complete, OMSTA Hawaii is assigned the highest ranking (lowest number) month not assigned to other stations. Fortunately, this particular situation requires no conflict resolution which means the highest-ranking (lowest-number) month in each allowable interval is ultimately selected.

The final estimated off-air/maintenance schedule is given in Table 6.5-3. Next to the month is shown the month's rank (out of 12 months). For comparison, the current schedule is

G-13589
1/26/89

Month	Station							
	A	B	C	D	E	F	G	H
January		8	11		5	3	10	10
February		6	12		3	4		9
March	5	7	9		7	6	9	7
April	3	9	7	5		8	7	5
May	1	10	5	1		12	4	1
June	2	4	3	2	9	11	3	2
July	4	2	2	3	4	10	2	3
August	6	1	1	4	1	9	1	4
September	7	3	4	6	2	7	5	6
October		5	6		6	5	6	8
November			8			1	8	12
December		11	10		8	2	9	11

Figure 6.5-1 Station Coverage Rankings (Inverse Order) Overlayed on Allowable Monthly Intervals for Stations' Annual Maintenance Months

shown together with its associated rankings. Notice that in two cases (OMSTAs Liberia and Argentina), the "best-estimate" month and the current month are the same. The cases in which the ranks are lower (numbers higher) are those in which months of highest coverage happen to occur during those months permitted for annual maintenance. The two schedules can be compared by noting that the average ranking for the best-estimate schedule is 3.75 while that for the current schedule is 5.25.

More definitive results must await the computer coding and testing of the scheduling algorithm described in Appendix E. Special considerations, such as the periodic need for a station to be off-air for 2-3 months (e.g., OMSTA Hawaii in 1987), are not included in the current structure of the algorithm and would require individual analytical treatment.

Table 6.5-3 Best Estimate of Station Off-air/Maintenance Schedule and Rank Order (out of 12 months); Also Showing Current Annual Maintenance Months (and Rank Orders)

STATION	BEST ESTIMATE MONTH	RANK	CURRENT MONTH (RANK)
A	JUNE	2	AUGUST (6)
B	FEBRUARY	6	FEBRUARY (6)
C	OCTOBER	6	JUNE (3)
D	MAY	1	JULY (3)
E	AUGUST	1	SEPTEMBER (2)
F	MARCH	6	MARCH (6)
G	SEPTEMBER	5	NOVEMBER (8)
H	JULY	3	OCTOBER (8)

7. SUMMARY, CONCLUSIONS, AND RECOMMENDATIONS

7.1 SUMMARY

This report focuses on developing a measure of Omega system performance called the system availability index, and its initial application to a variety of system options. The emphasis is placed on building models and algorithms; detailed numerical analyses of system options must await the full development of signal coverage databases and algorithm coding. The numerical results appearing in this report are of two types: (1) sample calculations using the fully developed system availability algorithm with the two-hour/four-month database and (2) approximate, "first-cut" calculations of parameters required for system alternatives/options. The principal developments and results for the system availability model and its application to system options are summarized in this section.

The system availability index/model is described in terms of four elements: Omega receiver reliability, transmitting station reliability, signal coverage, and geographic distributions of Omega users/user requirements. System availability has a system management application as a periodic index of system performance as well as a probabilistic interpretation from the viewpoint of Omega users. Suggested operational applications include an hour/frequency-averaged P_{SA} which is reported monthly together with a tabulation of those stations having reliabilities which fall below that needed to achieve a required minimum P_{SA}. Included in the system options examples is the effect on system availability of an off-air period at OMSTA Hawaii suggesting that loss of this station is likely to nearly double system *unavailability*.

Signals from the VLF Communications Station Network are compared with Omega signals in terms of signal coverage, receiver utilization, and government policy. Signal coverage comparison focuses on VLF station NPM at Lualualei, Oahu Is., Hawaii and OMSTA Hawaii at Haiku, also on Oahu Is. The coverage comparison is based mainly on SNR, since modal information on VLF signals above 14 kHz is relatively sparse. An upper-bound estimate of NPM coverage limited by SNR and modal interference is given under the assumption that modal interference is at least as extensive (both in time and space) at 23.4 kHz as at 13.6 kHz. Comparison of receiver utilization of the two types of signals indicates that VLF signals are treated with more caution than Omega signals and that use of receivers in a VLF-only mode is implicitly

discouraged in conventional receivers. Both U.S. Navy and FAA policies are reviewed regarding the use of VLF communication station signals for navigation. Both agencies agree that the VLF stations do not have a navigation mission and that the signals should be used for navigation only in a support, or backup, mode.

As an example of how the system availability model can be used to support the determination of system options, a method for assigning "optimal" station power levels is described. This assignment is based on minimizing the total cost required to maintain output power level at each station, while maintaining a minimum acceptable P_{SA} of 0.95. The structure of an algorithm to calculate this assignment is described and the practicality of the resulting assignment is found to depend on whether P_{SA} is a concave or convex function of the eight station power levels. Estimates are developed for an upper bound on the amount of power reduction per station, assuming power levels are equally reduced at each station.

As a second application of the system availability model, the scheduling of station off-air/maintenance periods is addressed. A performance function is defined in terms of P_{SA} as a function of month/station-off-air combination. This is motivated by the observation that a station's effective global coverage (measured by P_{SA}) varies with month (hour of the day held constant) due to asymmetries in global ground conductivity, etc. Thus, the system is penalized less if a station is off-air for maintenance during a month in which P_{SA} is low with that station off-air than if the maintenance is done during a month in which P_{SA} is high with that station off-air. The permitted months for maintenance (requiring off-air) at each station due to environmental/economic conditions are used as constraints on the scheduling problem. An estimated off-air/maintenance schedule is developed based on signal coverage interpolated monthly from the 2-hour/4-month database and constrained by the environmental/economic conditions at each station.

7.2 CONCLUSIONS

The system availability index is a comprehensive and accurate measure of Omega system performance which is superior to those indicators (e.g., station reliability) which measure only one aspect of system performance. Not only does this indicator reflect total system performance, but it is also properly sensitive to changes in Omega station reliability and signal coverage. By design, the index also incorporates Omega receiver reliability and geographic

priorities of various types of users, although their effects on P_{SA} are not demonstrated in detail in this report. No firm requirement for a minimally acceptable system availability threshold (P_{SAT}) for Omega is currently known to exist, although a default value of 0.95 is frequently used for numerical computations. Given an assumed minimum level for P_{SA}, this procedure can be inverted to find minimally acceptable station reliability figures to serve as operational guidelines. The time interval found to be appropriate for the calculation of P_{SA} is the month, which is long compared to the average off-air period but shorter than the seasonal variation in coverage or the upgrade cycle in the production of Omega receivers. The month is also the period during which each station conducts annual maintenance, an activity which dominates the station reliability figures. A recommended operational use of the index is to compute P_{SA} for the immediate past month for all 24 hours, at both 10.2 and 13.6 kHz, for a minimum SNR of -20 dB (100 Hz noise bandwidth), and for a uniform distribution of users. Of these computations, only the minimum, maximum, and average P_{SA} over 24 hours at both 10.2 and 13.6 kHz is recommended for periodic system evaluation. It is also recommended that the index be computed for a minimum SNR threshold value corresponding to the "lowest" (least sophisticated) receiver class which, if maintained above P_{SAT}, guarantees that P_{SA} for all other receiver classes will exceed P_{SAT}. Sample calculations using the 2-hour/4-month 10.2 kHz database indicate the following system behavior:

- Exclusion of regions with poor geometry reduces P_{SA} by about 1%
- Absence of OMSTA Hawaii signals reduces P_{SA} below 0.95 and increases system unavailability by a factor of 1.73 (from about 0.037 to 0.064) for all month/hour conditions tested
- Exclusion of concurrent scheduled off-airs does not show large improvement in P_{SA} (but decreases required minimum station reliability (P_T) by 1-3%) because scheduled off-airs for the sample calculation (1985) were relatively short; however, the practice is expected to lead to dramatic improvements in P_{SA} when several stations require lengthy scheduled off-airs
- Power level increases of 10 dB at all stations increase P_{SA} by 3-4% or, equivalently, decrease system unavailability by a factor of 4.63; for P_{SA} = 0.95, the minimum station reliability, P_T, is reduced by about 15%
- An increase of 10 dB in receiver sensitivity (in the presence of noise) has the same effect as a similar power level increase.

Signals from the VLF Communications Station Network are a useful supplement to Omega signal processing in most conventional airborne Omega receivers. Because they are

intended for communications, however, these signals do not have the same supporting information base as Omega. Hence, only rudimentary propagation corrections are available and information on modal behavior exists on relatively few paths. Based on the assumption that modal effects on the 23.4 kHz signal from Lualualei, Hawaii (NPM) are at least as extensive as those found on OMSTA Hawaii signals, estimates of 44-64% coverage for the month of February are projected for NPM. Examination of the limited observational data and theoretical results for this station site/frequency suggests that modal effects may be even more extensive than at Omega frequencies. In terms of their use in most Omega/VLF receivers, VLF signals (>14 kHz) serve a *supporting* role to Omega signals in the receiver's navigation filter. The written record of the U.S. Navy and Federal Aviation Administration correspondence on the use of VLF signals for navigation over the last 15 years indicates a consistent policy of retaining a protected communications role for these stations and providing only routine and "after-the-fact" information on station maintenance periods, outages, frequency changes, etc.

Applications of the system availability model to two plausible options for system improvement — re-assignment of station power levels to reduce system cost and rescheduling of station annual maintenance off-air months to improve system performance — demonstrate the utility of using the system availability index as a yardstick for system performance. With the system availability formulation, algorithms can be readily devised to support such system-level inquiries. A "quick-look" assessment of the station power level assignment problem indicates that a power level reduction of 5 dB at each station increases system *unavailability* by a factor of 1.45 but may be acceptable if the goal is to ensure that the *average* P_{SA} (over 24 hours) exceeds 0.95. Initial analysis indicates that a 10 dB reduction in power at each station increases system unavailability by a factor of 1.75 and would be unacceptable unless the minimum acceptable P_{SA} is lowered by a few percent. Estimates for a *single* station (OMSTA Hawaii) suggest that a power level reduction of 5 dB increases system unavailability by a factor of about 1.16, though maintaining P_{SA} above the default lower threshold of 0.95; similarly, a power level reduction of 10 dB increases system unavailability by a factor of about 1.27 and yields a P_{SA} which ranges above and below the default threshold of 0.95 depending on the hour/month condition. An initial analysis of the station off-air/maintenance scheduling problem (using coverage data alone) suggests an alternative schedule which (in terms of rankings) could yield a 30% improvement over the current schedule. Scheduling of extraordinary station maintenance or repair needs (such as those requiring more than 30 days off-air) are outside the scope of the recommended algorithm and require a specifically tailored methodology.

7.3 RECOMMENDATIONS

The system availability model satisfies one of the principal goals of this effort: to develop a measure of system performance which can be applied to answer questions about system alternatives, e.g., the impact of station off-airs. The system availability model provides a means of system assessment and the algorithms formulated herein demonstrate how this model can be applied to assist tradeoff studies in station disestablishment, power level reduction, and off-air/maintenance scheduling. It is recommended that these algorithms be further refined, translated into designed software (computer code), and tested to produce operational tools. It is further recommended that the 24-hour/4-month/2-frequency database be expanded to include signal coverage parameters for *all* Omega stations to supply the algorithms with critical input data. The operational algorithms can then be used to refine/modify the numerical results presented in this report regarding important system options. Moreover, these tools should be integrated into a signal coverage display package for the 24-hour/4-month/2-frequency database to provide the system evaluator with a visual understanding of the tradeoffs and alternatives involved in calculations of system availability parameters.

The system availability model, as presented in this report, is structured as a probabilistic model to account for the randomness inherent in station off-air occurrences/durations. The radiated signals and noise are assumed deterministic as a first approximation. The statistical distribution of VLF atmospheric noise amplitudes is known to be fairly wide (standard deviation of 2-4 dB) as is the uncertainty in specifying the phase of higher-mode signals. The random variation of these quantities is expected to have a substantial impact on the probabilistically-defined P_{SA}. It is therefore recommended that the system availability model be extended to embrace the statistical characteristics of signal amplitude, phase, and atmospheric noise in the Omega/VLF band. This, together with other known statistically-distributed parameters, will provide a consistent, comprehensive, probabilistic model of system availability.

VLF signals above 14 kHz, radiated by the U.S. Navy and NATO communication stations, have been used, together with Omega signals, as an aid to navigation on aircraft since the early 1970s. Evaluation of this signal resource as an alternative to Omega navigation is hampered by a lack of information on the spatial extent of the multi-modal behavior of these signals. If FAA policy refinements emerging from the current requirements definition study articulate a more critical role for VLF signals in aircraft navigation, it is recommended that semi-empirical calculations of SNR (using the VLFACM program) and full-wave calculations be carried out

systematically on 35-50 radial paths, of length 19 Mm, from each of the nine VLF stations to properly evaluate these signals as a primary navigational source. This information can then be used as a basis for determining the signal coverage, limited by SNR and modal interference, of the VLF signals. The signal coverage predictions should then be validated with observational data and integrated into the database supporting Omega system availability calculations.

As discussed in Appendix B, little consistent information is available on the threshold SNR/phase-tracking capabilities of modern Omega receiving systems. This information is important since it is used to formulate a signal access criterion applied to determine signal coverage. It is recommended that a cross section of conventional receiver systems (including airborne, marine, and special sensors) be tested in a common testbed facility (equipped with an Omega simulator) to determine minimum SNR/phase-tracking thresholds.

APPENDIX A

ANALYTICAL DEVELOPMENT OF THE SYSTEM AVAILABILITY MODEL

A.1 DEVELOPMENT OF THE SYSTEM AVAILABILITY INDEX

A.1.1 Derivation of Expression for P_{SA}

The system availability index, P_{SA}, is the probability that, for any location on the earth at any time/time interval, an Omega user's receiver will be properly functioning and three or more Omega signals can be effectively used for navigation. Expressed analytically, P_{SA} is given very generally as

$$P_{SA} \equiv \frac{1}{N} \sum_{i=1}^{n_c} n_i P_{R_i} P_{A_i} \qquad \text{(A.1-1)}$$

where $P_{R_i} \equiv$ probability that a receiver of class i is functioning normally and being operated correctly; also termed "receiver reliability"

$P_{A_i} \equiv$ probability that three or more usable signals are accessible by a receiver of class i at any point on the earth's surface at any time/time interval

$n_i \equiv$ number of receivers of class i currently in operation

$N \equiv \sum_{i=1}^{n_c} n_i$ = total number of receivers in the classes assumed

$n_c \equiv$ number of receiver classes assumed.

Using a uniform failure interval and repair time model, it can be shown that the reliability for a receiver of class i is

$$P_{R_i} = 1 - \frac{MTTR_i}{MTBF_i}$$

where $MTTR_i$ = mean time to repair figure for receivers of class i

$MTBF_i$ = mean time between failure figure for receivers of class i

Since only very rough approximations to n_i are known (see Ref. 26 for related information), P_{SA} for a single receiver class (i.e., $n_c = 1$) will generally be considered.

Let X_3 be the event that three or more usable signals are available at a given point in time and space, i.e.,

$X_3(\theta, \phi, t) \equiv$ event that three or more usable signals are accessible to a point (θ, ϕ) on the earth's surface at time t

Event X_3 depends on

- Signal coverage
- Transmitting station reliability.

A signal's coverage is not only a function of space and time but also depends on the signal access *criteria* which define the usability of a signal. Thus, $P(X_3)$, the probability measure on event X_3, depends on receiver class i through the signal coverage/access criteria which, in general, change with different i.

P_A is just the weighted average of $P(X_3(\theta, \phi, t))$ over time and space, i.e.,

$$P_A = \frac{1}{N_w T} \int_{t_1}^{t_2} \int_0^{2\pi} \int_0^{\pi} P(X_3(\theta, \phi, t)) w(\theta, \phi) R_E^2 \sin\phi \; d\theta \; d\phi \; dt$$

where $$N_w = \int_0^{2\pi} \int_0^{\pi} w(\theta, \phi) R_E^2 \sin\theta \; d\theta \; d\phi$$

$T = t_2 - t_1$

$w(\theta, \phi)$ = weight assigned to location (θ, ϕ) based on user's geographic priority

R_E = radius of earth

(θ, ϕ) = conventional angular spherical coordinates.

If time is partitioned into two dimensions (e.g., hour and day), then the integration will usually be carried out over day with hour fixed. In this case, T – 30 days, since longer time intervals would involve signal coverage changes.

$X_3(\theta, \phi, t)$ depends on which stations are on-air, in addition to the signal coverage dependence on space and time. Using the notation of Chapter 3, i.e.,

$T_i \equiv$ event that station i is on-air (i=1,2,...8)

$\overline{T}_i \equiv$ event that station i is off-air (i=1,2,...8)

$B_{ijk...} \equiv$ event that only stations i,j,k,... are concurrently off-air; i,j,k,... = 1,2,...8 and all indices distinct.

The universe (all possible events) can then be formed as

$$U = B_o + \sum_{i=1}^{8} B_i + \sum_{i=1}^{8} \sum_{j=i+1}^{8} B_{ij} + ... + \sum_{i=1}^{8} \sum_{j=i+1}^{8} \sum_{k=j+1}^{8} \sum_{l=k+1}^{8} \sum_{m=l+1}^{8} B_{ijklm} + ... + B_{12345678}$$

Notice that the sums are over the possible *combinations* of indices, not permutations, since the $B_{ijk...}$ are symmetric under all possible interchanges of indices (i.e., it only matters *which* stations are off-air, not the order). This particular decomposition of the universe is used because the events $B_{ijk...}$ are *mutually exclusive*. Now, by definition of the universe* (in the following, the θ, ϕ, t dependence of X_3 is suppressed)

$$X_3 \, U = X_3$$

and

$$X_3 \, B_{i_1 i_2 ... i_m} = 0$$

for m>5 since three or more signals cannot be available if more than five stations are concurrently off-air. Thus,

$$P(X_3) = P(X_3 \, U)$$

$$= P(X_3 \, B_o + \sum_{i=1}^{8} X_3 \, B_i + ... + \sum_{i=1}^{8} \sum_{j=i+1}^{8} \sum_{k=j+1}^{8} \sum_{l=k+1}^{8} \sum_{m=l+1}^{8} X_3 \, B_{ijklm})$$

$$= P(X_3 \, B_o) + \sum_{i=1}^{8} P(X_3 \, B_i) + ... + \sum_{i=1}^{8} \sum_{j=i+1}^{8} \sum_{k=j+1}^{8} \sum_{l=k+1}^{8} \sum_{m=l+1}^{8} P(X_3 \, B_{ijklm})$$

*In operations with events, product implies set intersection and sum implies set union. Thus, in set theory, the universe is equivalent to the identity operator.

where the last step follows because the $B_{ijk...}$ are all mutually exclusive.* Writing each of the above terms in terms of conditional probabilities, i.e.,

$$P(X_3\ B_{ijk...}) = P(X_3/B_{ijk...})\ P(B_{ijk...})$$

yields

$$P(X_3) = P(X_3/B_o)\ P(B_o) + \sum_{i=1}^{8} P(X_3/B_i)\ P(B_i) + \sum_{i=1}^{8}\sum_{j=i+1}^{8} P(X_3/B_{ij})\ P(B_{ij})$$

$$+ \ ... + \sum_{i=1}^{8}\sum_{j=i+1}^{8}\sum_{k=j+1}^{8}\sum_{l=k+1}^{8}\sum_{m=l+1}^{8} P(X_3/B_{ijklm})\ P(B_{ijklm}) \ . \qquad \text{(A.1-2)}$$

Since $X_3 = X_3(\theta, \phi, t)$, Eq. A.1-2 expresses a *local* definition (in space and time) of P_A. Thus, the factor

$$P(X_3(\theta, \phi, t)/B_{ijk...})$$

is a local coverage element (LCE). The second factor in each term in Eq. A.1-2, i.e.,

$$P(B_{ijk...})$$

is assumed approximately independent of time (up to a period of one month; see Section A.2) and is called the network reliability factor (NRF). Space and time integration of Eq. A.1-1 gives a relation of the same form but written as

$$P_A = Q_o\ R_o + \sum_{i=1}^{8} Q_i\ R_i + ... + \sum_{i=1}^{8}\sum_{j=i+1}^{8}\sum_{k=j+1}^{8}\sum_{l=k+1}^{8}\sum_{m=l+1}^{8} Q_{ijklm}\ R_{ijklm}$$

where

$$Q_{ijk...} = \frac{1}{N_W T} \int_{t_1}^{t_2} \int_0^{2\pi} \int_0^{\pi} P(X_3(\theta, \phi, t)/B_{ijk...})\ w(\theta, \phi)\ R_E^2 \sin\theta\ d\theta\ d\phi\ dt$$

*Events produced by intersections of one or more events with a set of mutually exclusive events are also mutually exclusive.

are called the global coverage elements (GCEs) and

$$R_{ijk...} = P(B_{ijk...})$$

are the NRFs.

P_{SA} is then given by Eq. A.1-1 in which the dependence on receiver class *i* is reflected through the GCEs.

A.1.2 Derivation of Expressions for the NRFs

The scheduled and unscheduled off-air probabilities are defined by

$$\bar{T}_i \equiv \bar{T}_i^u + \bar{T}_i^s \qquad i = 1,2,....8$$

where

$\bar{T}_i^u \equiv$ unscheduled off-air event for the i^{th} station

$\bar{T}_i^s \equiv$ scheduled off-air event for the i^{th} station

and, by definition,

$$\bar{T}_i^u \, \bar{T}_i^s = 0 \qquad i = 1,2,....8 \; . \qquad \text{(A.1-3a)}$$

Omega Navigation System operational doctrine bars the occurrence of concurrent scheduled off-airs at two or more stations. Thus

$$\bar{T}_i^s \, \bar{T}_j^s = 0 \qquad i,j = 1,2,....8 \qquad i \neq j \; . \qquad \text{(A.1-3b)}$$

Finally, the independence of an unscheduled off-air event at a given station from unscheduled/ scheduled off-air events at other stations is expressed as

$$P(\bar{T}_i^u \, \bar{T}_j^u) = P(\bar{T}_i^u) \, P(\bar{T}_j^u) \qquad i,j = 1,2,...8 \; , \; i \neq j \qquad \text{(A.1-4a)}$$

$$P(\bar{T}_i^u \, \bar{T}_j^s) = P(\bar{T}_i^u) \, P(\bar{T}_j^s) \qquad i,j = 1,2,...8 \; , \; i \neq j \qquad \text{(A.1-4b)}$$

Before proceeding, it is necessary to establish the independence of unscheduled off-air events at a given station from on-air events at other stations, a property which can be derived from

Eqs. A.1-4a and A.1-4b. An indirect approach is employed which is used several times in this Appendix. The procedure begins by expanding $P(\bar{T}_i^u)$ and recalling U ≡ universe is equivalent to the identity operator. Thus

$$P(\bar{T}_i^u) = P(\bar{T}_i^u U) = P(\bar{T}_i^u(T_j + \bar{T}_j)) = P(\bar{T}_i^u T_j + \bar{T}_i^u \bar{T}_j)$$
$$= P(\bar{T}_i^u T_j) + P(\bar{T}_i^u \bar{T}_j)$$

where the last step follows because events $\bar{T}_i^u T_j$ and $\bar{T}_i^u \bar{T}_j$ are mutually exclusive.* Rearranging the above relation gives

$$P(\bar{T}_i^u T_j) = P(\bar{T}_i^u) - P(\bar{T}_i^u \bar{T}_j)$$
$$= P(\bar{T}_i^u) - P(\bar{T}_i^u(\bar{T}_j^u + \bar{T}_j^s))$$
$$= P(\bar{T}_i^u) - P(\bar{T}_i^u \bar{T}_j^u + \bar{T}_i^u \bar{T}_j^s)$$
$$= P(\bar{T}_i^u) - P(\bar{T}_i^u \bar{T}_j^u) - P(\bar{T}_i^u \bar{T}_j^s)$$

where the last step follows because events $\bar{T}_i^u \bar{T}_j^u$ and $\bar{T}_i^u \bar{T}_j^s$ are mutually exclusive.* Now applying Eqs. A.1-4a and A.1-4b to the second and third terms on the RHS of the above relation yields

$$P(\bar{T}_i^u T_j) = P(\bar{T}_i^u) - P(\bar{T}_i^u)P(\bar{T}_j^u) - P(\bar{T}_i^u)P(\bar{T}_j^s)$$
$$= P(\bar{T}_i^u)[1 - P(\bar{T}_j^u) - P(\bar{T}_j^s)] = P(\bar{T}_i^u)[1 - P(\bar{T}_j^u + \bar{T}_j^s)]$$
$$= P(\bar{T}_i^u)[1 - P(\bar{T}_j)]$$

where the mutually exclusive property of $\bar{T}_i^u$ and $\bar{T}_j^u$ (Eq. A.1-3a) and the definition of $\bar{T}_j$ are used. Thus, by definition, the above relation gives

$$P(\bar{T}_i^u T_j) = P(\bar{T}_i^u)P(T_j) \qquad \text{(A.1-4c)}$$

Based on the above assumptions, the NDFs may now be computed in terms of the individual station off-air probabilities. Before considering the general case, a sample NRF calculation will be performed to illustrate the required component calculations. Consider R_{12}, i.e.,

*If events A and B are mutually exclusive and C and D are two other unrestricted events, then AC and BD are also mutually exclusive.

$$P(B_{12}) = P\left[(\overline{T}_1^u + \overline{T}_1^s)(\overline{T}_2^u + \overline{T}_2^s)\ T_3\ T_4\ T_5\ T_6\ T_7\ T_8\right]$$

$$= P\left[\overline{T}_1^u\overline{T}_2^u V + \overline{T}_1^u\ \overline{T}_2^s V + \overline{T}_1^s\ \overline{T}_2^u V + \overline{T}_1^s\ \overline{T}_2^s V\right] \qquad \text{(A.1-5)}$$

where $V = T_3T_4T_5T_6T_7T_8$.

The last term/event inside the bracket in Eq. A.1-5 vanishes because of the concurrent scheduled off-air exclusion (Eq. A.1-3b). The remaining terms/events are mutually exclusive as expressed by Eq. A.1-3a. With these results and the repeated use of Eqs. A.1-4a, A.1-4b, and A.1-4c, then Eq. A.1-5 becomes

$$P(B_{12}) = P(\overline{T}_1^u)\ P(\overline{T}_2^u)\ P(V) + P(\overline{T}_1^u)\ P(\overline{T}_2^s V) + P(\overline{T}_2^u)\ P(\overline{T}_1^s V) \qquad \text{(A.1-6)}$$

Thus, the NRF has been reduced to an expression involving single station off-air probabilities, except for P(V), $P(\overline{T}_2^s V)$, and $P(\overline{T}_1^s V)$ (similar results hold for reduction of other NRFs). Since $V = T_3T_4T_5T_6T_7T_8$, it is clear that $P(\overline{T}_1^s V)$ and $P(\overline{T}_2^s V)$ represent identical calculations, with $1 \rightarrow 2$.

To compute P(V), first calculate $P(T_1T_2)$ and extend the result to higher-order products. As before, an indirect approach is used, in which $P(T_1)$ is expanded as

$$P(T_1) = P(T_1U) = P(T_1(T_2 + \overline{T}_2)) = P(T_1\ T_2 + T_1\ \overline{T}_2)$$
$$= P(T_1T_2) + P(T_1\overline{T}_2)$$

where the last step follows since T_1T_2 and $T_1\overline{T}_2$ are mutually exclusive events. Rearranging the above relation and using the definitions yield

$$P(T_1\ T_2) = P(T_1) - P(T_1\ \overline{T}_2) = P(T_1) - P(T_1\ (\overline{T}_2^u + \overline{T}_2^s))$$
$$= P(T_1) - P(T_1\ \overline{T}_2^u + T_1\ \overline{T}_2^s)$$
$$= P(T_1)\ (1 - P(\overline{T}_2^u)) - P(T_1\ \overline{T}_2^s) \qquad \text{(A.1-7)}$$

where the last step followed from Eq. A.1-4c and the fact that events $T_1\overline{T}_2^u$ and $T_1\overline{T}_2^s$ are mutually exclusive. Now, the quantity $P(T_1\overline{T}_2^s)$ is calculated using an approach similar to that used for $P(T_1T_2)$, but now expanding $P(\overline{T}_2^s)$, i.e.,

$$P(\overline{T}_2^s) = P(\overline{T}_2^s U) = P(\overline{T}_2^s\ (T_1 + \overline{T}_1)) = P(\overline{T}_2^s\ T_1 + \overline{T}_2^s\ \overline{T}_1)$$
$$= P(\overline{T}_2^s\ T_1) + P(\overline{T}_2^s\ \overline{T}_1)$$

because $\overline{T}_2^s T_1$ and $\overline{T}_2^s \overline{T}_1$ are mutually exclusive. Thus

$$\begin{aligned} P(T_1\overline{T}_2^s) &= P(\overline{T}_2^s) - P(\overline{T}_2^s\ \overline{T}_1) \\ &= P(\overline{T}_2^s) - P(\overline{T}_2^s\ (\overline{T}_1^u + \overline{T}_1^s)) \\ &= P(\overline{T}_2^s) - P(\overline{T}_2^s\overline{T}_1^u) \end{aligned}$$

where the definition of $\overline{T}_1$ and the concurrent scheduled off-air exclusion (Eq. A.1-3a) was used. With the use of Eq. A.1-4b, the above expression yields

$$P(T_1\overline{T}_2^s) = P(\overline{T}_2^s)\ (1 - P(\overline{T}_1^u)) \qquad \text{(A.1-8)}$$

Substituting this result into Eq. A.1-7 gives

$$P(T_1T_2) = P(T_1)\ (1 - P(\overline{T}_2^u)) - P(\overline{T}_2^s)\ (1 - P(\overline{T}_1^u)) \qquad \text{(A.1-9)}$$

Now, by definition,

$$P(T_1) = 1 - P(\overline{T}_1) = 1 - P(\overline{T}_1^u + \overline{T}_1^s) = 1 - P(\overline{T}_1^u) - P(\overline{T}_1^s)$$

Thus

$$1 - P(\overline{T}_1^u) = P(T_1) + P(\overline{T}_1^s)$$

and, similarly, for $P(T_2)$,

$$1 - P(\overline{T}_2^u) = P(T_2) + P(\overline{T}_2^s)$$

Substituting these last two equations into Eq. A.1-9 yields

$$P(T_1T_2) = P(T_1)P(T_2) - P(\overline{T}_1^s)P(\overline{T}_2^s) \qquad \text{(A.1-10)}$$

This result, which is properly symmetric in stations 1 and 2 shows explicitly the error in assuming on-air probabilities T_1 and T_2 independent.

To compute $P(\overline{T}_1^s V)$, it is again convenient to start with $P(\overline{T}_1^s T_2)$ and extrapolate the result for additional factors. Equation A.1-8 gives, with indices 1 and 2 interchanged,

$$P(\overline{T}_1^s T_2) = P(\overline{T}_1^s)(1 - P(\overline{T}_2^u))$$

Using a procedure identical to that used to derive Eq. A.1-8, it can be shown that

$$P(\overline{T}_1^s T_2 T_3) = P(\overline{T}_1^s)(1 - P(\overline{T}_2^u))(1 - P(\overline{T}_3^u))$$

and, in general,

$$P(\overline{T}_{i_1}^s T_{i_2} T_{i_3} \ldots T_{i_n}) = P(\overline{T}_{i_1}^s) \prod_{j=2}^{n} (1 - P(\overline{T}_{i_j}^u)) \qquad \text{(A.1-11)}$$

This general result can be used to decompose both $P(\overline{T}_1^s V)$ and $P(\overline{T}_2^s V)$.

To calculate the general form $P(T_{i_1} T_{i_2} .. T_{i_n})$, a procedure similar to that used above is employed. Thus,

$$\begin{aligned} P(T_{i_1} T_{i_2} \ldots T_{i_{n-1}}) &= P(T_{i_1} T_{i_2} \ldots T_{i_{n-1}} U) \\ &= P(T_{i_1} T_{i_2} \ldots T_{i_{n-1}} (T_{i_n} + \overline{T}_{i_n})) \\ &= P(T_{i_1} T_{i_2} \ldots T_{i_n}) + P(T_{i_1} T_{i_2} \ldots T_{i_{n-1}} \overline{T}_{i_n}) \end{aligned}$$

because complementary sets are mutually exclusive. Thus,

$$\begin{aligned} P(T_{i_1} T_{i_2} \ldots T_{i_n}) &= P(T_{i_1} T_{i_2} \ldots T_{i_{n-1}}) - P(T_{i_1} T_{i_2} \ldots T_{i_{n-1}} (\overline{T}_{i_n}^u + \overline{T}_{i_n}^s)) \\ &= P(T_{i_1} T_{i_2} \ldots T_{i_{n-1}}) - P(T_{i_1} T_{i_2} \ldots T_{i_{n-1}} \overline{T}_{i_n}^u) \\ &\quad - P(T_{i_1} T_{i_2} \ldots T_{i_{n-1}} \overline{T}_{i_n}^s) \end{aligned}$$

Now, Eq. A.1-4c is applied to the second term and Eq. A.1-11 is used to reduce the third term. Hence,

$$\begin{aligned} P(T_{i_1} T_{i_2} \ldots T_{i_n}) &= P(T_{i_1} T_{i_2} \ldots T_{i_{n-1}}) (1 - P(\overline{T}_{i_n}^u)) \\ &\quad - P(\overline{T}_{i_n}^s) \prod_{j=1}^{n-1} (1 - P(\overline{T}_{i_j}^u)) \end{aligned} \qquad \text{(A.1-12)}$$

Equation A.1-12 is in the form of a recursion relation for $P(T_{i_1} T_{i_2} \ldots T_{i_n})$. Although the symmetry on interchange of indices is not evident in this form, it is immediately adaptable to programming on a computer. For n = 3, Eq. A.1-12 can be manipulated to yield the expression

$$P(T_1T_2T_3) = P(T_1)P(T_2)P(T_3) - P(\overline{T}_1^s)P(\overline{T}_2^s)P(\overline{T}_3^s) - \left[P(T_1)P\overline{T}_2^s)P(\overline{T}_3^s)\right.$$
$$\left. + P(\overline{T}_1^s)P(T_2)P(\overline{T}_3^s) + P(\overline{T}_1^s)P(\overline{T}_2^s)P(T_3) + P(\overline{T}_1^s)P(\overline{T}_2^s)P(\overline{T}_3^s)\right]$$

This relation is expressly written to exhibit the complete symmetry on interchange of indices 1, 2, and 3.

Thus, all terms and factors in the expression for $P(B_{12})$ (Eq. A.1-6) can be computed with the aid of Eqs. A.1-11 and A.1-12. For example, P(V) is computed from Eq. A.1-12 with $i_1 = 3$, $i_2 = 4$, $i_3 = 5$, $i_4 = 6$, $i_5 = 7$, $i_6 = 8$, and $n = 6$. Similarly, $P(\overline{T}_1^s V)$ is computed from Eq. A.1-11 with $i_1 = 1$, $i_2 = 3$, $i_3 = 4$, $i_4 = 5$, $i_5 = 6$, $i_6 = 7, i_7 = 8$, and $n = 7$. $P(\overline{T}_2^s V)$ is computed the same way except that $i_1 = 2$.

The general NRF, $R_{i_1 i_2 \ldots i_n}$, may be written as

$$P(B_{i_1 i_2 \ldots i_n}) = P\left[(\overline{T}_{i_1}^u + \overline{T}_{i_1}^s)(\overline{T}_{i_2}^u + \overline{T}_{i_2}^s) \ldots (\overline{T}_{i_n}^u + \overline{T}_{i_n}^s) T_{i_{n+1}} T_{i_{n+2}} \ldots T_{i_8}\right]$$

Although the above expression may appear formidable, the exclusion rule, Eq. A.1-3b, reduces the number of terms inside the brackets to just $n + 1$. Expanding the indicated product in brackets and using Eqs. A.1-2,3,4 yields the following general expression for the NRF:

$$R_{i_1 i_2 \ldots i_n} = P(W) \prod_{j=1}^{n} P(\overline{T}_{i_j}^u) + \sum_{j=1}^{n} \prod_{k=1}^{n} \left[P(\overline{T}_{i_k}^u)(1 - \delta_{jk}) + P(\overline{T}_{i_k}^s W)\delta_{jk}\right]$$

where $W = T_{i_{n+1}} T_{i_{n+2}} \ldots T_{i_8}$

$\delta_{jk} = 1 \quad j = k$ (Kronecker δ)

$= 0 \quad j \neq k$

In this expression, P(W) is determined by means of Eq. A.1-12 and $P(\overline{T}_{i_k}^s W)$ is computed with the use of Eq. A.1-11. Note that $n \leq 5$ since

$$P(X_3/B_{i_1 i_2 \ldots i_n}) = 0 \text{ for } n > 5$$

i.e., no more than 5 stations can be concurrently off-air.

It should be mentioned that the independence assumption regarding unscheduled off-air events is only approximate and is most accurate when the scheduled and unscheduled off-air probabilities are small. This is consistent with the definition of the off-air probabilities as ratios of total off-air duration to total time in a month as shown in Section A.2.

A.2 OFF-AIR PROBABILITY FUNCTIONS

A.2.1 Off-air Occurrence Probability Functions

A reasonable description of unscheduled (random) off-air occurrence is given by the probability density function shown in Fig. A.2-1(a). The probability density describes the situation in which an off-air occurs at time t = 0 and the probability per unit time of the next off-air occurrence is indicated by the plot. The probability density following the off-air is zero and gradually increases to a peak at time $1/\lambda$ which represents the average interval between off-air occurrences (based on empirical data). The probability density then gradually decreases to permit normalization. The normalized probability density function may be expressed as

$$p_{OAO}(t) = \lambda^2 t e^{-\lambda t} \qquad \text{(A.2-1)}$$

For scheduled off-airs the process is entirely deterministic so that the probability density function is given by the Dirac-delta function δ (t - T) where T is the known time of off-air occurrence referenced to a convenient initial point (such as the beginning of a month). This distribution is illustrated in Fig. A.2-1(b).

A.2.2 Off-air Duration Probability Functions

In the case of unscheduled off-airs, the off-air duration may be described by a simple exponential probability density function, which, in its normalized form is given by

$$p_{OAD}(t) = \mu e^{-\mu t} \qquad \text{(A.2-2)}$$

where $1/\mu$ is the average off-air duration, obtained from empirical data. Figure A.2-2(a) shows a plot of this function and Fig. A.2-2(b) illustrates the corresponding distribution function (integral of the density function) which describes the probability that the off-air duration is less than some value, T.

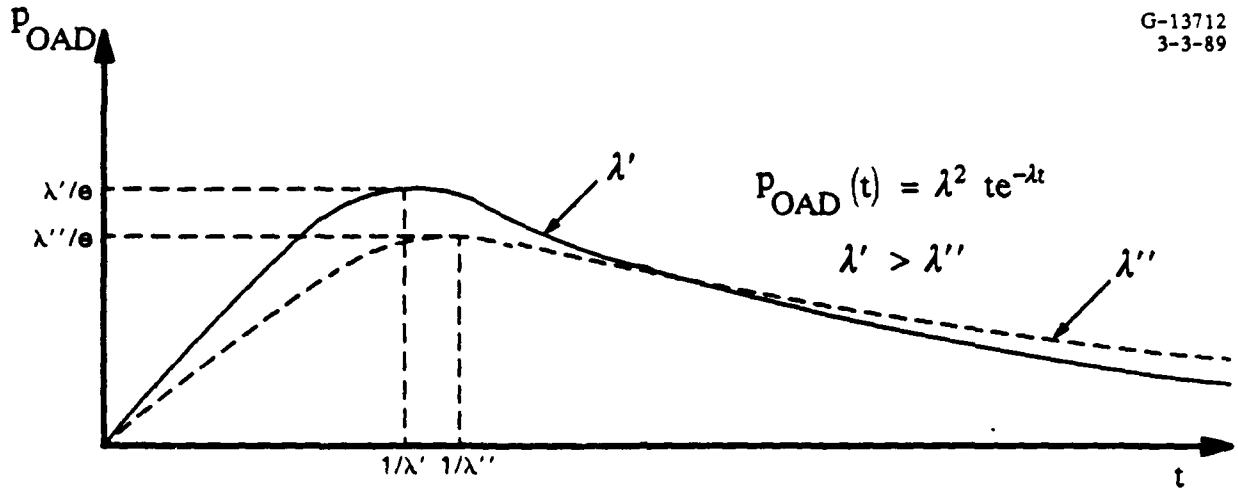

a) Unscheduled (random) Off-air Occurrence Probability Density Function for Two Values of the Average Time between Off-airs ($1/\lambda$)

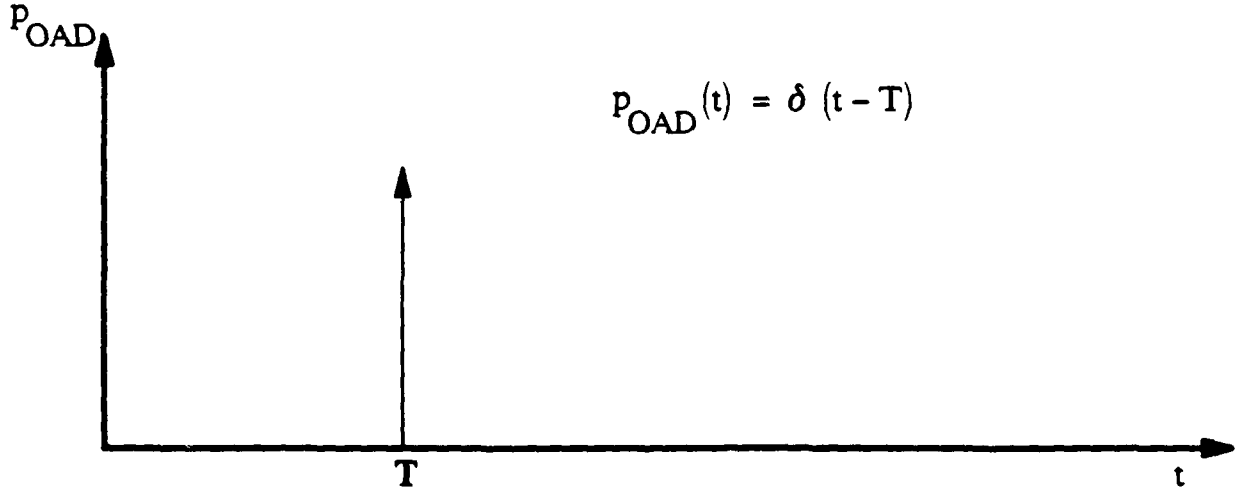

b) Scheduled (Deterministic) Off-air Occurrence Probability Density Function

Figure A.2-1 Off-air Occurrence Probability Density Functions for Unscheduled (random) and Scheduled (deterministic) Off-air Conditions

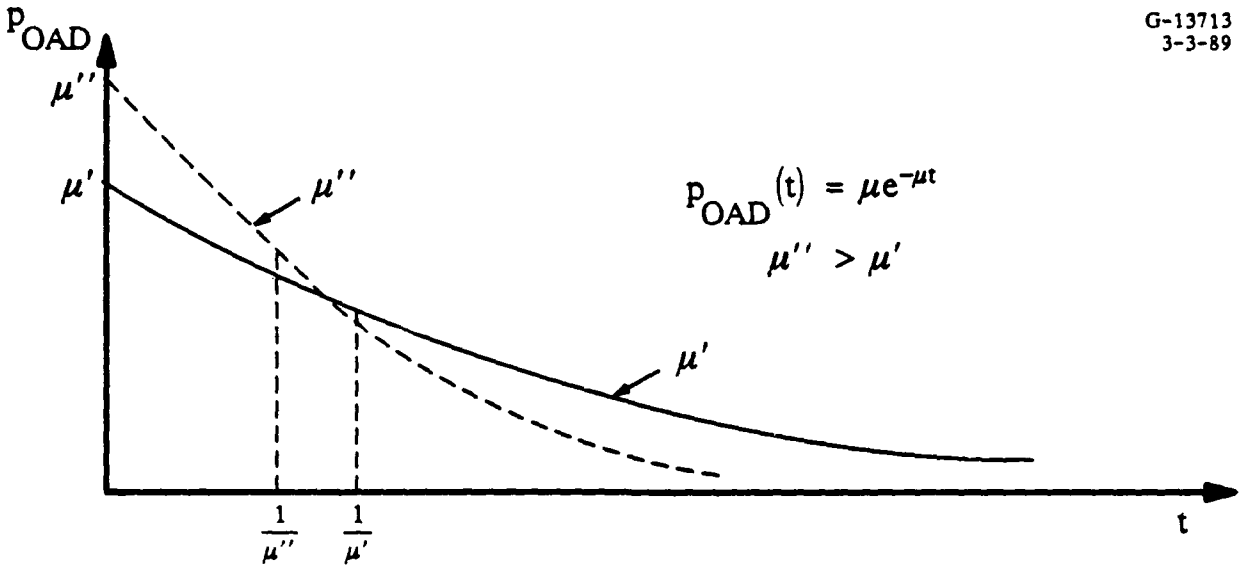

a) Off-air Duration Probability Density Function for Two Values of the Average Off-air Duration (1/μ)

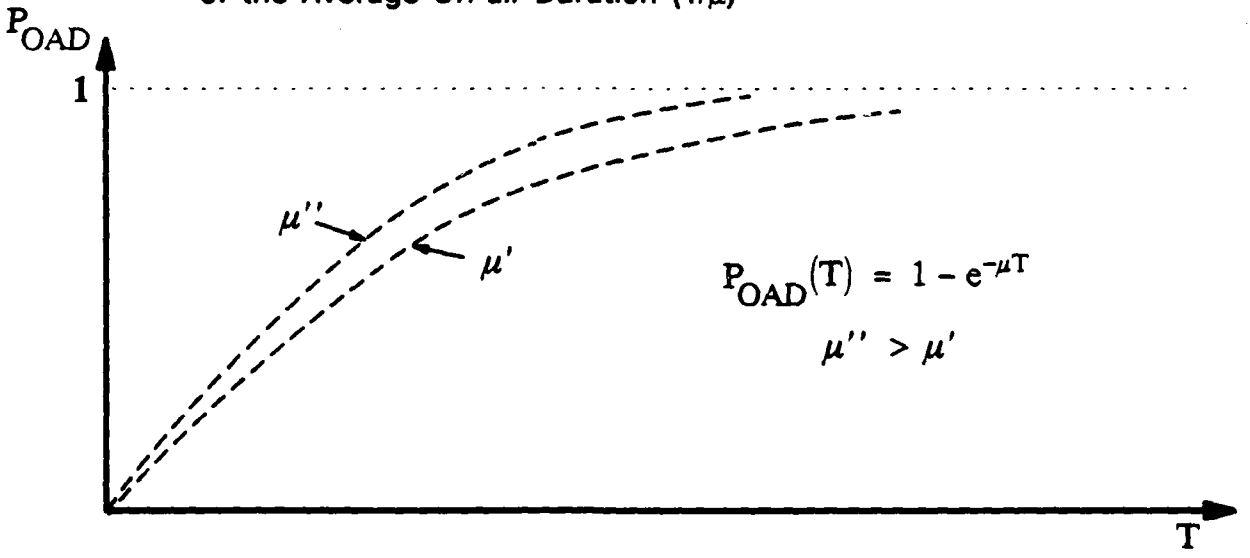

b) Off-air Duration Probability Distribution Function for Two Values of the Average Off-air Duration (1/μ)

Figure A.2-2 Off-air Duration Probability Density and Distribution Functions for Unscheduled (random) Off-air Conditions

This density function differs from the off-air occurrence density function (aside from normalization constants) by a factor of t. This factor occurs in the expression for $p_{OAO}(t)$ to explicitly exclude very short intervals between off-air occurrences (e.g., before the station achieves an on-air condition). An unscheduled off-air condition may be indefinitely short, however, since immediate action is always taken to restore the on-air condition. Thus, the exponential factor appears alone (leading to a monotonically decreasing density function) in the expression for $p_{OAD}(t)$.

Since the duration of scheduled off-airs is a deterministic quantity, the probability density function has the same form as for off-air occurrences, i.e., δ $(t-\Delta T)$ where ΔT is the known off-air duration. This density function is similar to the one shown in Fig. A.2-1(b).

A.2.3 Probability that a Station is Off-air at an Arbitrary Time

Assuming that the time of off-air occurrence is independent of the duration of the corresponding off-air period, the probability that a station is off-air at some arbitrary time t is

$$P_{OA}(t) = \int_{t'<t} dt' p_{OAO}(t') \int_{t-t'<t''} dt'' \; p_{OAD}(t'')$$

In words this says that in order that a station be off-air at time t, the off-air (beginning at t') must begin before t *and* the off-air duration (t'') must be longer than the current elapsed time since the off-air occurrence ($t-t'$). This reasoning is illustrated in Fig. A.2-3. With an arbitrary zero-time reference, the above may be written

$$P_{OA}(t) = \int_{0}^{t} dt' \; p_{OAO}(t') \int_{t-t'}^{\infty} dt'' \; p_{OAD}(t'') \qquad \text{(A.2-3)}$$

For the case of unscheduled off-airs, Eqs. A.2-1 and A.2-2 are used for the off-air occurrence and off-air duration probability density functions, respectively. When inserted in Eq. A.2-3, the off-air probability becomes

$$P_{OA}(t) = \mu\lambda^2 \int_{0}^{t} dt' \; t'e^{-\lambda t'} \int_{t-t'}^{\infty} dt''e^{-\mu t''}$$

This integral is easily evaluated to give

$$P_{OA}(t) = \frac{\lambda^2}{\mu - \lambda}\left[\frac{e^{-\mu t}}{\mu - \lambda} + te^{-\lambda t} - \frac{e^{-\lambda t}}{\mu - \lambda}\right] \qquad \text{(A.2-4)}$$

To evaluate this quantity, the assumption is made that the average time interval between successive off-airs is much larger than the average off-air duration, i.e.,

$$\frac{1}{\lambda} >> \frac{1}{\mu} \qquad \text{or} \qquad \lambda << \mu$$

Thus, for $t \neq 0, e^{-\lambda t} >> e^{-\mu t}$ and the first term in brackets in Eq. A.2-4 can be neglected in comparison to the second and third terms. Since $\mu >> \lambda$, the exponential in the third term in brackets in Eq. A.2-4 is essentially multiplied by $1/\mu$. Thus, for $t >> 1/\mu$ (i.e., for times large compared to an off-air duration), the third term in brackets in Eq. A.2-4 may be neglected in comparison to the second term. Thus, with t large compared to the average off-air duration, the off-air probability at time t may be written

$$P_{OA}(t) = \frac{\lambda^2}{\mu - \lambda} te^{-\lambda t} \equiv \frac{\lambda^2}{\mu} t\, e^{-\lambda t}$$

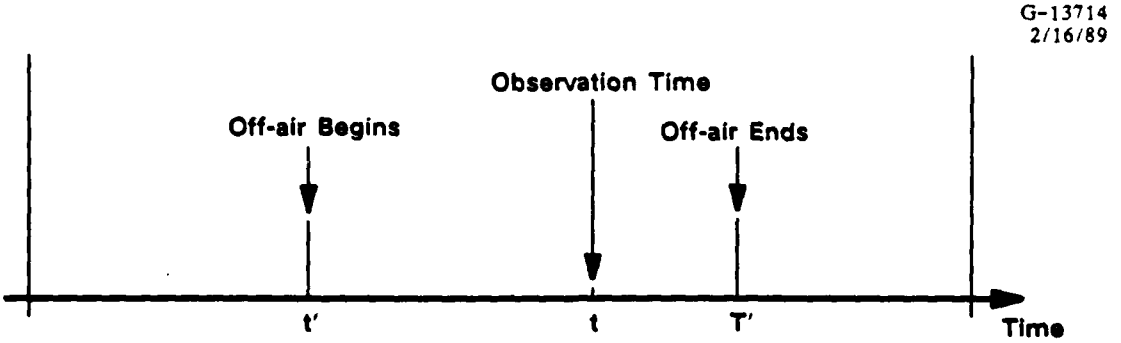

Figure A.2-3 Conditions Under Which a Station is Off-air at Time, t

since $\mu >> \lambda$. Defining the month to begin at $t = 0$ and end at $t = T$, the average value of $P_{OA}(t)$ over the month may be computed as follows:

$$< P_{OA}(t) > \equiv \frac{1}{T} \int_0^T P_{OA}(t)\, dt$$

$$= \frac{\lambda^2}{\mu T} \left[\frac{1}{\lambda^2} (1 - e^{-\lambda T}) - \frac{T}{\lambda} e^{-\lambda T} \right] \qquad \text{(A.2-5)}$$

Now, assuming an average of about 3 off-air occurrences per month (i.e., $3/\lambda \approx T$)*, the exponential terms occurring inside the brackets in Eq. A.2-5 may be dropped in comparison to the non-exponential term. Thus,

$$< P_{OA}(t) > \equiv \frac{\lambda^2}{\mu T} \left(\frac{1}{\lambda^2} \right) = \frac{1}{\mu T} = \frac{1/\mu}{T} = \frac{T_{OA}}{T} \qquad \text{(A.2-6)}$$

where T_{OA} is the average off-air duration and T is the total time in the month.

"Scheduled" off-airs which are not planned until after the beginning of the month can be modeled using the *a priori* probability functions (occurrence/duration) treated above with λ, μ given by historical reliability figures† for each station. Once the scheduled off-air is planned/announced, the randomness vanishes (for that particular kind of off-air) and the problem becomes deterministic. Equation A.2-6 may still be used as an approximation to the off-air probability, however, since it is valid except for those intervals during which advance information is known. For the completely deterministic cases/intervals, Eq. A.2-6 simply becomes a fractional off-air figure subject to the exclusion of concurrent scheduled off-airs from different stations (see Eq. A.1-3).

*This assumption is based on a sampling of off-airs (>1 min) in four separate months during 1988.

†Excluding scheduled off-airs for annual maintenance which are known well before the month begins and are thus completely deterministic.

APPENDIX B

OMEGA RECEIVERS AND SIGNAL COVERAGE

Signal coverage is a crucially important element of the system availability model. A critical aspect of signal coverage is the set of signal access criteria which specify the limiting thresholds on signal use. The signal access criteria address the following signal parameters contained in the 24-hour/4-month/2-frequency database (not all of these are included in the 2-hour/4-month/2-frequency database).

- Phase deviation (difference between mode-1 and mode-sum phase with respect to the nearest lane)
- Dominant mode number
- Signal-to-noise ratio (SNR)
- Short-path/long-path amplitude ratio
- Path-terminator crossing angle
- Geometric Dilution of Precision (GDOP) of accessible signals.

To provide accurate predictions of signal coverage for a wide range of users, the signal access criteria for each of the signal parameters above must be representative of that achievable by conventional Omega receivers. The limits on the phase deviation are determined by the probability of cycle slip (including a safety margin) which is a general property, not limited to particular receiver implementations. The criterion for dominant mode number is determined by the propagation corrections (PPCs) used to convert received signal phase to a standard geodetic reference which can be used for navigation. In all cases known, the PPCs use a mode-1 model (Ref. 14), thus limiting the dominant mode number to 1. The criterion governing short-path/long-path amplitude ratio depends somewhat on the receiver system in terms of its ability to reject/suppress an unwanted narrowband signal of the same frequency. The extent of long-path interference/domination is not fully understood at this time but a minimum (short-path/long-path) ratio of 3 dB is a generally accepted criterion. The minimum path-terminator crossing angle is generally not dependent on receiver type (except possibly for non-adaptive, long-time-constant receivers) but rather on the possibility of off-path interference (Ref. 27). The maximum allowable GDOP depends on the receiver mechanization/navigation filter but

sample calculations suggest that GDOP has little effect on P_{SA}. This leaves SNR as the only signal coverage parameter having a threshold condition which depends significantly on receiver type/class and is known to substantially affect coverage. The geographic location of the SNR threshold is also a quantity which is available from both the 2-hour/4-month/2-frequency and the 24-hour/4-month/ 2-frequency databases.

Based on the above reasons, the minimum SNR threshold is the principal focus of the investigation into Omega receiver systems. The findings presented in this appendix are based on interviews with representatives of six North American Omega receiver manufacturers. To protect proprietary rights, receiver characteristics are not associated with a particular manufacturer, and only summary findings are explicitly discussed.

B.1 CLASSES OF OMEGA RECEIVER SYSTEMS

Omega receiver systems are manufactured for a variety of applications including airborne, surface (marine/land), and special sensors. Receiver systems within each application area can differ markedly (e.g., those marine receivers which are used for surface ships and those used for submarines). However, in terms of minimum SNR threshold effects, two classes of receiver systems are distinguished:

1. Modern airborne/marine Omega systems
2. Omega sensors/early-generation systems.

Airborne systems for airliners and high-performance military aircraft are usually quite sophisticated and include VLF signal processing, rate aiding from true air speed and heading sensors, electronically steerable crossed-loop H-field antennas, and coupling into the autopilot and mission computer. Omega systems for general aviation aircraft are generally less sophisticated and feature E-field antennas because of the closer proximity to the engine. Surface marine systems normally do not include VLF signal processing since the speed of the platform is such that propagation-induced phase changes between successive VLF "lanes" may be significant. Rate aiding (speed through water and magnetic heading) and E-field antennas are found on most marine Omega systems. Receivers on board submerged vessels process signals in the hyperbolic

mode to eliminate the highly variable antenna to sea-surface segment of the propagation path.* Such systems use both loops and long horizontal wire antennas. Omega sensors are used in a number of applications including wind-finding and remote tracking of unmanned craft. Because of the large number of sensors required for a given application (an estimated 100,000 units/year are used on meteorological balloons, Ref. 29), their design emphasizes simplicity and low-cost. As a result, these sensors employ only rudimentary detection schemes and perform minimal processing. Early generation airborne Omega receivers did not generally employ phase lock loops and their tracking bandwidths are somewhat wider than modern receivers. Time constants on these earlier receivers were also shorter for some military aircraft to allow for greater maneuverability requirements.

B.2 RECEIVER CHARACTERISTICS/THRESHOLDS

Figure B.2-1 shows a schematic for a typical airborne Omega receiver system. Without the loop steering section and some of the outputs, this schematic can also describe Omega receiver systems for most other applications. Signal and noise (including harmonic interference) from all sources are received at the antenna (having a bandwidth of at least 4 kHz), pre-amplified and sent to the detector for conditioning. The bandwidth due to filtering at the front-end of the detector is typically 100 Hz. Since the signal bandwidth is very narrow (a few Hertz), the 100 Hz is effectively a *noise* bandwidth (BW) which is assumed to have a flat spectrum (across 100 Hz) from atmospheric sources. The 100 Hz BW is a design tradeoff between noise impulse definition/rejection (easier at wider BWs) and flat spectra noise (less at narrower BWs). The signal is also limited at this stage to prevent swamping due to large impulsive noise spikes. Typical limiter levels of 1-100 mV/m are also the result of a tradeoff — in this case, between lower levels to reduce the impulsive noise and higher levels to minimize intermodulation products which can corrupt the phase (Ref. 30). At this point, receiver mechanizations differ in the detection process: "Tuned RF" receivers process signals at the received frequencies while other receivers use heterodyning to process signals at intermediate (usually lower) frequencies. In any case, a reference signal is injected which is stable enough to make phase comparisons over a few time constants (minutes). In some receivers, a quadrature detection is performed in which the signal is decomposed into orthogonal sine and cosine components and the phase extracted as the inverse

*In sea water, the effective wavelength at 10 kHz is only 15 meters so that surface sea state variability (on the order of meters) can substantially perturb phase (on time scales of ≤ 1 minute).

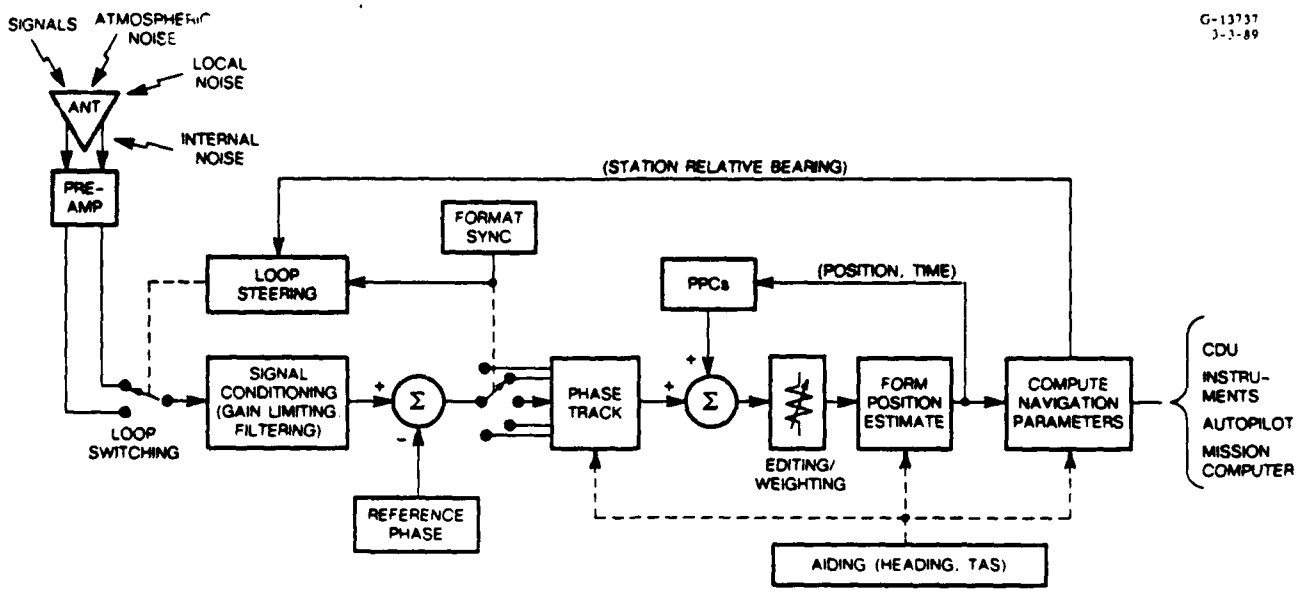

Figure B.2-1 Functional Block Diagram for Conventional Airborne Omega Navigation Receiver System (Ref. 31)

tangent. Other receivers use purely digital techniques with first-order and/or second-order phase-lock loops to provide phase estimates. VLF signal processing requires signal doubling to uniquely extract phase components from the MSK-modulated communication signal.

Later stages in the receiver bring in external parameters such as propagation corrections and DR inputs. It is here that comparison is made with modal maps (if available), geometrical effects, and general figures of merit. Some of these latter calculations may be included in the navigation filter which may also incorporate navigation estimates from independent aids, such as inertial systems.

B.2.1 Theoretical Relationship between Phase Error and SNR

Noise which has a non-zero mean level when sampled over intervals of 1-10 μsec contributes directly to phase error in navigation systems. Figure B.2-2 shows a sinusoidal waveform representing an Omega signal perturbed by a mean noise level, N(0) near $\phi = 0$. Phase is usually measured as a zero-crossing with respect to a common standard (analog or digital). The mean noise level near $\phi = 0$ shifts the zero-crossing at $\phi = 0$ to $\phi' = -\Delta\phi$. Assuming the

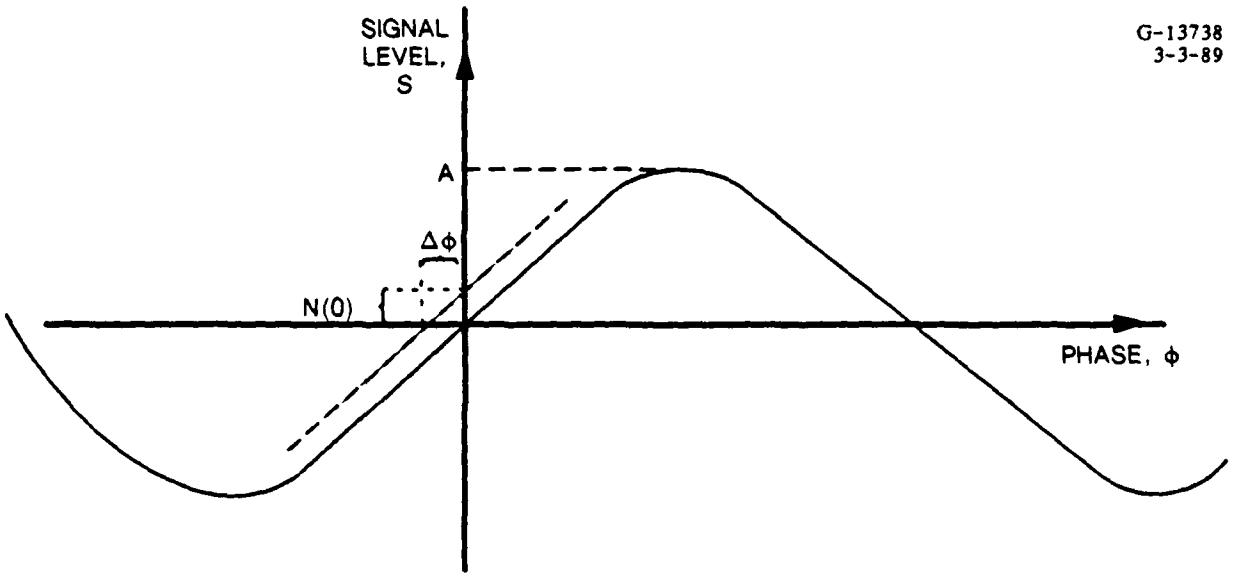

Figure B.2-2 Displacement of a Sinusoidal Signal Zero-crossing due to Mean Noise Level near $\phi = 0$

noise level is approximately constant over the interval $\Delta\phi$ *, the error in the zero-crossing, $\Delta\phi$ can be estimated by first noting that

$$\frac{N(0)}{\Delta\phi} \equiv \left.\frac{dS}{d\phi}\right|_{\phi = 0}$$

which is approximately valid in the near-linear regime of the sinusoid and thus

$$\Delta\phi \equiv \frac{N(0)}{dS/d\phi|_{\phi=0}} = \frac{N(0)}{A} \qquad \text{(B.2-1)}$$

where A is the amplitude of the signal $S(\phi)$. If the average power (to within a constant factor) developed by the signal $S(\phi)$ is denoted by C, then

$$C = \frac{1}{2\pi}\int_0^{2\pi} S^2(\phi)d\phi = \frac{A^2}{2\pi}\int_0^{2\pi} \sin^2\phi d\phi = A^2/2$$

*$\Delta\phi$ cannot be too large because the noise signal N must lie in a 100 Hz BW about the Omega signal and hence must vary somewhat over a signal period; $\Delta\phi$ must also be small to satisfy the linearity assumption inherent in Eq. B.2-1.

since $S(\phi)$ is sinusoidal. Denoting the noise power near $\phi = 0$ by N, Eq. B.2-1 becomes

$$\Delta\phi = \frac{1}{(A/N(0))} = \frac{1}{\sqrt{2C/N}} \qquad \text{(B.2-2)}$$

where $\Delta\phi$ is in radians and N is the noise power for a fixed bandwidth. The bandwidth can be approximated from knowledge of the receiver time constant, modified by the 10% duty cycle of the Omega station-signal/common-frequency transmissions.

A simple example will help to clarify these considerations. Assume a typical airborne receiver time constant of 80 seconds (marine receiver time constants are typically longer by a factor of 3). With a 10% duty cycle, this corresponds to 8 seconds of actual integration time and a corresponding bandwidth of 0.125 Hz. Assume further a threshold phase error of 5 centicycles which corresponds to 0.314 radian. With this value for $\Delta\phi$, Eq. B.2-2 can be inverted to yield

$$C/N = 5.066 \rightarrow 7.05 \text{ dB} \quad (0.125 \text{ Hz BW})$$

For a 100 Hz BW this signal-to-noise ratio (SNR) is reduced by 29.03 dB to

$$C/N = -21.98 \text{ dB} \quad (100 \text{ Hz BW})$$

It is interesting to note that increasing the minimum accuracy by a factor of two (e.g., $\Delta\phi$ =4 cec → 2 cec) increases the minimum required SNR by 6 dB. Increasing the time constant by a factor of 2, however, decreases the effective BW by the same amount which lowers the minimum SNR by 3 dB. In aircraft, time constants are limited by maneuverability constraints, e.g., tracking during a 2-minute turn requires a time constant of well under 120 seconds. As shown above, the minimum SNR is more sensitive to accuracy uncertainty threshold than time constant. For fixed time constant, minimum SNR thresholds are lowered if larger maximum phase tracking errors can be tolerated. However, phase tracking error translates directly into position error and thus should not be compromised.

B.2.2 Receiver Estimates of SNR

The above analysis is useful for understanding the procedures and connections between the various quantities. However, signal processing in conventional receivers includes factors not addressed in the above analysis. For example, requirements are usually given in terms of

position accuracy, not phase-tracking accuracy. Because of the large contribution of propagation correction errors to the position error budget, phase-tracking accuracy is not well-correlated with total position accuracy. Another problem is related to the definition and statistics of the VLF noise. In deriving Eq. B.2-2, the noise "level" was assumed constant over $\Delta\phi$ (or equivalently, over time interval, $\Delta t = \Delta\phi/\omega$). If, instead, an RMS value of noise is assumed, there is some evidence that the effective minimum SNR threshold increases by -6 dB when impulsive noise is present. This suggests the noise impulses, even after limiting, occur with sufficient frequency and duration so as to carry significant energy. The signal coverage diagrams specify median atmospheric noise (for a given hour/month), a statistic which is independent of receiver limiter level if the median noise is below the limiter level. If the pre-amplifier raises the median noise to or above the limiter level, the median noise will be reduced to the limiter level in the post-limiting portion of the receiver. In this case the receiver would experience a larger signal-to-median noise level than that measured at the antenna. Some research has shown that this difference may be as much as 15 dB (Ref. 37). RMS noise measurements depend on the entire distribution of noise samples and thus are sensitive to limiter levels even when the pre-amplifier does not make the detector front-end atmospheric noise limited.

The actual minimum SNR/phase-tracking *capability* of the receiver is really not the central issue for determining signal coverage. In modern receiver systems, tests are performed in software to determine whether or not a signal should be tracked or used for navigation. These tests are performed by computing figures-of-merit which involve a number of factors in addition to SNR (e.g., GDOP). If these non-SNR factors are held constant or ignored, the figure-of-merit depends only on the SNR which is internally computed/estimated. Although estimation techniques vary depending on the receiver mechanization, they all involve the computation of a tracking parameter(s) which is expected to be directly related to SNR (i.e., increase (decrease) if SNR increases (decreases)). For example, some digital phase lock loop implementations compute the cosine of the phase estimate error resulting from the feedback loop, i.e.,

$$< \cos \phi > \; = \frac{1}{N} \sum_{n=1}^{N} \cos (\phi_n - \phi_{n-1})$$

where ϕ_n is the phase estimate at the n^{th} cycle and N is the number of samples in a 10 second, or longer, period. Since the difference, $\phi_n - \phi_{n-1} \equiv \Delta\phi_n$ is expected to be relatively small for all n, the above becomes, approximately,

$$< \cos \phi > \equiv \frac{1}{N} \sum_{n=1}^{N} (1 - (\Delta\phi_n)^2/2) = 1 - \frac{1}{2N} \sum_{n=1}^{N} (\Delta\phi_n)^2$$

Since $\Delta\phi_n$ is small, use of Eq. B.2-2 is justified, yielding

$$< \cos \phi > = \frac{1}{4N} \sum_{n=1}^{N} (N/C)_n$$

Thus, the average noise-to-signal ratio is

$$\frac{1}{N} \sum_{n=1}^{N} (N/C)_n = 4(1 - < \cos \phi >)$$

and an *estimate* of the signal-to-noise ratio is just the reciprocal or

$$(C/N)_{\text{estimate}} = \frac{1}{4(1 - < \cos \phi >)}$$

Mathematically, this estimate cannot be less than -9 dB which is an acceptable limit since the SNR is computed in the processing BW which is typically less than 1 Hz.

In receivers with quadrature detection, the "variance" (VAR) is computed as the sum of the squares of the time-averaged quadrature components, i.e.,

$$\text{VAR} = \overline{\sin}^2 + \overline{\cos}^2$$

where

$$\overline{\sin} = \frac{1}{T} \int_0^T \sin \phi(t)\, dt \quad ; \quad \overline{\cos} = \frac{1}{T} \int_0^T \cos \phi(t)\, dt$$

and the time integration unit is typically 100 msec with $T \geq 10$ seconds. Assume that ϕ varies linearly with time over the interval [0,T], i.e., $\dot{\phi} \equiv d\phi/dt$ = constant. Then, integration by parts gives for $\overline{\sin}$, ($\dot{\phi} \neq 0$)

$$\overline{\sin} = \frac{1}{T} \int_{\phi(0)}^{\phi(T)} \sin \phi \frac{d\phi}{\dot{\phi}} = \frac{1}{\dot{\phi}T} \int_{\phi(0)}^{\phi(T)} \sin \phi\, d\phi = \frac{\cos \phi(0) - \cos \phi(T)}{\dot{\phi}T}$$

$$= \frac{2 \sin \left(\frac{\phi(0) + \phi(T)}{2} \right) \sin (\Delta\phi/2)}{\Delta\phi}$$

where $\Delta\phi = \phi(T) - \phi(0) = \dot{\phi}T$. Similar operations with $\overline{\cos}$ yield

$$\overline{\cos} = \frac{2 \cos\left(\frac{\phi(0)+\phi(T)}{2}\right) \sin(\Delta\phi/2)}{\Delta\phi}$$

From these expressions for $\overline{\sin}$ and $\overline{\cos}$ it follows that

$$\text{VAR} \equiv \overline{\sin}^2 + \overline{\cos}^2 = \frac{4 \sin^2(\Delta\phi/2)}{(\Delta\phi)^2} \qquad \text{(B.2-3)}$$

Note that VAR $\rightarrow 1$ as $\Delta\phi \rightarrow 0$. For small $\Delta\phi$, Eq. B.2-3 may be approximated as

$$\text{VAR} \equiv \frac{4}{(\Delta\phi)^2} \left[\Delta\phi/2 - \frac{1}{3!} (\Delta\phi/2)^3\right]^2$$

Neglecting all terms higher than second order in $\Delta\phi$ yields

$$\text{VAR} \equiv 1 - \frac{1}{12} (\Delta\phi)^2$$

Since $\Delta\phi$ is small, Eq. B.2-2 may be used to give

$$\text{VAR} = 1 - \frac{1}{24\ (C/N)}$$

Thus

$$C/N = \frac{1}{24(1 - \text{VAR})}$$

is the estimate for signal-to-noise ratio in terms of the VAR measurement.

With these internal estimates of SNR, the receiver processor computes the figure of merit and compares with pre-determined thresholds to determine whether the signal will be tracked or used for navigation.

B.2.3 Manufacturers' Estimates of Minimum SNR

Table B.2-1 summarizes the findings for the six North American Omega and Omega/VLF receiver manufacturers. Those in the first receiver class, which include most of the modern

Table B.2-1 Minimum SNR Thresholds and Platform-generated VLF Noise Levels for Receiver Types/Classes Produced by a Sample of North American Omega Receiver Manufacturers

RECEIVER TYPE (by application/platform)	RECEIVER CLASS (by similar SNR threshold)	MINIMUM SNR THRESHOLD (100 Hz BW)	PLATFORM-GENERATED VLF NOISE* (above atmospheric noise)
Modern Airborne	1	-20 to -25 dB	0 to +10 dB
Modern Marine	1	-18 dB	0 dB
Underwater Systems	1	-18 dB	0 dB
Older Airborne/Marine	2	-13 dB	- 0 dB†
Special-purpose Sensor	2	-10 dB	0 dB

*At antenna location.

†400 Hz/60 Hz spectral line strength < 1 mV/m.

navigation systems have minimum SNR thresholds which lie within a few dB of -20 dB (100 Hz BW). This figure is the most commonly used signal access criterion for SNR in the currently available signal coverage diagrams. The second class of receivers includes early generation systems and Omega special-purpose sensors which numerically exceed the number of receivers in the first class (though perhaps less critical in terms of navigation safety). The second class of receiving systems have minimum SNR thresholds of about -11 or -12 dB (100 Hz BW) reflecting shorter time constants and low-cost design. Though based on manufacturers' estimates, the minimum SNR threshold figures in Table B.2-1 are not definitive due to the uncertainties in the noise characteristics and processing procedures outlined above.

B.3 LOCAL VLF NOISE CHARACTERISTICS

Signal coverage calculations presume that VLF noise arises only from natural sources (e.g., lightning discharges) which can be predicted from physical models (Ref. 4). However, artificially-generated noise in the VLF band can also be severe. Sources such as welding torches, generators, large transformers, or engines are especially potent generators of VLF noise. This artificially-generated noise is usually grouped into two categories: broadband and discrete spectra. Broadband noise (e.g., from welding torches) has a flat spectrum across the 100 Hz bandwidths surrounding each Omega carrier frequency. Discrete spectra are usually manifest as

harmonics of strong electric power sources, i.e., 60 and 400 Hz. For example, 10.2 kHz is the 170^{th} harmonic of 60 Hz and 13.6 kHz is the 34^{th} harmonic of 400 Hz. These narrowband noise sources are potentially quite damaging since they are unfiltered and directly contribute to phase error in the tracking loop bandwidth. Fortunately, however, the 60 and 400 Hz power generating systems are not tightly controlled in frequency and thus tend to wander in and out (over time) of the narrow bands surrounding each Omega frequency.

To minimize the effect of these extraneous noise sources on vehicles such as aircraft, a skin-mapping is performed. In this procedure, a spectrum analyzer (or sometimes, an Omega sensor) is used to measure noise sources at or near Omega frequencies at all candidate antenna sites throughout the aircraft. Measurements are made with all aircraft power subsystems both on and off and compared with measurements made at a site remote from the aircraft. In many cases (for aircraft), manufacturers report that they are able to find antenna locations where the measured noise matches the remote measurement, i.e., the noise of the antenna location is dominated by atmospheric noise sources. Table B.2-1 summarizes the results for various receiver types. The table indicates that aircraft are generally the noisiest vehicles in the Omega frequency band.

If a worst-case assumption is made that locally-generated VLF noise is 10 dB above atmospheric noise for all users, then the median noise levels used in the signal coverage database would be increased by 10 dB for all hours/months. However, this degradation may be compensated for by the effect of receiver limiter levels below the median atmospheric noise mentioned in Section B.2.

B.4 SUMMARY/CONCLUSIONS

The discussion in this Appendix has illustrated the important connection between Omega receiver characteristics and signal coverage. The relationship is established by the signal access criteria which specify the level of acceptability of the critical signal/path parameters. The signal access criteria for most signal parameters can be derived from general/external considerations but minimum signal-to-noise ratio is largely a function of receiver type and mechanization. Since signal coverage cannot be tailored to apply to individual receiver-types, it is necessary to identify generic classes of receivers in which receivers belonging to the same class have similar minimum SNR thresholds. Two such receiver classes are identified: (1) Modern

airborne/marine Omega marine systems and (2) Omega sensors/early-generation receiving systems.

The theoretical relationship between phase-tracking error and SNR provides a useful context for the discussion of minimum SNR. The derivation of this relationship illustrates the necessary assumptions regarding noise, SNR, and bandwidth/time-constant. Simple examples show that -20 dB (100 Hz BW) is a "ballpark" minimum SNR figure and that minimum SNR is more sensitive to phase-tracking accuracy threshold than receiver time constant.

The effect of hard limiting, a feature of most conventional receivers, is to reduce the noise in the signal detection stage of the receiver. In many receivers, an initial pre-amplifier is sufficient to boost incoming narrowband noise (irrespective of the presence of a signal) to a level at or near the limiter level. Thus, the receiver is in a limiting condition much of the time and large noise impulses are cut off. If median noise level is the "N" specified by the SNR signal coverage parameter and the limiter level is above this median level, then the SNR, internal and external to the receiver, is essentially unchanged. However, if the median noise level is above the limiter level, then an SNR gain is realized internal to the receiver. This gain depends on pre-amplifier gain, atmospheric noise level, and pre-detection bandwidth and may be as large as 15 dB. Conventional receivers provide estimates of internal SNR by averaging phase estimation errors in digital phase-lock-loop implementations or by averaging squared quadrature components in other kinds of systems.

In a survey of six North American Omega receiver manufacturers, minimum SNR thresholds ranging from -10 to -25 dB (100 Hz BW) were identified by engineering representatives from each manufacturer. Local, platform-generated VLF noise, observed by manufacturers' field engineers on vehicle installations, varied from 0 to 10 dB above atmospheric noise.

In conclusion, it appears that no firm minimum SNR threshold figure can be given at this time. However, operational figures can be obtained by assuming gains due to the action of receiver limiting and modified by additional platform-generated VLF noise are 7-10 dB exclusive of gains considered in the manufacturers' estimates. This means that, with respect to noise levels computed from atmospheric noise models (i.e., independent of local noise), minimum SNR thresholds of -20 dB (receiver class (2)) to -30 dB (receiver class (1)) are indicated.

APPENDIX C

SIGNAL COVERAGE DATABASES

The system availability index, P_{SA}, depends on the signal coverage information contained in signal coverage databases. Two databases are referenced in this report:

(1) The 2-hour/4-month/2-frequency signal coverage database
(2) The 24-hour/4-month/2-frequency signal coverage database.

Database (1) is used for sample calculations of P_{SA} and Database (2) is used both in connection with estimates of VLF station coverage and for estimates of bounds on station power level reductions. Each of these databases is briefly described in this appendix.

C.1 TWO-HOUR/FOUR-MONTH/TWO-FREQUENCY DATABASE

This database (Database (1)) originated as a result of compiling a large number of calculations to construct signal coverage diagrams (Refs. 32 and 33). These calculations were made using computer programs based on a full-wave waveguide-mode model of VLF signal propagation (Ref. 8). Signal parameters were computed for a minimum set of 24 radials at a nominal spacing of 15° from each Omega station at 0600 and 1800 UT during the months of February, May, August and November for both 10.2 and 13.6 kHz. VLF noise is computed in a 100 Hz bandwidth (BW) about 10.2 kHz and 13.6 kHz for the UT-hours and months mentioned above using the semi-empirically-derived NRL/WGL VLF noise model (Ref. 9). Among the many signal parameters computed at points (spaced 100-200 km) along each radial path, the following are identified because they pertain specifically to signal coverage:

- Mode-sum signal phase
- Mode-1 signal phase
- Mode-sum signal amplitude
- Dominant mode number
- Median noise level.

The calculations assume that three modes adequately represent the signal on daytime paths with a horizontally homogeneous ionosphere; similarly, five modes are assumed for nighttime paths

with a horizontally homogeneous ionosphere. Path calculations of the signal parameters in transition regions (at terminator crossings) were computed using a mode conversion model/program (Ref. 13). Radial path calculations were not carried out beyond 19 Mm to exclude antipodal* effects. These effects which occur within one Mm of the antipode include:

- Long-path/short-path† interference
- Long-path dominance over short path
- Navigation difficulties associated with rapidly changing station bearings.

From the signal coverage parameters listed above, signal access criteria are formed which define signal usability for a broad range of system users. For this database, signal access criteria are formulated in terms of:

- Signal phase deviation ($\Delta\phi$) which is the absolute difference between the mode-sum and mode-one signal phase assuming that the whole-cycle value nearest the mode-sum phase is known
- Ratio of mode-sum signal amplitude to noise level (SNR)
- Geometric dilution of precision (GDOP) computed for three or four stations (calculation of GDOP is described in Ref. 33).

Signal access criteria differ somewhat between 10.2 and 13.6 kHz databases since they were compiled at widely separated times (- five years). Thus, the signal access criteria for 10.2 kHz are:

(1) $\Delta\phi \leq 20$ centicycles

(2) a) SNR $\geq$ -20 dB (100 Hz BW)
b) SNR $\geq$ -30 dB (100 Hz BW)

(3) GDOP $\leq$ 1 km/centicycle of phase difference error for at least one combination of 3- or 4-station signals satisfying criteria (1) and (2).

---

*The antipode here refers to the point on the earth diametrically opposite from the station, i.e., the point on the earth at maximum distance (20 Mm for a spherical earth) from the station.

†From any point on a spherical earth, two great-circle paths to a station can be formed: the longer of the two paths is called the *long-path*, the shorter is called the *short-path*.

For 13.6 kHz, the signal access criteria are:

(1) $\Delta\phi \leq 20$ centicycles

(2) SNR $\geq$ -20 dB (100 Hz BW)

(3) GDOP $\leq$ 0.5 km/centicycle of phase difference error for at least one combination of 3- or 4-station signals satisfying criteria (1) and (2).

These signal access criteria were applied to the radial path calculations and the threshold points (spatial locations where the "equal signs" apply in criteria (1), (2), and (3)) were connected to form contours (for 10.2 kHz, separate contours are shown for -20 and -30 dB). These global contours are given for each station individually (in which case the GDOP criterion does not apply) or overlayed for all stations (GDOP criterion applies). Each set of contours is given for the 8 month/hour times (0600 and 1800 UT in the months of February, May, August, and November). Additionally "nighttime modal interference" contours are given which are the loci of points for which $\Delta\phi = 20$ centicycles, assuming a nighttime ionospheric profile everywhere on the globe. The actual "signal coverage database" consists of coordinates (either latitude/longitude or range/bearing from each station) of the contours for each station at each of the eight times.

At 10.2 kHz, an additional body of information, which may be considered part of the database, furnishes lists of global coverage fractions (GCFs). These lists contain fractional coverage (relative to the earth's surface area) for each station combination having a non-zero GCF. Table C.1-1 illustrates a GCF list for May 0600 UT, with SNR $\geq$ -20 dB and GDOP $\leq$ 1 km/cec. All station combinations with non-zero GCFs are listed on the left and the GCF is given under the column corresponding to the number of stations in the combination. For example, 4-Station Combination BEGH covers 0.0584 of the earth's surface area. A column total is given as the first row at the bottom showing that 4-station coverage is the most prevalent, covering approximately 40% of the earth's surface. The next row shows the cumulative total area covered by the number of stations at the top of column plus the area covered by all higher numbers of station combinations. Thus, approximately 97% of the earth's surface area is covered by 3 or more stations. The bottom row indicates the fractional coverage of each individual station, indicating a maximum coverage of 64% for station H and a minimum coverage of 40% for Station A. These GCFs are rearranged into a specific combinatorial ordering before being placed in a data file to be read by the program which computes P_{SA}. GCF lists are also given for SNR $\geq$ -30 dB and for GDOP unrestricted.

Table C.1-1 Global Coverage Fractions for May/0600 UT/10.2 kHz with SNR ≥ -20 dB, $\Delta\phi \leq 20$ cec and GDOP ≤ 1 km/cec

Number of Stations

	0	1	2	3	4	5	6	7	8
G H			0.0006						
F G			0.0013						
F G H				0.0001					
E H			0.0083						
E G H				0.0188					
E F				0.0006					
E F G				0.0008					
E F G H					0.0378				
D G H				0.0090					
D E G H					0.0031				
D E F				0.0005					
D E F G H						0.0022			
C G H				0.0009					
C F G				0.0017					
C F G H					0.0316				
C E G H					0.0083				
C E F G			0.0016		0.0001				
C E F G H			•	0.0014		0.0128			
C D			•						
C D H			•	0.0196					
C D G H				•	0.0884				
C D F				•					
C D F H					0.0007				
C D F G					0.0096				
C D F G H					•	0.0509			
•					•	•			
•					•	•			
•									
A B D H					0.0001				
A B D F					0.0070				
A B D F H						0.0005			
A B D E H						0.0000			
A B D E F						0.0241			
A B D E F H							0.0010		
A B C E					0.0005				
A B C E H						0.0014			
A B C E G						0.0001			
A B C E G H							0.0003		
A B C E F						0.0019			
A B C E F H							0.0187		
A B C D					0.0004				
A B C D H						0.0067			
A B C D G H							0.0074		
A B C D F						0.0276			
A B C D F G							0.0077		
A B C D E H							0.0142		
A B C D E G H								0.0013	
A B C D E F							0.0026		
A B C D E F H								0.0070	
COL TOTAL	0.0	0.0	0.0123	0.0813	0.4044	0.3584	0.1174	0.0083	0.0
CUM TOTAL	0.9821	0.9821	0.9821	0.9698	0.8885	0.4841	0.1257	0.0083	0.0
STATION	A	B	C	D	E	F	G	H	
COVERAGE	0.3978	0.4794	0.5521	0.5819	0.6156	0.6068	0.5710	0.6359	

C.2 TWENTY-FOUR-HOUR/FOUR-MONTH/TWO-FREQUENCY DATABASE

This database (Database (2)) is also compiled from calculations of signal parameters using a full-wave waveguide-mode model but with slightly different version of the program (Ref. 10). As with the database described in Section C.1, many signal, noise, and geometrical parameters were output in the original calculations but only those parameters required by the signal access criteria are extracted to form this signal coverage database. These parameters include

- Ratio of short-path mode-sum amplitude to noise level in 100 Hz BW (SNR)
- Short-path mode-sum amplitude
- Phase deviation $\equiv \Delta\phi = \mathrm{MOD}_1 \, |\phi_{MS} - \phi_{M1}|$ where ϕ_{MS} is the mode-sum phase (cycles), ϕ_{M1} is the mode-1 phase (cycles), and MOD_1 means modulo one cycle.
- Dominant mode number*
- Illumination, condition (day, night, or transition) at the path point
- Angle between the great-circle propagation path and great-circle terminator (computed as the angle between the normals to the planes containing the two great circles).
- Mode-1 phase (short-path) = ϕ_{M1}
- Long-path mode-sum amplitude.

The original computations were made at path intervals of 100-300 km but to facilitate data extraction and long-path/short-path comparisons, data at the original computation points were interpolated† at fixed 500 km intervals along all paths. To obtain long-path information, calculations were carried out to ranges of 39 Mm along each path. Radial path calculations of the signal parameters were made at bearing intervals of 10° (starting at 0° geographic north and proceeding clockwise). Additional radial path calculations for intervening bearings were made for cases requiring more coverage definition/resolution, e.g., in those angular intervals where paths are nearly tangent to edges of low-conductivity regions or where modal parameters change rapidly. Table C.2-1 lists for each station the radial path bearings for which path

* The modes are generally numbered in order of increasing phase velocity. The odd-numbered modes are the transverse magnetic (TM) modes and the even numbers refer to transverse electric (TE) modes.

† Values normally expressed in dB (e.g., SNR and amplitude) are converted to the actual (non-logarithmic) values prior to interpolation.

Table C.2-1 Additional Station Radials

STATION NAME	ADDITIONAL RADIALS	
	Geographic Bearing Angle of Radials (deg) at the Station	TOTAL NUMBER
Norway (A)	45, 105, 115, 225, 285, 295	6
Liberia (B)	17, 156, 165, 175, 178, 197, 336, 345, 355, 358	10
Hawaii (C)	5, 25, 27, 152, 163, 167, 185, 205, 207, 332, 343, 347	12
North Dakota (D)	8, 35, 44, 165, 188, 215, 224, 345	8
La Reunion (E)	13, 23, 148, 155, 167, 174, 193, 203, 328, 335, 347, 354	12
Argentina (F)	5, 16, 22, 152, 175, 178, 185, 196, 202, 332, 355, 358	12
Australia (G)	5, 18, 165, 173, 185, 198, 345, 353	8
Japan (H)	2, 5, 26, 165, 172, 175, 182, 185, 206, 345, 352, 355	12

calculations were made in addition to the 36 paths at bearing intervals of 10° computed at all stations.

For the effort described in this report, only the full-wave calculations for Omega Station (C) Hawaii (OMSTA Hawaii) are used in compiling the signal coverage database. Following the interpolation of the data to 0.5 Mm path intervals, the long-path amplitude data are associated with the short-path amplitude data according to the following relationship

$$A_S(r,\beta) \longleftrightarrow A_L\,(2\pi R_E - r, \beta + \pi)$$

where $A(s,\gamma)$ is the signal amplitude for Station C propagating along a path of length s and bearing γ (in radians) measured clockwise from geographic north at the station. Thus, 39 data records (20 Mm x 1 data record/0.5 Mm -1 (no record at 20 Mm)) are computed for each path/bearing and the 48 path/bearings computed for the station comprise one data file. Each data file represents path calculations from a station at a given signal frequency for one particular hour/

month combination. Since there are 96 computation times (4 months x 24 hours), 96 data files are created for each frequency (10.2 and 13.6 kHz). Figure C.2-1 illustrates how the data is organized. Each row of 48 radial path/bearings represents one data file and is labeled by a month/hour.

Each data record contains the signal/noise/geometric parameters listed above. Figure C.2-2 shows sample records from the beginning of a data file. The file header labels the file as Station C (OMSTA Hawaii), 13.6 kHz, February, 0100 UT. The last two items indicate path segment length (0.5 Mm) and number of segments/path (39). The second record of the header indicates the path bearings of the additional radials in degrees (3 digits/datum). Note that only six are listed; the remaining six are obtained by adding 180° to each of the first six. The first data record corresponds to a point 0.5 Mm due north of OMSTA Hawaii (radial bearing of 0°). The first datum, SNR, has units of dB in a 100 Hz BW. Both mode-sum amplitude (second datum) and long-path amplitude (last datum) have units of dB relative to 1 μV/m. Both phase deviation (third datum) and mode-1 phase (seventh datum) have units of centicycles but phase deviation is, by definition, always positive (0 to 99 cec) whereas mode-1 phase (-999 to +999)

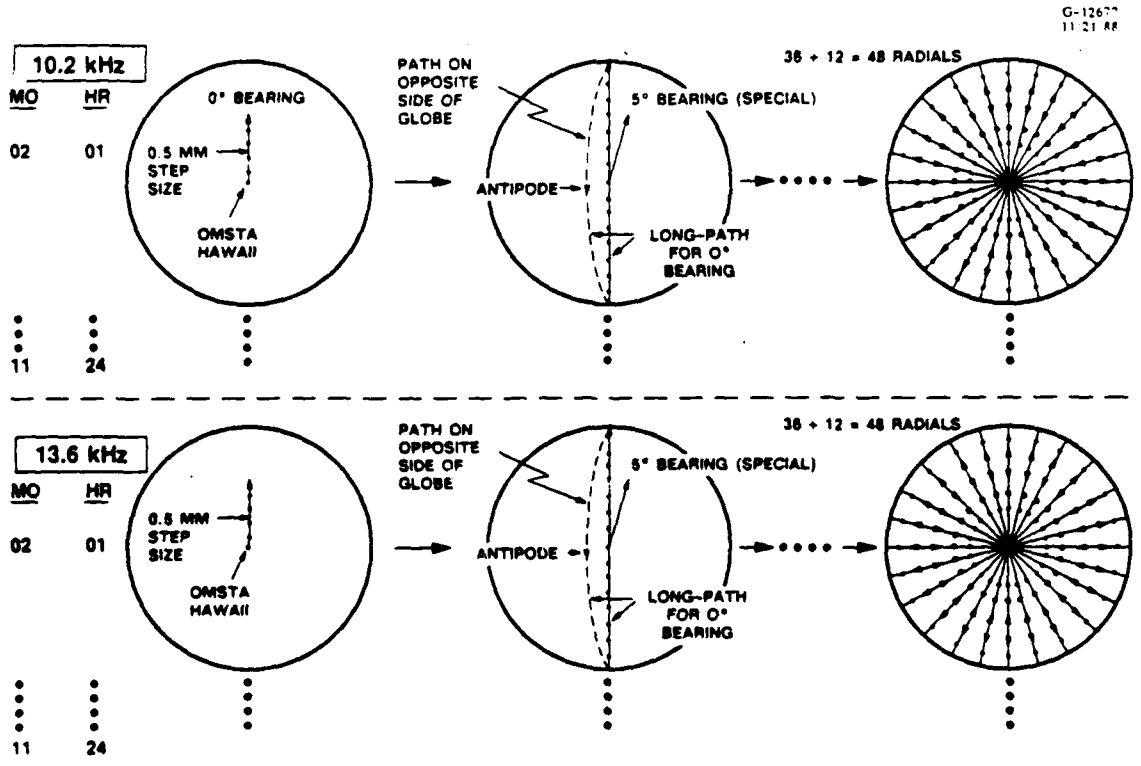

Figure C.2-1 Illustration of 24-Hour/4-Month/2-Frequency Database Organization for OMSTA Hawaii

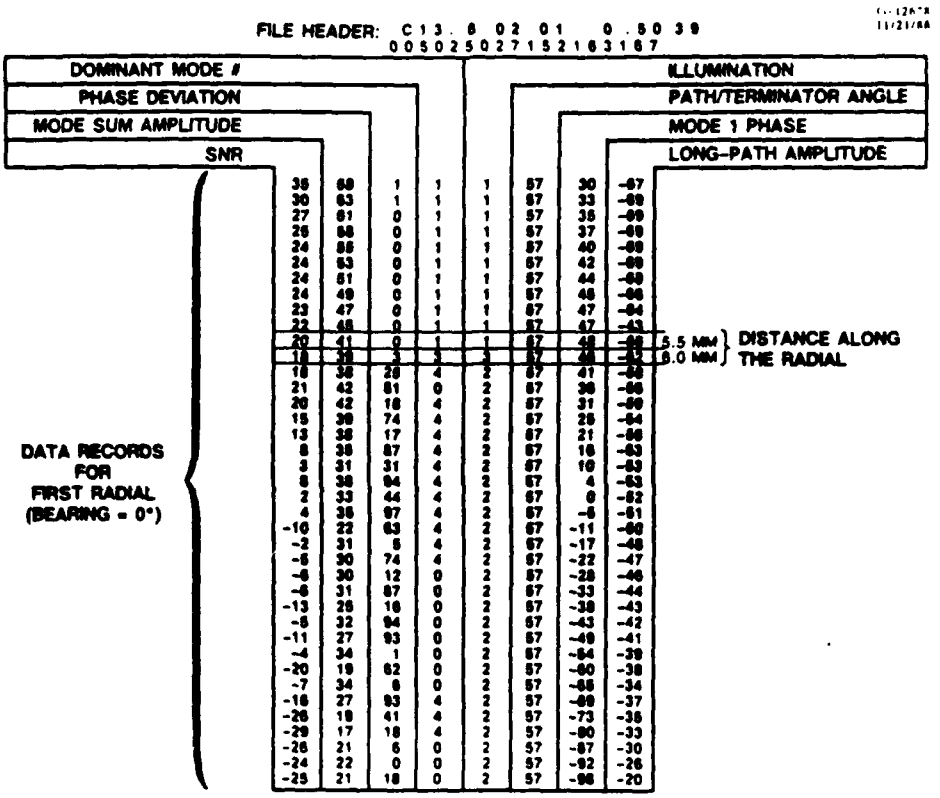

Figure C.2-2 Data Records for Sample Data File from OMSTA Hawaii 24-Hour/4-Month/2-Frequency Database

can range over both positive and negative values of multiple lanes. Dominant mode number (fourth datum) displays a zero if no mode is dominant* and an asterisk if mode X is dominant (Ref. 10). Illumination condition (fifth datum) is indicated by 1(day), 2(night), or 3(transition†). The sixth datum is a quantity which is 100 times the absolute value of the cosine of the path/terminator angle.

The data described above is structured on a range-azimuth "grid" centered at the station. Because coverage data and display are now being targeted for a matrix/cell format (instead of contours) to support system availability calculations and other applications, the range-azimuth data is interpolated onto the latitude/longitude grid structure shown in Table C.2-2. This provides a matrix of 444 cells, each of which contains (for the 96 times) the data items shown in Fig. C.2-2 (except for Mode-1 phase). To determine signal coverage, signal access criteria are applied to the coverage data and combined appropriately. The signal access criteria may be determined by the database user (although default values can be used) to tailor the coverage for a

*A mode is dominant if its amplitude is more than 2 dB larger than: (1) any other mode amplitude and (2) the amplitude of the vector sum of the other component modes.

†Solar zenith angle is 90° within the 0.5 Mm path segment.

Table C.2-2 Latitude/Longitude Dimensions of Cells in Grid Structure for Signal Coverage Database (Matrix Format)

LATITUDE RANGE*	LATITUDE DIMENSION OF CELL	LONGITUDE DIMENSION OF CELL	NUMBER OF CELLS IN BOTH HEMISPHERES
0° TO 40°	10°	10°	288
40° TO 60°	10°	15°	96
60° TO 75°	15°	15°	48
75° TO 90°	15°	60°	12
TOTAL NUMBER OF CELLS = 444			

*Same for northern and southern hemisphere

particular application. This freedom is not provided in the 2-hour/4-month database since only contour coordinates or the list shown in Table C.1-1 are available (although two options (-20 dB and -30 dB) are included for SNR). Default signal access criteria are given as:

- SNR $\geq$ -20 dB (100 Hz BW)
- $\Delta\phi \leq 20$ centicycles
- Dominant mode number = 1
- Path-terminator angle $\geq 5°$
- Ratio of short-path amplitude to long-path amplitude $\geq$ 3 dB

This format also allows GDOP or other accuracy figure as a signal access criterion if sufficient external information is available.

Table C.2-3 shows a sample of the signal coverage database in matrix format for OMSTA Hawaii, 13.6 kHz, February, 1800 UT. The signal access criteria may be expressed as

SHORT-PATH SNR $\geq$ -37.2 dB (100 Hz BW)
AND
DOMINANT MODE=1
AND
$[(0 \leq \Delta\phi \leq 20 \text{ cec}) \text{ OR } (80 \text{ cec} \leq \Delta\phi \leq 100 \text{ cec})]$

The first column in Table C.2-3 gives the cell number, while the second and third show range (Mm) and bearing (clockwise from geographic north in degrees) from OMSTA Hawaii to the center of the cell. The fourth and fifth columns list short-path and long-path SNR (dB in 100 Hz BW), respectively. The table shows that the short-path SNR criterion is satisfied everywhere and the smallest short-path amplitude to long-path amplitude ratio* (not a signal access criterion) is 6 dB for cell 16. Phase deviation (centicycles) is given in the sixth column, and the corresponding signal access criterion is seen to fail at cells 18, 26, 29, and 30. The seventh column shows a figure which is 100 times the absolute value of the cosine of the path-terminator crossing angle. When invoked, this coverage criterion only applies when the terminator cuts the short path

Table C.2-3 Sample of Signal Coverage Database in Matrix Format for OMSTA Hawaii/13.6 kHz/February/1800 UT; Signal Access Criteria: SNR ≥ -37.2 dB and Dominant Mode=1 and ($0 \leq \Delta\phi < 20$ cec or 80 cec $\leq \Delta\phi \leq 100$ cec)

CELL	RANGE (Mm)	BEARING (Degrees)	SHORT-PATH SNR(dB)	LONG-PATH SNR(dB)	$\Delta\phi$ (cec)	CROSSING ANGLE*	DOMINANT MODE NUMBER	WEIGHT	COVERAGE
1	6.8	1.2	13.0	-99.0	2	92	1	1	1
2	7.3	7.6	14.0	-81.0	6	95	3	1	0
3	8.1	6.2	13.0	-77.0	3	94	3	1	0
4	8.4	359.0	10.0	-99.0	1	90	1	1	1
5	7.9	352.7	9.0	-96.0	1	86	1	1	1
6	7.1	353.4	10.0	-96.0	2	86	1	1	1
7	5.2	352.4	12.0	-99.0	2	86	2	1	0
8	5.1	0.2	15.0	-99.0	3	91	1	1	1
9	5.2	8.0	15.0	-91.0	2	95	1	1	1
10	5.5	14.7	16.0	-67.0	0	96	3	1	0
11	6.0	19.7	15.0	-56.0	0	97	3	1	0
12	6.6	22.8	13.0	-37.0	1	97	1	1	1
13	7.2	24.2	7.0	-29.0	1	97	1	1	1
14	7.8	24.0	1.0	-26.0	2	97	1	1	1
15	8.4	22.4	-4.0	-29.0	4	97	1	1	1
16	9.0	19.5	-14.0	-20.0	1	97	3	1	0
17	9.5	15.6	-7.0	-30.0	8	96	3	1	0
18	9.8	10.9	-4.0	-49.0	38	95	2	1	0
19	10.0	5.6	2.0	-87.0	9	94	2	1	0
20	10.1	359.9	6.0	-99.0	0	91	1	1	1
21	10.0	354.2	4.0	-98.0	1	87	1	1	1
22	9.8	348.9	2.0	-80.0	1	83	1	1	1
23	9.4	344.2	0.0	-51.0	15	78	2	1	0
24	9.0	340.3	3.0	-42.0	85	74	2	1	0
25	8.4	337.5	6.0	-41.0	88	71	2	1	0
26	7.8	336.0	9.0	-41.0	67	69	2	1	0
27	7.1	335.8	11.0	-42.0	88	69	2	1	0
28	6.5	337.3	11.0	-42.0	81	71	2	1	0
29	6.0	340.5	11.0	-43.0	77	74	2	1	0
30	5.5	345.6	11.0	-56.0	24	80	2	1	0

*100 x | cos (Path / Terminator Angle) |

*The ratio of long-path and short-path amplitudes is the same as the ratio of the corresponding SNRs since the common noise cancels.

between the station and the cell. Dominant mode number is listed in the eighth column and numbers other than one (a failure of the criterion) appear in a large percentage of the cells shown. In fact, this criterion is responsible for negating coverage in every uncovered cell shown (occasionally sharing equal responsibility with phase deviation). The ninth column shows the weight attached to a particular cell to indicate geographic priority of that cell for an Omega user or group of users. Here, the default uniform distribution (all cells weighted "1") is used. The last column indicates the cell coverage, i.e., the collective result of applying the signal access criteria.

C.3 PLAN FOR OMEGA ACCESS UPGRADE AND INCORPORATING VLF

Omega Automated Composite Coverage Evaluator of System Signals (Omega ACCESS) (Ref. 35) is a microcomputer-based software package which can be used to extract and display coverage data available from Database (1). Additional data were supplied to permit portrayal of coverage for each Omega station at two power levels: 10 kW and 2.5 kW. In addition, coverage data for OMSTA Japan at 6.3 kW, 4 kW, 1.6 kW and 1 kW were included in the software package. To make use of Database (2) and present coverage information in a matrix display format, Omega ACCESS must be upgraded. VLF station data can also be accommodated in the matrix format and composited with the Omega information. The nature of the input data and candidate output screens are presented in the following sections.

C.3.1 Input Data

A key issue in providing an upgraded Omega ACCESS for the Omega user community is the level of information to provide. Two principal questions to be answered are: (1) What size matrix cell should be used and (2) how much raw data should be provided? The sizes that have been investigated are cells with a nominal 10 degree x 10 degree and 5 degree x 5 degree size. Table C.2-2 gives the latitude and longitude intervals for 10 degree x 10 degree cells; intervals for 5 degree x 5 degree cells are obtained by dividing each latitude and longitude interval shown in the table by 2. For most applications the 10 degree x 10 degree cell structure has adequate resolution and is consistent with the resolution of the underlying data.

The information which must be available to the Omega ACCESS user on a cell-by-cell basis is:

- Short-path SNR
- Short-path/long-path SNR ratio and corresponding signal access criterion
- Phase deviation/dominant mode number and corresponding signal access criterion
- Path/terminator crossing angle and corresponding signal access criterion.

To provide this information, the upgraded Omega ACCESS database must have at least one number (short-path SNR) and three flags* for every matrix cell. The flags can also be derived from the short-path SNR, short-path amplitude, long-path amplitude, phase deviation, dominant mode number, and crossing angle. This "raw data" may be useful to some users or to ONSCEN for some types of analyses. Although it will increase the size of the ACCESS database, it is recommended that the raw data, rather than just flags, be stored.

The resolution required for all the parameters stored in the ACCESS database is the nearest whole number (dB, cec, or degree). Therefore, one byte will be required for each parameter, or four bytes per matrix cell†. At the 10 degree x 10 degree size, there are 444 cells to cover the world for one time (hour/month), station, and frequency. Each frequency/time/station matrix will require 1776 bytes of storage (4 x 444). The complete 24-hr/4-month/2-frequency database will have 1536 matrices (24 x 4 x 2 x 8 stations) of 444 cells each. This amounts to about 2.6 megabytes of storage. On a typical floppy disk, some space is wasted due to constraints on the minimum allocation of space (sectors and clusters). If each matrix is stored as a separate file, then each would use 2048 bytes of disk space and the entire database would require 3.0 megabytes of storage. For purposes of distribution, the entire database would fit onto three high density 5.25 inch floppy disks (1.2 megabytes each), possibly with space for the program and map files to fit as well. It should be noted that, if only flags are stored in the database rather than values for three of the parameters, exactly half as much storage space is required.

---

*For example, if the phase deviation of a particular signal accessed at a given cell exceeds the corresponding signal access criterion (typically, 20 cecs) then a "modal" flag would be attached to that signal/cell combination (for a given time).

†Dominant mode number is combined with phase deviation such that the combination is stored as one byte. This is done by adding zero if the dominant mode number is 1 and adding 100 if the dominant mode number is not 1. This allows unique identification since the phase deviation ranges between 0 and 99 (cec).

The nine VLF stations shown in Table C.3-1 range in frequency from 16 kHz to 24.8 kHz. At present only SNR information is readily available for these stations. However, the same database structure used for the Omega data will be used for the VLF data to provide uniformity and space for possible additional VLF station parameters.

The required storage space for the VLF database (10 degree x 10 degree-size cells, all parameters) is 3.375 megabytes. This database also should fit on three 1.2 megabyte floppy disks.

The other input data required by an updated Omega ACCESS is a definition of the cell structure. This data defines the corners of the cells in latitude/longitude and in the screen coordinates for the map projections supported by Omega ACCESS.

C.3.2 Output Screens

The Setup Screen for the updated Omega/VLF ACCESS would be very similar to that for the current version of ACCESS. However, the Display Screens will be different, reflecting the matrix form of coverage display. The revised Setup Screen is shown in Fig. C.3-1. Rather than select/deselect stations on the map as in the current ACCESS, the station selection may be

Table C.3-1 VLF Stations for Omega/VLF ACCESS

STATION ID	LOCATION	LATITUDE	LONGITUDE	FREQUENCY (kHz)	POWER (kW)
GBR*	Rugby, U.K.	52° 22'N	1° 11'W	16.0	65
JXZ*	Noviken, Norway	66° 58'N	13° 53'E	16.4	-200
NDT**	Yosami, Japan	34° 58'N	137° 01'E	17.4	38
GBZ*	Anthorne, U.K.	54° 55'N	3° 16'W	19.0	80
NSS†	Annapolis, MD, U.S.	38° 59'N	76° 27'W	21.4	390
NWC†	Exmouth, Australia	21° 49'S	114° 10'E	22.3	1800
NPM†	Lualualei, HI, U.S.	21° 26'N	158° 09'W	23.4	530
NAA†	Cutler, Me, U.S.	44° 39'N	67° 17'W	24.0	1740
NLK†	Jim Creek, Washington, U.S.	48° 12'N	121° 55'W	24.8	192

*Operated by the North Atlantic Treaty Organization (NATO).

†Operated by the U.S. Navy (USN).

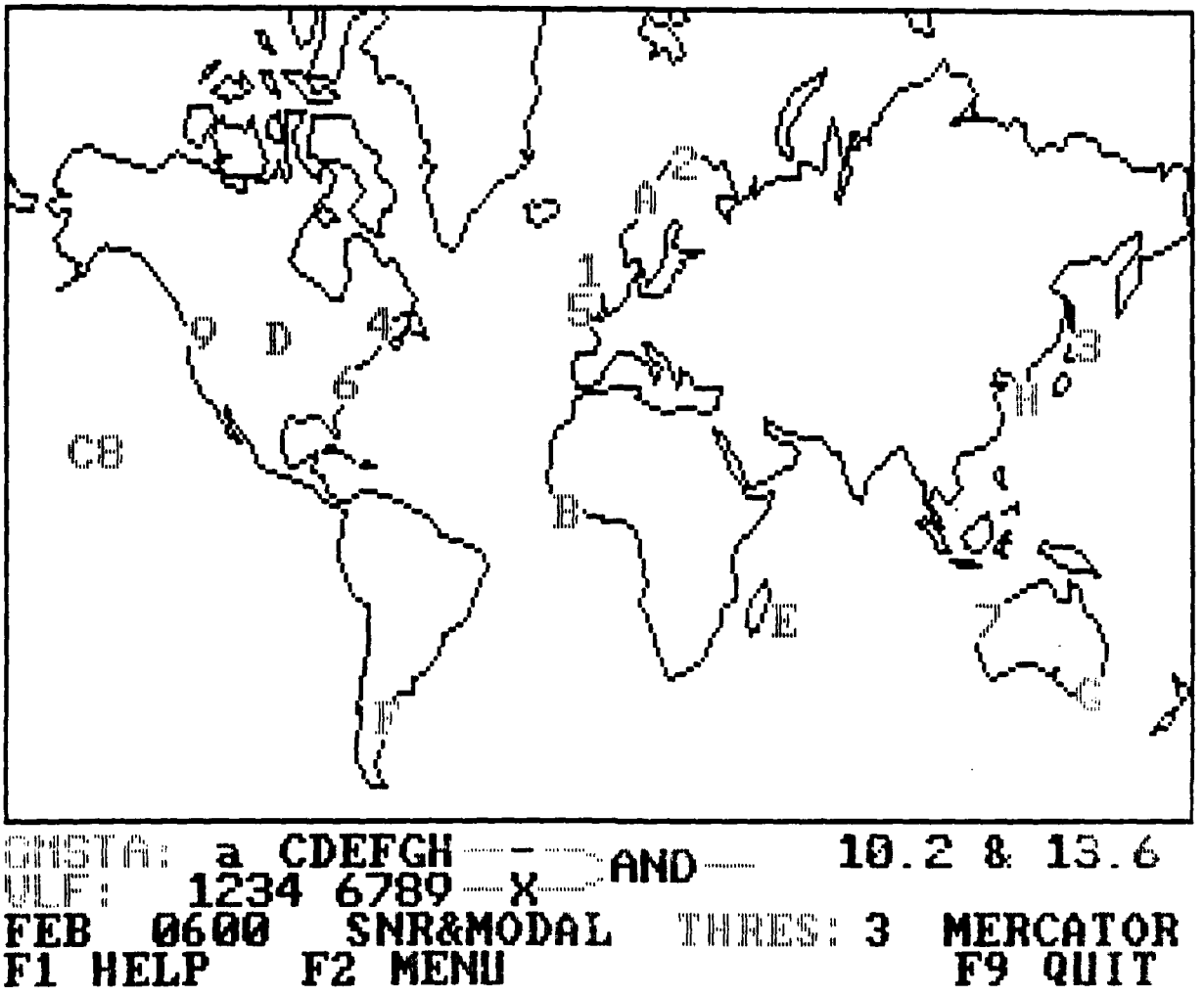

Figure C.3-1 Sample Setup Screen for Omega/VLF ACCESS

toggled by clicking on the station letters and numbers at the bottom of the screen. Either or both Omega and VLF station sets may be selected and combined. The "-" and "X" indicators to the right of the numbers/letters in the example in the figure indicate that the Omega stations are selected and the VLF stations are deselected. These selectors may be toggled by clicking on them. The word "AND" to the right of these selectors indicates how to combine the Omega station and VLF station coverages, if they are both selected. This option toggles between "AND" and "OR" to indicate the logical operations which are performed. The remaining options on this screen are the same as for the current Omega ACCESS.

The multi station Display Screen is the same as for the current Omega ACCESS. Coverage areas where the number of available stations are greater than, equal to, or less than the selected threshold level are indicated by colors. The display is generated by compositing cells rather than overlaying coverage areas generated by contours. Therefore the time required to generate the screen should be much less than for the current Omega ACCESS. The query function will operate much differently in the new Omega/VLF ACCESS. Figure C.3-2 shows an example of the Display Screen with the pop-up query window overlaid. The window shown lists all the available parameters for all the Omega stations for the matrix cell which was selected (by

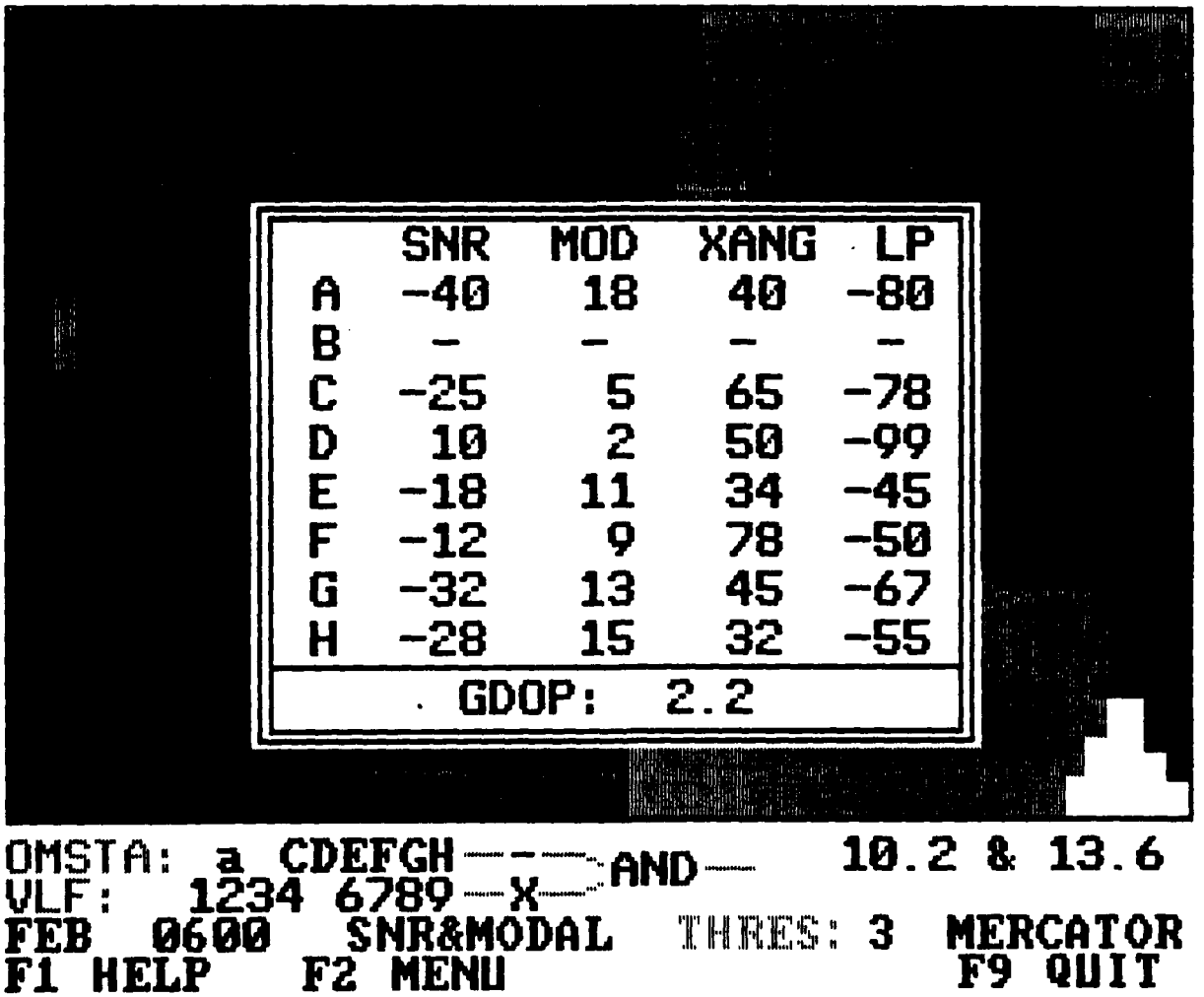

Figure C.3-2 Sample Multi-station Display Screen for Omega/VLF ACCESS

cursor placement). The parameters, left to right, are short path SNR in dB, phase deviation* (Modal) in cec, path/terminator crossing angle in degrees, and long-path SNR in dB. The GDOP for a point in the center of the selected cell is shown at the bottom of the window.

The output screens for the upgraded Omega (or Omega/VLF) ACCESS differ most from the current Omega ACCESS in the single-station Display Screen. In the current Omega ACCESS, the single-station display screen is simply a degeneration of the multi-station screen. The area of coverage (as determined by the selected criterion) is currently displayed on this screen. For the upgraded ACCESS, the single-station screen shows:

- The gradation of short-path SNR
- Modal areas (excessive phase deviation or dominant mode number not equal to 1)
- Areas of low path/terminator crossing angle
- Areas where the long-path SNR is too high relative to the short path SNR.

A sample single-station display screen is shown in Fig. C.3-3 with a query window overlaid on it. The query window displays specific values of the coverage parameters at the designated latitude/longitude.

C.3.3 Conclusions

The changes to Omega ACCESS necessary to incorporate Database (2), matrix display format, and VLF data are straightforward in nature. The development of a new Omega/VLF ACCESS would be facilitated by incorporating all three changes in a single upgrade. The upgraded Omega/VLF ACCESS would retain the user friendliness and compatibility with industry-standard microcomputers which is built into the current Omega ACCESS.

*Dominant mode number is included with this parameter as explained earlier.

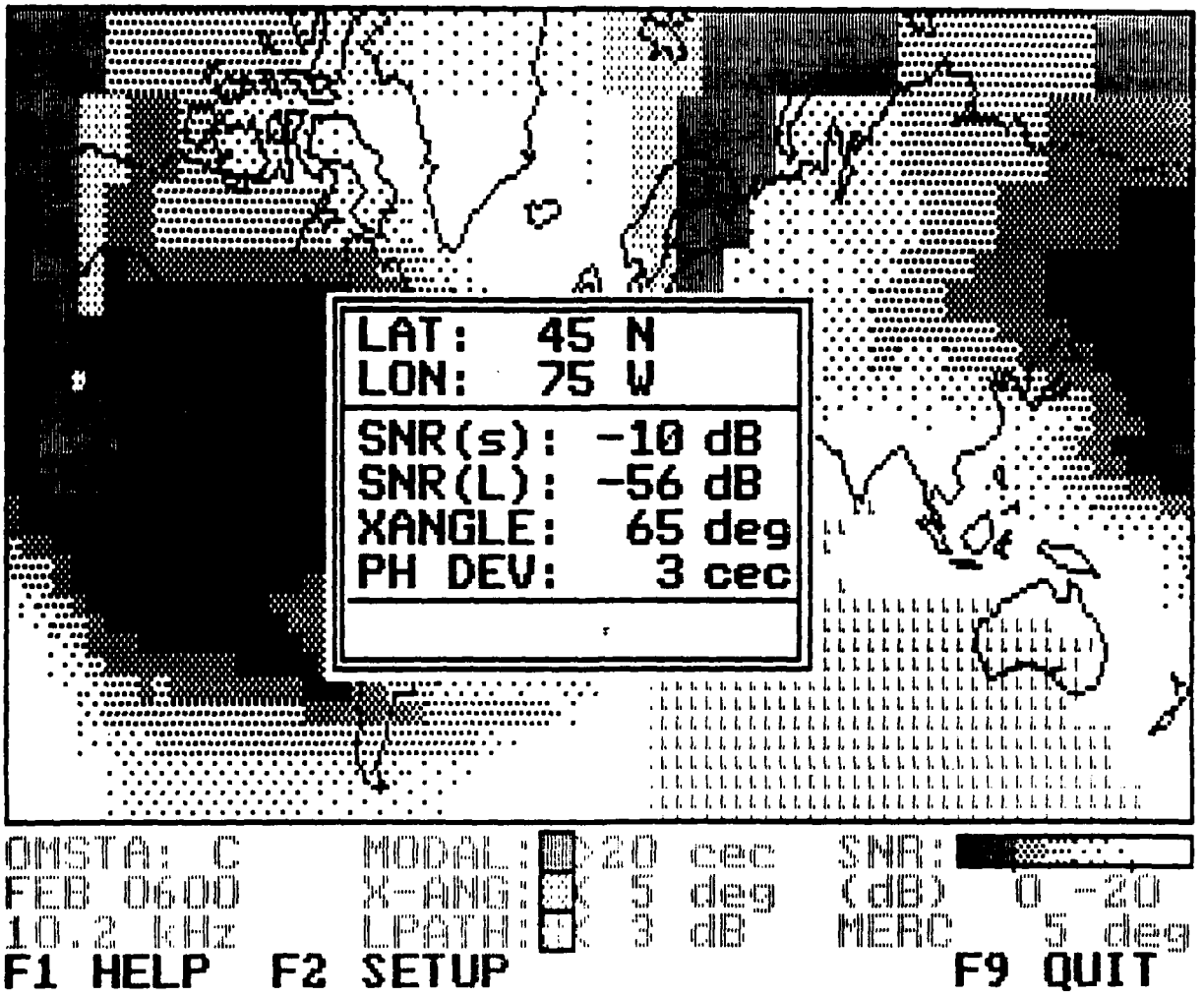

Figure C.3-3 Sample Single Station Display Screen for Omega/VLF ACCESS

APPENDIX D

STATION POWER LEVEL ASSIGNMENT ALGORITHM

The possibility of revising the existing station power level assignments is investigated in light of the emerging availability of comprehensive signal coverage diagrams and the need to reduce costs and increase reliability at all levels of system operation. The objective is to reduce station electric power costs by lowering station power levels to the point that a minimum-acceptable system availability index, P_{SAT}, is achieved. A cost function is developed which accounts for the differing costs to produce power at each station (referenced to a common monetary basis), i.e.,

$$CF \equiv \beta \sum_{i=1}^{8} a_i P_i$$

where:

$\beta \equiv$ normalizing factor $= 1/\sum_{i=1}^{8} a_i$

$P_i \equiv$ power level for station i

The cost function CF is to be minimized subject to the constraint

$$P_{SA}(\vec{P}) \geq P_{SAT} \; ; \; \vec{P} = (P_1, P_2, \ldots P_8)$$

Since CF and P_{SA} both increase (decrease) with increasing (decreasing) P_i, the constraint becomes the equality

$$P_{SA}(\vec{P}) = P_{SAT}$$

Thus, the problem is reduced to finding the $\{P_i\}$ such that CF is a minimum subject to $P_{SA} = P_{SAT}$.

The power level assignment problem can be viewed as a minimization problem in an 8-dimensional space. The desired power level vector $\vec{P}$ results from the intersection of a hyperplane $CF = \beta\vec{a}\cdot\vec{P} = \eta'$ and $P_{SA}(\vec{P}) = P_{SAT}$. An implicit constraint in this problem is that the components, P_i, lie between 0 and 10 kW (represented by an 8-dimensional hypercube), although the upper limit could easily be extended without affecting the operation of the algorithm.

Because it involves signal coverage over the entire earth's surface, P_{SA} is a very complicated function of $\vec{P}$. However, two general shapes of the $P_{SA}(\vec{P}) = P_{SAT}$ hypersurface are distinguished in this problem — concave and convex. Since the $a_i > 0$ for all i, the intersection of the hyperplane $CF = \beta\vec{a}\cdot\vec{P}$ with a *concave* $P_{SA}(\vec{P}) = P_{SAT}$ hypersurface results in a $\vec{P}'$ which is expected to be well into the interior of the hypercube. On the other hand, the intersection of the hyperplane with a *convex* $P_{SA}(\vec{P}) = P_{SAT}$ hypersurface results in a $\vec{P}'$ which lies on the boundary of the hypercube ($P_i = 0$ or 10 kW for one or more values of *i*). These concepts are illustrated by a two-dimensional cut through the space for the two kinds of surfaces as shown in Fig. D-1.

D.1 SEARCH STEP SIZE

Starting at the initial point $\vec{P}_{10} \equiv (10,10,10,10,10,10,10,10)$, the $P_{SA} = P_{SAT}$ surface is located by proceeding along the hypercube diagonal ($P_1 = P_2 = P_3 = \ldots = P_8$) or along the negative gradient of the hyperplane, $\beta\vec{a}$. Once located, the $P_{SA} = P_{SAT}$ surface is searched to find the minimum CF. If 1 kW steps are assumed (in the interval 0 to 10 kW)*, then search of the entire $P_{SA}(\vec{P}) = P_{SAT}$ hypersurface requires on the order of 10^7 test calculations (for both convex and concave hypersurfaces). If the hypersurface is convex and the entire boundary of the hypercube is searched for a minimum CF, the same number (to an order of magnitude) of iterations is required. To reduce the number of iterations, it is useful to determine the minimum step size.

Figure D.1-1 shows the earth's surface area broken up into cells in a matrix format. In this signal coverage format, each cell contains signal coverage data on all station signals for a fixed hour/month. Only SNR will be addressed here since it is the only signal coverage parameter which is affected by station power level†. The figure shows for a sample cell a schematic representation of SNR (vertical axis) for each station. The "floor" is shown at SNR = -20 dB

*Steps of 1 to 10 dB in power reduction (assuming a 1 kW minimum power level) can also be used. Numerically, this yields the same number of steps but, being logarithmic, the values are different.

†Signal coverage parameters/criteria (e.g., modal, long-path) which "pre-empt" the SNR criterion will be considered to the extent that they exclude certain station signals/cells. For example, if station B is modal in a certain cell (at a given time), it is excluded from consideration since power level changes at the station will not change its modal status.

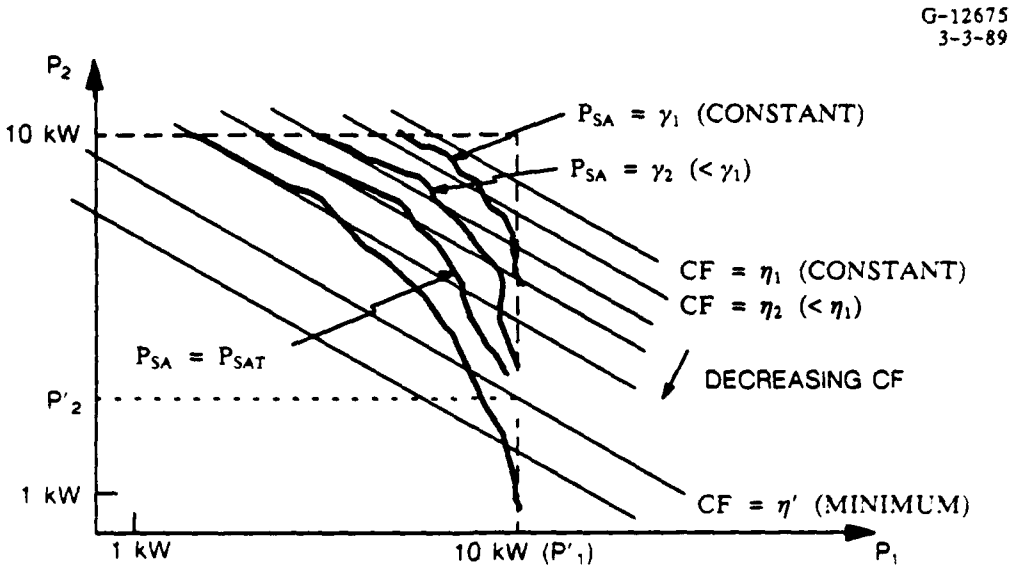

a) Convex Form of P_{SA} Contour

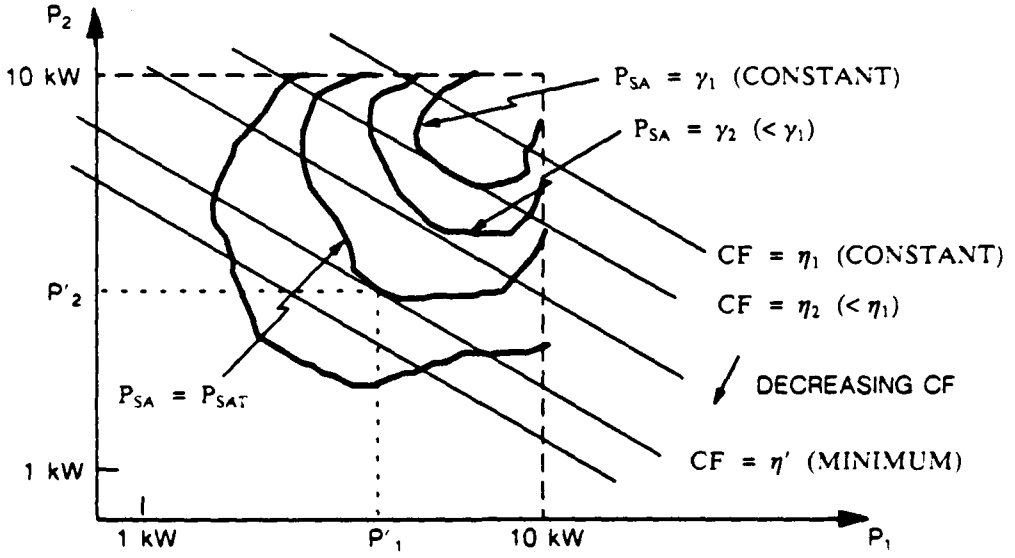

b) Concave Form of P_{SA} Contour

Figure D-1 Illustration of Station Power Level Assignment Algorithm in Two Dimensions for Type Types of P_{SA} Contours Defined by $P_{SA} = P_{SAT}$

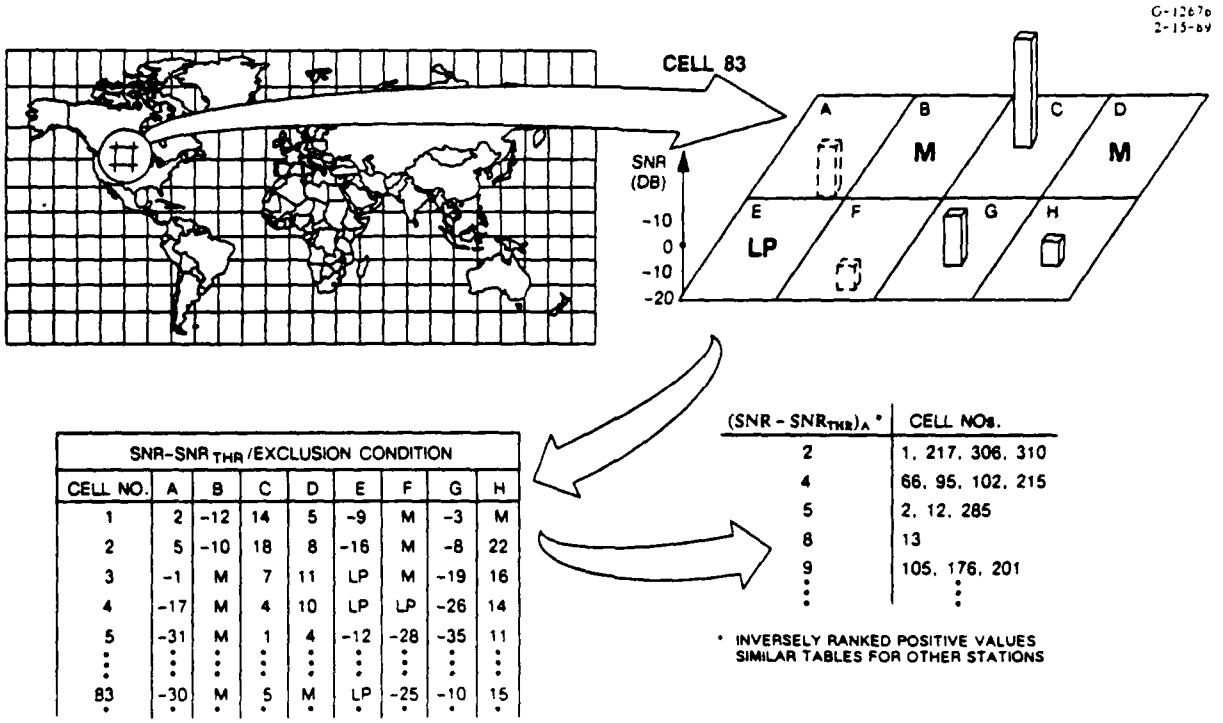

SNR-SNR THR /EXCLUSION CONDITION								
CELL NO.	A	B	C	D	E	F	G	H
1	2	-12	14	5	-9	M	-3	M
2	5	-10	18	8	-16	M	-8	22
3	-1	M	7	11	LP	M	-19	16
4	-17	M	4	10	LP	LP	-26	14
5	-31	M	1	4	-12	-28	-35	11
⋮	⋮	⋮	⋮	⋮	⋮	⋮	⋮	⋮
83	-30	M	5	M	LP	-25	-10	15
•	•	•	•	•	•	•	•	•

$(SNR - SNR_{THR})_A$ *	CELL NOs.
2	1, 217, 306, 310
4	66, 95, 102, 215
5	2, 12, 285
8	13
9	105, 176, 201
⋮	⋮

* INVERSELY RANKED POSITIVE VALUES
SIMILAR TABLES FOR OTHER STATIONS

Figure D.1-1 Methodology for Determining Power Level Reduction Increments for Station Power Level Assignment

corresponding to the signal access criterion (all stations at 10 kW) and each station is associated with a rectangular segment in the horizontal plane. Thus, stations A and F have SNRs below -20 dB, stations B and D are modal, and Station E is long-path-dominated. Since power-level reduction is being considered, Stations A and F are excluded, as further power decreases will depress their SNRs further below the SNR floor. Stations B, D, and E are excluded because they fail signal access criteria which are power-level independent. The lower left panel of the figure shows a table which lists, for each station, the difference (in dB) between the SNR and the threshold SNR (-20 dB) or any exclusion condition which pre-empts the SNR criterion. Only the positive, numerical quantities in each row are of interest, since these represent station signals which have a margin above the SNR floor and thus can tolerate a power reduction (for that cell only). If the *positive* values of $SNR-SNR_{THR}$ are ranked from smallest to largest for each station, the sample table (for Station A) in the lower right panel is obtained. This table shows the important result that if Station A's power level is reduced by less than 2 dB, cell coverage will not change and, hence, P_{SA} will not change. Similarly, coverage will not change again until A's power level is reduced another 2 dB (to 4 dB below 10 kW). Similar considerations apply to greater power reductions. Thus, for example, there is no need to test Station A's power level at

3 dB below 10 kW (i.e., 5 kW), assuming the 2 dB reduction was already tested, since P_{SA} cannot change between the two levels of reduction. Care must be taken, in deriving the table of rankings, that a station's power reduction value for a given cell must not be entered if less than three positive numbers occur for that cell in the table on the lower left, since otherwise the cell cannot be covered for any positive value of power reduction. More than just step size, this methodology specifies the particular SNR values at which the steps are to be taken.

D.2 ALGORITHM FOR CONCAVE HYPERSURFACE

Figure D.2-1 illustrates the procedure for finding $\vec{P}'$ in the hypercube which results from the intersection of the CF-hyperplane with minimum parameter (η') and the concave $P_{SA} = P_{SAT}$ hypersurface. The first row of the functional blocks in the figure serve to locate the $P_{SA} = P_{SAT}$ hypersurface, requiring less than 10 steps*. Once the $P_{SA} = P_{SAT}$ hypersurface is reached, a steepest descent method (Ref. 34) can be used to find the minimum CF=η' In

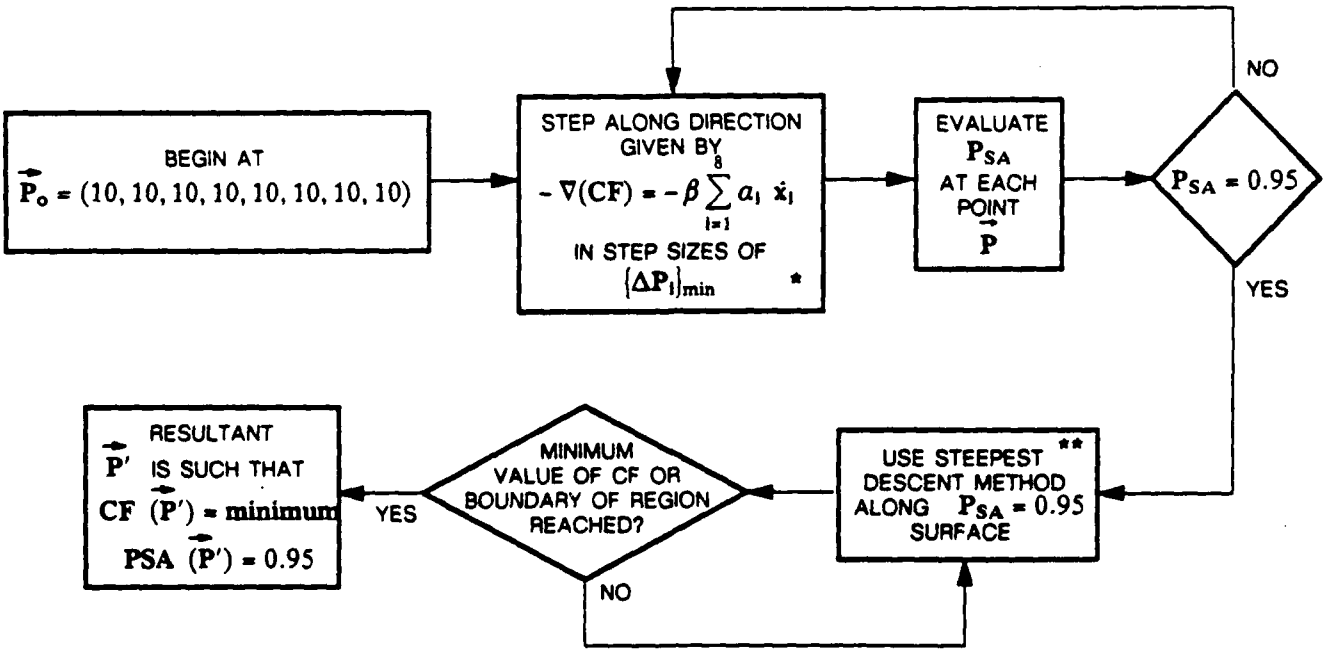

Figure D.2-1 Station Power Level Assignment Algorithm for Concave $P_{SA} = P_{SAT}$ Hypersurface

*Each step requires a calculation of P_{SA} for a given hour/month/frequency, etc.

applying this method, "steepest" refers to the negative gradient of CF, i.e., the vector, $-\beta\vec{a}$. Most versions of this method include checks for local minima and re-initializing the search for the global minimum. If the $P_{SA} = P_{SAT}$ hypersurface is everywhere concave, then the minimum $\vec{P} = \vec{P}'$ is generally single-valued and located in the interior of the hypercube. If the hypersurface is only locally concave, then multiple minima and boundary minima are possible.

D.3 ALGORITHM FOR CONVEX HYPERSURFACE

Figure D.3-1 illustrates the procedure for finding $\vec{P}'$ on the boundary of the hypercube which results from the intersection of the CF-hyperplane with minimum parameter (η') and the convex $P_{SA} = P_{SAT}$ hypersurface. Note that this procedure assumes that the 7-dimensional $P_{SA} = P_{SAT}$ hypersurface intersects the 7-dimensional boundary of the hypercube at a finite number of points (in general, a 6-dimensional "hypercurve"). This assumption is supported by sample calculations which show that, for $P_{SAT} = 0.95$, the $P_{SA} = P_{SAT}$ hypersurface intersects the boundary of the hypercube. The basic idea of the procedure is to search along each edge (eight 1-dimensional edges, seven 2-dimensional edges, etc.) for $P_{SA} = P_{SAT}$. If $P_{SA} = P_{SAT}$ along one or more edges, the corresponding CF values are checked and the edge with the minimum CF then serves as the basis for searching edges in the next higher set of dimensions. This continues until a minimum CF is found or until search is complete through the last 7-dimensional "face".

In the top row of the functional flow in Fig. D.3-1, the search of the eight 1-dimensional edges is illustrated. The example shown is the search along the P_3 "edge" using the steps indicated in Section D.1. If $P_{SA} = P_{SAT}$ is detected, CF is computed and stored. If $P_{SA} = P_{SAT}$ is not detected, the minimum P_{SA} for the P_3 edge is stored. This process is repeated for all edges and when complete, the minimum CF among those computed for each edge is denoted as CF' and the corresponding edge and power level value (in this case, edge P_7 and power level value P_7') are stored as that component of the minimizing vector $\vec{P}'$. If $P_{SA} = P_{SAT}$ is not detected on any edge, the minimum of the minimal P_{SA} values along each edge is stored along with the corresponding P-component. With $P_7 = P_7'$ fixed, the search proceeds in the same way along the seven remaining components. The example in the figure indicates edge P_4 is to be tested for $P_{SA} = P_{SAT}$. The minimum CF-value over all edge points for which $P_{SA} = P_{SAT}$ is now stored as CF' and the minimum edge/power level value shown in the example (see bottom row of the

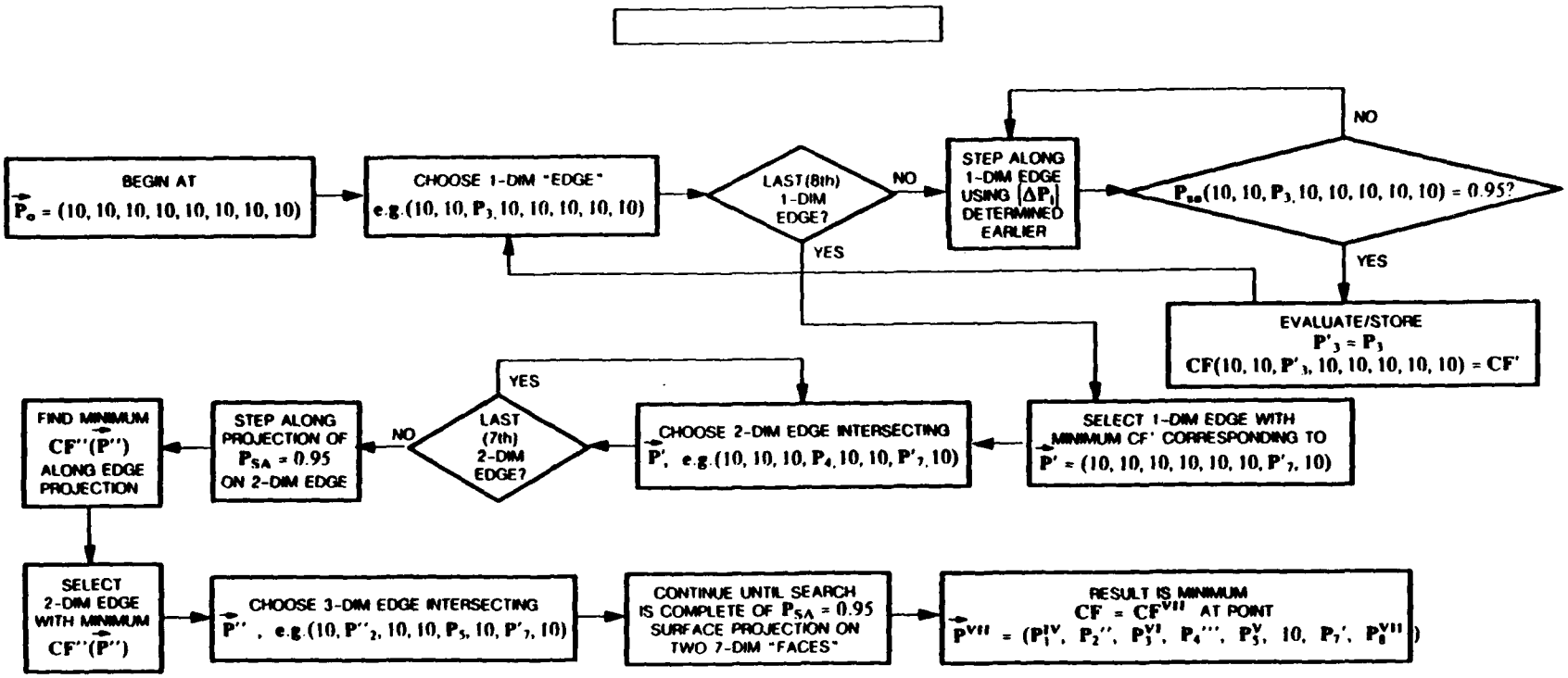

Figure D.3-1 Station Power Level Assignment Algorithm for Convex $P_{SA} = P_{SAT}$ Hypersurface

figure) is P_2. Again, if no $P_{SA} = P_{SAT}$ value is detected, the minimum of the minimal P_{SA} values (and the corresponding P-component) is stored. Note that the search in each new space is 1-dimensional although the search space is augmented by one-dimension each time a new set of edges is introduced. The procedure is continued until seven components are computed. At the conclusion of the algorithm, the intermediate CF-values, e.g., CF', CF'', CF''', are checked to determine if any intermediate minimum is the absolute minimum.

It should be mentioned that this algorithm does not guarantee optimality, i.e., that the minimum CF and corresponding $\vec{P}$ will always be found for $P_{SA} = P_{SAT}$. The algorithm is relatively rapid, however requiring only about 350 steps. An alternative, but longer, procedure is to search the seven-dimensional boundary using a steepest descent algorithm.

APPENDIX E

STRUCTURE OF THE OFF-AIR/MAINTENANCE SCHEDULING ALGORITHM

Off-air periods for each Omega station's required annual maintenance and equipment/structural repair are generally much longer than other scheduled off-airs. As a result, it is important that these off-airs be scheduled so as to maximize system performance. Figure E-1 shows the current (1989) monthly schedule for each station's annual maintenance period.

E.1 PERFORMANCE FUNCTION AND CONSTRAINTS

Since the objective is to maximize *annual* system performance, an algorithm is designed to maximize a performance function given by

$$PF = \sum_{i=1}^{8} w_i \, \bar{P}_{SA}(\vec{P}_i, m_i) \quad \text{(E.1-1)}$$

where

$$\bar{P}_{SA}(\vec{P}_i, m_i) = \frac{1}{T_H} \sum_{h=1}^{T_H} P_{SA}(\vec{P}_i, m_i, h)$$

$P_{SA}(\vec{P}_i, m_i, h)$ = system availability index for month m_i, hour h, and station power level vector $\vec{P}_i$

T_H = total number of hours over which average is desired (limited by database)

$(\vec{P}_i)_j = 10(1 - \delta_{ij})$ in kW, where δ_{ij} is the Kronecker delta

w_i = weighting factor for station i

m_i = annual maintenance month for station i

Here, the station power levels are assumed to be fixed at 10 kW although any fixed level (different or the same for each station) could be used without affecting the execution of the algorithm.

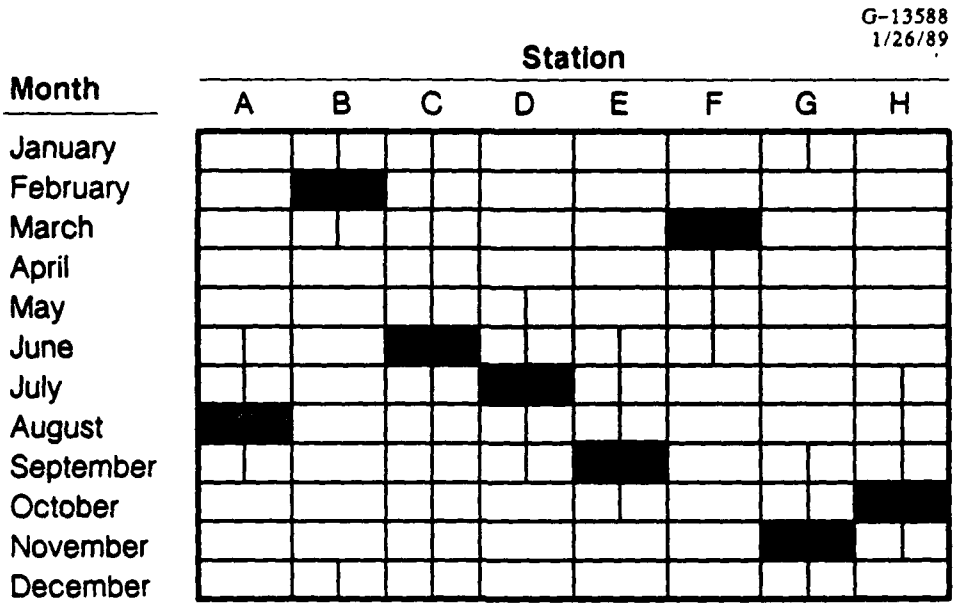

Figure E-1 Allowable Monthly Intervals for Each Station's Annual Maintenance Month (Current Maintenance Month is Shaded)

Unscheduled and scheduled off-air probabilities based on historical reliability figures are used in the monthly calculations of $\bar{P}_{SA}(\vec{P}_i, m_i)$. However, for the i^{th} term in the sum, the i^{th} station is effectively off-air ($P_i = 0$) so that historically-based off-air statistics for annual maintenance of station i are not reflected. For other stations, j ($j \neq i$), which, historically, use m_i as their annual maintenance month, the historical off-air probabilities for annual maintenance are not included in the calculation of $\bar{P}_{SA}$, since the computation is made assuming m_i is station i's annual maintenance month. For these reasons, the following two considerations are included in the calculation of PF:

(1) $\bar{P}_{SA}(\vec{P}_i, m_i)$ does not include *any* historically-based station reliability statistics for annual maintenance

(2) A weight, w_i, is inserted to characterize the expected duration of the off-air maintenance period based on historical figures. Note that w_i is tied to the station, *not* the historically-associated month.

The constraints on month m_i, i.e., the allowable monthly intervals for each station's annual maintenance, are illustrated in Fig. E-1. These intervals are 4-5 contiguous months (except for OMSTA Hawaii, which is unconstrained) which result from climatic, monetary, and contractual considerations.

E.2 SCHEDULING ALGORITHM

The algorithm determines the set $\{m_i\}$ which maximizes PF subject to the constraints on m_i shown in Fig. E-1. With no constraints on the m_i, $24!/4! - 2 \times 10^7$ iterations (calculations of PF) are required, but when constrained, this number is decreased by more than 3 orders of magnitude. A search, which is guided by the behavior of the component terms of PF, however, can reduce the number of iterations by 1-2 orders of magnitude.

Figure E.2-1 shows a series of plots of $w_i\bar{P}_{SA}(\vec{P}_i, m_i)$ as a function of m_i. These plots do not represent actual calculations (although they do approximate the behavior shown in Table 6.5-2) but serve to illustrate operation of the algorithm. The algorithm begins by selecting the value of m_i which maximizes $w_i\bar{P}_{SA}(\vec{P}_i, m_i)$ over the allowable months for station *i*, i.e.,

$$\text{Find } m_i \in \{M_i\} \text{ for which } w_i\bar{P}_{SA}(\vec{P}_i, m_i) \text{ is maximum}$$

where $\{M_i\}$ is the set of allowed maintenance months for station *i*. The algorithm proceeds by finding the maximum $w_i\bar{P}_{SA}(\vec{P}_i, m_i)$ within each allowable set of months for all stations. When the process is complete and all m_i are *distinct*, the algorithm terminates. However, if one or more m_i have the same value, then *conflict resolution* must be invoked.

Figure E.2-2 indicates the procedure to be followed when the algorithm schedules the same month for two different stations. To resolve the conflict, the conflicting month is deleted from the allowable set for station *i* (this is the meaning of the set $\{M_i - m_i'\}$ and the maximum value of $w_i\bar{P}_{SA}(\vec{P}_i, m_i)$ is computed over the remaining months, resulting in $m_i = m_i''$. The same procedure is followed for station *j*, resulting in $m_j = m_j''$. Thus the highest and second-highest values for $w\bar{P}_{SA}$ are computed for both stations. The next two boxes indicate calculations of two possible alternatives:

(1) the sum of the highest value of $w\bar{P}_{SA}$ for station *i* (satisfying the constraints) and the second-highest value of $w\bar{P}_{SA}$ for station *j*.

(2) the sum of the highest value of $w\bar{P}_{SA}$ for station *j* (satisfying the constraints) and the second-highest value of $w\bar{P}_{SA}$ for station *i*.

If sum(1) is larger than sum(2), then the conflict is resolved in favor of station *i* ($m_i = m_i'$) and station *j* is assigned the month ($m_j = m_j''$) corresponding to the second-highest value of $w\bar{P}_{SA}$. If sum(2) is larger than sum(1), then the conflict is resolved in favor of station *j*

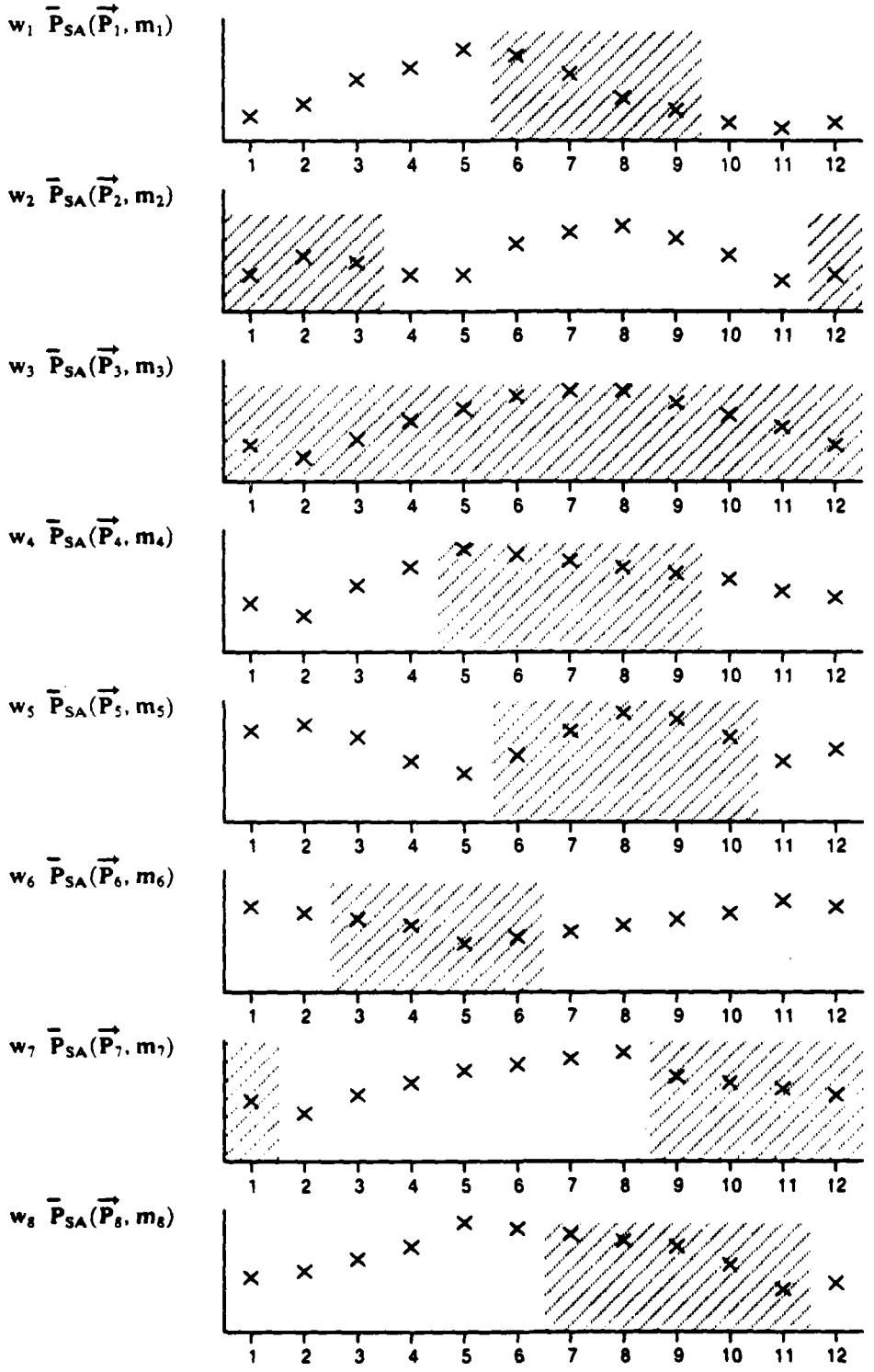

Figure E.2-1 Illustrative Plots of Performance Function Components Used in Off-air/Maintenance Scheduling Algorithm

G-13820
3-14-89

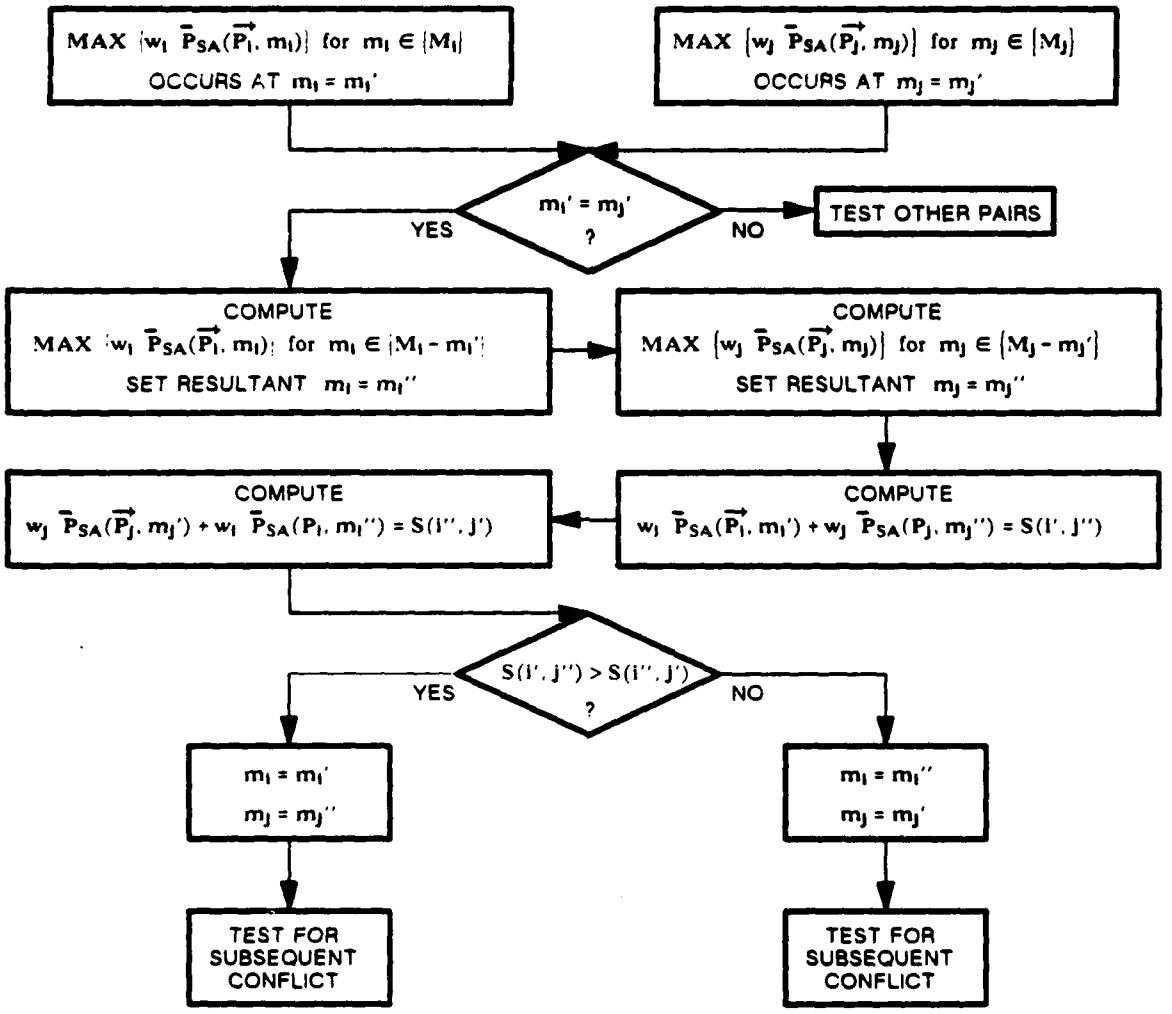

Figure E.2-2 Pairwise Conflict Resolution in Off-air/Maintenance Scheduling Algorithm

($m_j = m_j'$) and station *i* is assigned the month ($m_i = m_i''$) corresponding to the second-highest value of $w\bar{P}_{SA}$. Following this step, subsequent pairs are checked for conflicts. If subsequent conflicts are found and resolved, the algorithm cycles back to check previous re-assignments resulting from conflict resolution. If a loop is formed, preventing algorithm termination, then the next lowest-ranking values of $w\bar{P}_{SA}$ are compared.

REFERENCES

1. Pierce, J.A., *J.A. Pierce and the Origin of Omega*, IOA Newsletter (Special Edition), R. Revel, Editor, June 1988.

2. U.S. Department of Defense and U.S. Department of Transportation, *Federal Radionavigation Plan*, **Report No. DoD 4650.4/DOT-TSC-RSPA-87-3**, 1986.

3. Wenzel, Commander R.J., Omega System Status Update — 1988, *Proceedings of the Thirteenth Annual Meeting of the International Omega Association*, Munich, FRG, October 1988.

4. deBuda, R., Coherent Demodulation of Frequency-shift Keying with Low Deviation Ratio, *IEEE Transactions on Communication (Concise Papers)*, Part I, Vol. COM-20, June 1972 pp. 429-435.

5. Mathwich, H.R., Balcewicz, J.F. and Hecht, M., The Effect of Tandem Band and Amplitude Limiting of the E_b/N_o Performance of Minimum (frequency) Shift Keying (MSK), *IEEE Transactions on Communication*, Vol. COM-22, October 1974, pp. 1525-1540.

6. Morris, P.B., and Gupta, R.R., Omega Navigation Signal Characteristics, *Navigation: Journal of the Institute of Navigation*, Vol. 33, No. 3, Fall 1986.

7. Hauser, J.P., Rhoads, F.J., and Kelly, F.J., *VLFACM Program Description and Operational Manual*, **NRL Report 8530**, November 1981.

8. Ferguson, J.A., *A Report on the Integrated Prediction Program with Nuclear Environment (IPP-2)*, Naval Electronics Laboratory Center, **NELC Technical Note TN 1890**, July 1971.

9. Kelly, F.J., Hauser, J.P., and Rhoads, F.J., *Computer Program Model for Predicting Horizontally and Vertically Polarized VLF Atmospheric Noise at Elevated Receivers*, **NRL Report 8479**, December 1981.

10. Gupta, R.R., *Two-Frequency 24-hour/4-month Signal Coverage Database Development*, The Analytic Sciences Corporation, **Technical Report TR-5351-5-2**, October 1988.

11. Watt, A.D., *VLF Radio Engineering*, International Series of Monographs in Electromagnetic Waves, Vol. 14, Pergamon Press, 1967.

12. Ferguson, J.A., and Snyder, F.P., *The Segmented Waveguide Program for Long-Wavelength Propagation Calculations*, **NAVOCEANSYSCEN TD 1071**, December 1986.

REFERENCES (Continued)

13. Ferguson, J.A., and Snyder, F.P., *Approximate VLF/LF Waveguide Mode Conversion Model*, **NAVOCEANSYSCEN TD 400**, November 1980.

14. Morris, P.B., and Cha, M.Y., *Omega Propagation Corrections: Background and Computational Algorithm*, **ONSOD 01-74**, December 1974.

15. Levine, P.H., Tests of a Simple Omega Phase Model Including Solar Flare Effects, *Proceedings of Fifth Annual Meeting of the International Omega Association*, Bergen, Norway, August 1980.

16. Letter correspondence from Honorable James E. Dow, Acting Administrator, Federal Aviation Administration (FAA) to Honorable Frank A. Schrontz, Department of Defense (DoD) Representative to FAA, 25 April 1975.

17. Letter correspondence from Honorable Frank A. Schrontz, Chairman, DoD, Advising Committee on Federal Aviation, to Honorable James E. Dow, Acting Administrator, FAA, 30 June 1975.

18. FAA Advisory Circular No. 20-101C, *Airworthiness Approval of Omega/VLF Navigation Systems for Use in the U.S. National Aerospace System (NAS) and Alaska*, U.S. Department of Transportation, September 1988.

19. Pierce, J.A., Palmer, W., Watt, A.D., and Woodward, R.H., *Omega, a World-wide Navigation System: System Specification and Implementation*, Omega Implementation Committee Report to U.S. Navy Department/Bureau of Ships, Published by Pickard & Burns Electronics, Waltham, MA, Pub. No. 886B, May 1966.

20. International Radio Consultative Committee, *World Distribution and Characteristics of Atmospheric Radio Noise*, International Telecommunications Union, **CCIR Report 332**, 1964.

21. Private communication, Commander R.J. Wenzel, Commanding Officer, U.S. Coast Guard Omega Navigation System Center, 28 October 1988.

22. Morfitt, D.G., *Effective Electron Density Distributions Describing VLF/LF Progagation Data*, **NOSC TR 141**, September 1977.

23. Ferguson, J.A., *Ionospheric Profiles for Predicting Nighttime VLF/LF Propagation*, **NOSC TR 530**, February 1980.

24. Gupta, R.R., and Morris, P.B., Overview of Omega Signal Coverage, *Navigation: Journal of the Institute of Navigation*, Vol. 33, No. 3, Fall 1986.

25. *Omega Station Performance Statistics*, Omega Navigation Systems Center, U.S. Coast Guard, Letter Correspondence to The Analytic Sciences Corporation, August 1988.

REFERENCES (Continued)

26. Endter, E.W., Survey of Worldwide Omega Users, *Proceedings of the Ninth Annual Meeting of the International Omega Association*, Seattle, Washington, August 1984.

27. Mannheimer, D., Lateral Bending Effects at the Ionospheric Height Transition, *Effect of the Ionosphere on Radiowave Systems*, ed. by J. Goodman, April 1981.

28. Project Office/PM-9, *Project Master Plan for Omega Navigation System*, Chief of Naval Material, Department of the Navy, April 1966.

29. Karhunen, P., Use of Omega in Upper-air Windfinding, *Proceedings of the Eleventh Annual Meeting of the International Omega Association*, Quebec City, P.Q., Canada, August 1986.

30. Lanoue, J.C., Omega/VLF Receiver Design and Signal Processing, *Proceedings of the Ninth Annual Meeting of the International Omega Association*, Seattle, Washington, August 1984.

31. International Omega Association, Omega Tutorial Slides, *Supplement to Proceedings of the Annual Meeting of the International Omega Association*, 1988.

32. Gupta, R.R., Donnelly, S.F., Creamer, P.M., Sayer, S., *Omega Signal Coverage Prediction Diagrams for 10.2 kHz*, Vols. I-IV, The Analytic Sciences Corporation, **Technical Report TR-3077-2**, October 1980.

33. Gupta, R.R., *Omega Signal Coverage Prediction Diagrams for 13.6 kHz*, The Analytic Sciences Corporation, **Technical Report TR 4418-6**, August 1985.

34. Himmelblau, D.M., *Applied Nonlinear Programming*, McGraw-Hill, Inc., 1972.

35. Warren, R.S., Tench, K.A., Gupta, R.R., and Morris, P.B., Omega ACCESS: A Microcomputer Display of Omega Signal Coverage Diagrams, *Proceedings of the Eleventh Annual Meeting of the International Omega Association*, Quebec City, P.Q., Canada, August 1986.

36. Watson, R.A., FAA Update of Omega Activities, *Proceedings of the Thirteenth Annual Meeting of the International Omega Association*, Munich, FRG, October 1988.

37. Swanson, E. and Adrian, D., *Omega Envelope Capability for Lane Resolution*, NELC **TR-1901**, November 1973.